



**University of
Zurich**^{UZH}

Loss and damage of climate change in tropical glacierized areas: from changes in water availability to GLOFs.

GEO 511 Master's Thesis

Author

Olafur Yngvi Stitelmann
20-751-574

Supervised by

Dr. Randy Muñoz Asmat

Faculty representative

Prof. Dr. Christian Huggel

28.01.2024

Department of Geography, University of Zurich

Acknowledgment

I would like to express my gratitude to Dr. Randy Muñoz Asmat and Prof. Dr. Christian Huggel for their guidance and trust throughout this work. I also wish to thank Dr. Holger Frey for sharing his work and valuable insights. Special thanks to Bastien Bornet for sharing the photographs of his 2016 expedition.

Further, I extend my heartfelt thanks to my family, friends, and the inhabitants of Villa Gassweid for their unwavering support during this endeavor. I would also like to express my sincere gratitude to Mareke for her invaluable advice and support in the completion of my studies.

Ultimately, I would like to give my thanks to my classmates for their enduring friendship, making these last years of study a radiant journey.

Abstract

Embedded within the Cordillera Blanca, the world's most glaciated tropical mountain range, the Quillcay sub-catchment is heavily affected by anthropogenic climate change. Warming temperatures and glacier retreat lead to increasing slope instability in the high-mountain, while ice-melt and changing precipitation patterns alter water supply. Water, both as a vital resource and as a source of natural hazard through GLOFs, is a major concern for local inhabitants and decision-makers. Based on the Coupled Model Intercomparison Project's Phase 6 (CMIP6) Shared Socio-economic Pathways (SSPs), this work attempts to co-assess the negative impacts or 'losses and damages' (L&Ds) of climate change, related to changing water availability and GLOFs in the Quillcay catchment until 2050. Future river flow regimes are simulated with hydrological modelling, permitting an assessment of impacts of changes in water availability in terms of potential shortages and agricultural economic loss. Spatial analysis of GLOFs' hazard zones permits to assess possible loss of lives, number of buildings and agricultural area exposed. While no water shortage could be simulated, agricultural economic loss is highest in SSP5-8.5, with a \$319'054'345 USD estimated over the entire period. GLOFs' L&Ds are differentiated, with more important L&Ds for scenarios of high magnitude and low probability of occurrence. With different metrics combined, this L&D co-assessment provides a better understanding of the impacts of climate change in the catchment area and contributes as a basis to develop appropriate mitigation strategies. Further, this study explores the relationship between social and environmental drivers—such as population increase and glacier retreat—and the L&Ds studied. From this exploration, a framework and suggestions for co-assessing cascading L&Ds emerge.

Resumen

Enclavada en la Cordillera Blanca, la cadena montañosa tropical con más superficie glaciar del mundo, la subcuenca de Quillcay se ve muy afectada por el cambio climático antrópico. El aumento de las temperaturas y el retroceso de los glaciares provocan una mayor inestabilidad de las laderas en la alta montaña, mientras que el deshielo y los cambios en el régimen de precipitaciones alternan el suministro de agua. El agua, como recurso vital y como fuente de riesgos naturales a causa de las inundaciones repentinas de los lagos glaciales (ing. GLOFs), es una de las principales preocupaciones de los habitantes locales y los responsables en la toma de decisiones. Basándose en las Vías Socioeconómicas Compartidas (ing. SSPs) de la Fase 6 del Proyecto de Intercomparación de Modelos Acoplados (ing. CMIP6), este trabajo intenta coevaluar los impactos negativos o "pérdidas y daños" (ing. L&Ds) del cambio climático, relacionados con la disponibilidad cambiante de agua y los GLOFs en la cuenca del Quillcay hasta 2050. Los futuros regímenes de caudal de los ríos se simulan con modelamiento hidrológico, lo que permite una evaluación de los impactos de los cambios en la disponibilidad de agua en términos de escasez potencial y pérdidas económicas agrícolas. El análisis espacial de las zonas de peligro de GLOFs permite evaluar la posible pérdida de vidas, el número de edificios y la superficie agrícola expuesta. Aunque no se pudo simular escasez de agua, las pérdidas económicas agrícolas son mayores en el SSP5-8.5, con una pérdida estimada de 319.054.345 USD durante todo el periodo. Los L&D de los GLOFs son diferenciados, con L&Ds más importantes para escenarios de alta magnitud y baja probabilidad de ocurrencia. Con diferentes métricas combinadas, esta coevaluación de L&D proporciona una mejor comprensión de los impactos del cambio climático en la subcuenca de Quillcay y contribuye como base para desarrollar estrategias de mitigación apropiadas. Además, este estudio explora la relación entre los factores sociales y medioambientales —como el aumento de la población y el retroceso de los glaciares— y los L&D estudiados. De esta exploración surgen un marco y sugerencias para la coevaluación en cadena de los L&D.

Contents

Acknowledgment.....	I
Abstract.....	I
Resumen	II
Table of Figures:.....	V
Table of Tables:	VI
Introduction	1
1.1 Context	1
1.2 Motivation	2
Study site	4
2.1 Regional and climatological setting.....	4
2.2 The hydrological system of the Quillcay catchment	6
2.3 Agriculture in the Quillcay catchment.....	7
2.4 History of GLOFs.....	9
State of the art	12
3.1 Glacier’s retreat impact on hydrology.....	12
3.2 Changes in water availability	13
3.3 Shared Socio-economic Pathways	14
3.4 Loss and damage	16
3.5 Integrated Assessments of GLOFs and Water availability	17
Methods.....	20
4.1 Hydrological Simulations	21
4.1.1 The HBV Model.....	21
4.1.2 Reference period simulations	23
4.2.3 Simulation of future discharges	25
4.3 Water demands	26
4.3.1 Estimation of agricultural demand and impact on revenue	26
4.3.2 Estimation of domestic demand and potential water shortages	28
4.4 GLOFs simulations	29
4.4.1 Overview of GLOF modelling	29
4.4.2 Estimation of damage within the city of Huaraz	30

4.4.3 Estimation of damage in agricultural areas.....	31
4.5 Framework for co-assessment of changes in water availability and GLOFs.....	32
Results.....	33
5.1 Glacio-hydrological simulations	33
5.1.1 Glacier extents	33
5.1.2 Hydrological simulations.....	34
5.2 Impacts of changing water availability.....	38
5.2.1 Impact on water balance	38
5.2.2 Impact on agricultural revenue	40
5.3 Impacts of GLOFs	41
5.3.1 Impacts within Huaraz.....	41
5.3.2 Impacts on agricultural land	43
5.4 Co-assessment.....	45
5.4.1 Overview of losses and damages.....	45
5.4.2 Connecting losses and damages with their drivers.....	46
Discussion	47
6.1 Robustness of simulations	47
6.1.1 Glacier retreat	47
6.1.2 Hydrological simulations.....	48
6.2 Losses and damages of changing water availability	49
6.2.1 Water balance	49
6.2.2 Loss of agricultural revenue	50
6.3 Loss and damage assessment of GLOFs.....	51
6.3.1 Losses and damages within Huaraz.....	51
6.3.2 Damage on agricultural land	52
6.4 Co-assessment of Loss and Damage	53
6.5 Limitations and uncertainties	57
Conclusion	58
References	60
Appendix.....	69

Table of Figures:

Figure 1. Callash valley (Bastien Bornet, 2016).....	5
Figure 2. Glaciers and mountain peaks on the South-Western part of the catchment, with Tullparaju in the background (Bastien Bornet, 2016).	5
Figure 3. Map of the hydrological system of the Quillcay catchment.	6
Figure 4. Map of Irrigation blocks and irrigation system.	7
Figure 5. Map of water intake points.....	8
Figure 6. Photography from NE view of the March 19, 2003 landslide area indicated by the narrow black line (photo by J. Klimes, July 2003, retrieved from Vilímek et al. 2005).	9
Figure 7. Photography of the panoramic view over the Palcacocha lake, showing the breached morain from the 1941 GLOF, by Martin Mergili, July 2017 (retrieved from Mergili et al., 2020).	10
Figure 8. Panoramic view over Huaraz and representation of the 1941 GLOF extent, by Martin Mergili, July 2017 (Retrieved from Mergili et al., 2020).	10
Figure 9. Evolution of the Palcacocha lake since the 1941 GLOF (Retrieved from Huggel et al., 2020)	11
Figure 10. Spatial propagation of the contribution of glacial melt to river flow for four hotspots in the tropical Andes: (Retrieved from Buytaert et al., 2017).....	12
Figure 11. Projected annual precipitation and temperature for the Condorcerro catchment. (Retrieved from Motschmann et al., 2022).....	14
Figure 12. Three-dimensional representation of the SSP scenarios and their five SSP families. (Retrieved from Meinshausen et al., 2020).	15
Figure 13. Matrix that compares probability of occurrence and exposure for GLOF and water scarcity. (Retrieved from Motschmann et al., 2020b).....	18
Figure 14. General scheme of the research’s method.....	20
Figure 15. Design of the hydrological modelling method.....	21
Figure 16. The HBV model (Retrieved from Seibert, 2005).....	22
Figure 17. Example of Open Building V3 polygons and confidence intervals at the confluence of Rio Quilcay and Rio Santa in Huaraz.	30
Figure 18. Map of historical glaciers extents from 1988 to 2016.....	33
Figure 19. Historical and future glacier extents according to SSPs projections.....	34
Figure 20. Monthly precipitation compared to discharge during the reference period and for the SSPs’ projections.....	35

Figure 21 & 22 (Left). Average dry season (Left) and rainy season (Right) discharge in mm for the reference period and SSPs' projections.....	36
Figure 23. Discharge balance of SSPs' projections compared with the reference period annual average of 825.7 mm for 1981-2016.....	36
Figure 24. Cumulated discharge during the dry season for the reference period and SSPs' projections.....	37
Figure 25. Cumulated discharge during the rainy season for the reference period and SSPs' projections.....	37
Figure 26. Glacier melt-water content in percentage of the discharge during the dry-season for SSPs' projections.....	38
Figure 27 & 28. SSP1-2.6 (Left) and SSP5-8.5 (Right) Water balance during the dry season (mm).....	39
Figure 29 & 30. SSP1-2.6 (Left) and SSP5-8.5 (Right) Annual water balance (mm).....	39
Figure 31. Yearly economic balance of agricultural revenue.....	40
Figure 32. Dry-season economic balance of agricultural revenue.....	41
Figure 33. Map of GLOF hazard zones.....	42
Figure 34. Population within GLOFs hazard zones.....	42
Figure 35. Map of NDVI classification (January 2021).....	43
Figure 36. Map of agricultural area (high NDVI) within GLOF hazard zones.....	44
Figure 37. Relationships between glacier retreat, population increase, and L&Ds from water availability and GLOFs in the Quillcay catchment.....	46

Table of Tables:

Table 1. Table showing categorization of L&D originating from cryosphere impacts (Huggel et al., 2018)..	17
Table 2. ANOVA and Post-hoc analysis with the Bonferroni method on the discharges of the reference period and the SSP1-2.6 & SSP5-8.5 projections.....	35
Table 3. Co-assessment table of L&D directly related to water scarcity and GLOFs.....	45
Table 4. Suggested framework for co-assessing cascading L&D of GLOFS & water scarcity.....	55

List of Abbreviations

ANA: Autoridad Nacional del Agua

BCRP: Banco Central de Reservas del Peru

CB: Cordillera Blanca

COP: Conference Of Parties

CMIP6: Coupled Model Intercomparison Project Phase 6

ELA: Equilibrium Line Altitude

ETP: Evapotranspiration

FAO: Food and Agriculture Organisation

FLH: Freezing Line Height

GAP: Genetic Algorithm Calibration

GLOF(s): Glacier Lake Outburst Flood(s)

INAIGEM: Instituto Nacional de Investigación en Glaciares y Ecosistemas de Montaña

INEI: Instituto Nacional de Estadística e Informática:

IPCC: International Panel for Climate Change

L&D(s): Loss(es) and Damage(s)

MBC: Multi-variate Bias Correction

MBR: Michael Bauer Research GmbH

MINAM: Ministerio Del Ambiente

NDVI: Normalized Difference Vegetation Index

NELD: Non-Economic loss and damage

PISCO: the Peruvian Interpolated data of the SENAMHI's Climatological and Hydrological Observations

RCP: Representative Concentration Pathways

RWE: Rheinisch-Westfälisches Elektrizitätswerk Aktiengesellschaft

SAT: Surface Air temperature

SIEA: Sistema Integrado de Estadísticas Agrarias

SMHI: Swedish Meteorological and Hydrological Institute

SSP(s): Shared Socio-Economic Pathway(s)

UNFCCC: United Nations Framework Convention on Climate Change

WIM: Warsaw International Mechanism

Introduction

1.1 Context

In 2015, a farmer and mountain guide named Saúl Luciano Lliuya sued the German company *Rheinisch-Westfälisches Elektrizitätswerk Aktiengesellschaft* (RWE) for being responsible of atmospheric emissions contributing to enhancing GLOF hazard in his hometown Huaraz (Burhans, 2022). This litigation has become famous amongst the scientific community dedicated to studying the impacts of climate change in mountainous regions. This event brings into light both the consequences of climate change and its systemic origin in an interconnected world. For evaluating and reducing negative consequences of climate change, an international climate policy mechanism has been developed: the loss and damage (L&D) approach (Motschmann, 2020). In November 2023, the L&D Fund was operationalized at the COP28 (UNFCCC, 2023). The fund aims at compensating for “economic and non-economic loss and damage associated with the adverse effects of climate change, including extreme weather events and slow onset events” (UNFCCC, 2023, p.1). The Cordillera Blanca (CB) suits well for a L&D assessment as this region is subject to increasing socio-environmental stresses induced by anthropogenic climate change (Schauwecker et al., 2014; Drenkhan et al., 2015; Motschmann et al., 2020). The CB contains about 20% of tropical glaciers’ area in the world and 41% of the glacier’s area of Peru (ANA, 2014b). Climate change in the CB has led to ice melt, with the glacier area reducing by 33% between 1970 and 2014 (Casassa et al., 2007; ANA, 2014b; Yap, 2015; Drenkhan, 2016). Hydrological cycles in the CB are also affected by global changes in precipitation patterns (Drenkhan et al., 2015; Guittard et al., 2020). On one hand, glacier melt and changes in precipitation patterns result in discharge variations within the Rio Santa and its tributaries. On the other hand, higher temperatures and loss of permafrost increase instability of high-mountain slopes, resulting in more likely occurrences of landslides and glacier lake outburst floods (GLOFs) (Frey et al., 2018). The significance of the changes in the CB’s cryosphere and their impact on local inhabitants has been widely recognized and investigated by the scientific community (Carey, 2005; Emmer 2017; Mark et al. 2017; Motschmann et al., 2020). In addition to physical changes in natural systems, population increase and economic development accentuates stresses on water supply. With increasing water demands and unstable environmental conditions, water availability and

occurrences of GLOFS are major concerns for local inhabitants and decision-makers. Furthermore, as is typically the case in high-mountain environments, changes in upper catchments can cascade into series of processes impacting populations downstream (Motschmann et al., 2020b).

1.2 Motivation

The ongoing social and physical processes connected to climate change in the CB have been widely studied by the scientific community (Carey, 2005; Vuille et al., 2008; Yap et al., 2015; Muñoz, 2017; Motschmann et al., 2020). However, little research has been done in integrative assessments of the impacts on climate change in terms of L&D (Motschmann et al., 2020b; Bahinipati & Gupta, 2022). Even though highly impacted by climate change, the mountain cryosphere and its cascading processes have remained rather disconnected from the L&D discussion (Huggel et al., 2018). As a mechanism of environmental policy, L&D inherently recognises the interconnections between climatological conditions, physical processes, and anthropogenic activities. According to Huggel et al., “L&D is connected, driven, and caused by climate and cryosphere change, [...] (and) is related to other factors and developments (e.g. social, political, economic)” (2018, p.1395). It is therefore relevant, when looking at impacts of climate change, to attempt not only a general mapping of L&Ds, but also to investigate the relationships between losses and damages, social development, and physical processes. In this line of thought, this study primarily aims at consolidating the current effort in investigating future changes in hydrological systems and impacts of GLOFs in the Quillcay catchment by quantifying their associated losses and damages. Reaching consistent results in estimating these changes and their consequences for local communities may help adaptive water management (Drenkhan, 2016). Further, this study explores the relationship between social and environmental variables—such as population increase and glacier recession—and L&D associated to changes in water availability and GLOFs.

This study’s framework delimitates L&D of water availability as impact on agricultural production value and water deficit for domestic demand. Agricultural production value is represented as an economic loss, with agriculture including only non-subsistence farming partly depending on irrigation. Small-scale subsistence and rain-dependent farming is excluded from this research. L&D of GLOFs are estimated in terms of number of lives impacted, as well as number of buildings and agricultural area potentially damaged.

This leads us to the main question this research will attempt to answer: what are the losses and damages of GLOFs events and changes in water availability due to climate change on local assets, agricultural revenue, and loss of lives until 2050? To comprehensively answer the question above, three other research-specific questions must be asked:

1. What are the impacts of changes in water availability on agricultural revenue and domestic consumption?
2. What is the extent of damage to buildings, agricultural area, and loss of lives related to GLOF events in the catchment?
3. How are these impacts spatially and temporally distributed?

Quantifying and analysing the distribution of the investigated L&Ds can serve informing global L&D mechanisms on possible assessment methods (Motschmann et al., 2020). On the local scale, presenting stakeholders with a range of L&Ds from plausible future scenarios can contribute to develop adequate adaptation strategies (Drenkhan et al., 2023). In addition, this study provides a usable base to assess water security within the Quillcay catchment. Water security is reflected in both water scarcity and water induced natural hazards such as GLOFs (Grey & Sadoff, 2007; Bakker, 2012; Drenkhan, 2016; Drenkhan & Castro-Salvador, 2023).

Study site

2.1 Regional and climatological setting

The Quillcay catchment is characterized by a semi-arid climate with total annual precipitation between 700 and 1000 mm/year (Drenkhan, 2016). As is typically the case for the tropical Andes, annual temperatures do not vary significantly, whereas precipitation's patterns are divided between the rain and dry season, respectively peaking between December to February and June to August (Drenkhan, 2016). There have been many efforts in modeling the evolution of precipitation and hydrological cycles in the tropical Andes (Condom et al., 2012; Neukom et al., 2015; Muñoz, 2017; Motschmann et al., 2020). Results indicate a decrease in precipitation for the CB towards the end of the 21st century (Motschmann et al., 2020). In high-mountainous regions such as the tropical Andes, climate change has a significant impact on the cryosphere (Huggel et al., 2018). On a national scale Peru's glacier cover has reduced by 43% from 1970 to 2010 (ANA, 2014a; Drenkhan 2016). In 2016, Glaciers represented 12.6% of the Quillcay catchment (ANA, 2023). Glaciers act as water storage for precipitation in the accumulation area. The accumulation period therefore also corresponds to the rainy season. In the ablation area, water is released as ice melts. With rain season taking place in the summer months, accumulation period also corresponds with higher volumes of ice melt. During the rainy season, high volume of water from melting ice as well as high precipitation leads to high discharge (Calizaya et al., 2021). In the dry season months between May and September both precipitation and glacier melt decrease. Due to very low precipitation, the proportion of water from glacier melt in the river stream becomes more significant during the dry season (Buytaert et al., 2017).

The location of the Quillcay catchment in a high-altitude mountain range separating the wet tropical climate zone of the rain forest on its East to the dry coastal desert on its West is favorable to the development of a micro-climate. In combination with changing climatic conditions, this signifies a highly variable start of growing season (Hänchen et al., 2022). The Quillcay catchment is composed of three distinct latitude zones characterized by distinctive environmental settings and land-use. In the lower altitudes lies the city of Huaraz surrounded by agricultural land. Then starts the national park with semi-arid climatic conditions and scarce vegetation (Figure 1). In the high-mountain are glaciated areas and lakes formed by ice-melt (Figure 2).



Figure 1. Callash valley (Bastien Bornet, 2016). The mid-altitude mountainous areas, ranging from about 4000 m.a.s.l. to the glacier tongues, present a semi-arid climate with scarce vegetation. Livestock roams free in the national park.



Figure 2. Glaciers and mountain peaks on the South-Western part of the catchment, with Tullparaju in the background (Bastien Bornet, 2016).

2.2 The hydrological system of the Quillcay catchment

The CB is located in the department of Ancash, whose capital, Huaraz, lies at an elevation of 3050 m.a.s.l. Our study area is the Quillcay catchment. It includes the capital city and extends west until the mountain tops of Palcaraju (6'274 m.a.s.l.), Chinchey (6'309 m.a.s.l.), and Tullparaju (5'787 m.a.s.l.). The catchment area is 250 km². The upper section of the catchment area is designated as a national park, constituting approximately 78% of the total catchment area. Within the national park lie about 40 lakes, with the biggest ones being located at the edge of glacier tongues. Most of the lakes are small lakes of less than one hectare while the biggest lakes are Palcacocha and Tullpacocha with 46.6 and 44.8 ha respectively (Muñoz, 2017). The Cojup, Quillcayhuanca and Shallap rivers flow from glacier tongues and lakes until they meet other smaller tributary streams. Then, the Cojup becomes the Paria and Quillcayhuanca and Shallap form the Auqui. The Paria and the Auqui meet in the city of Huaraz and form the Quillcay which then flows into the Santa River (Figure 3).

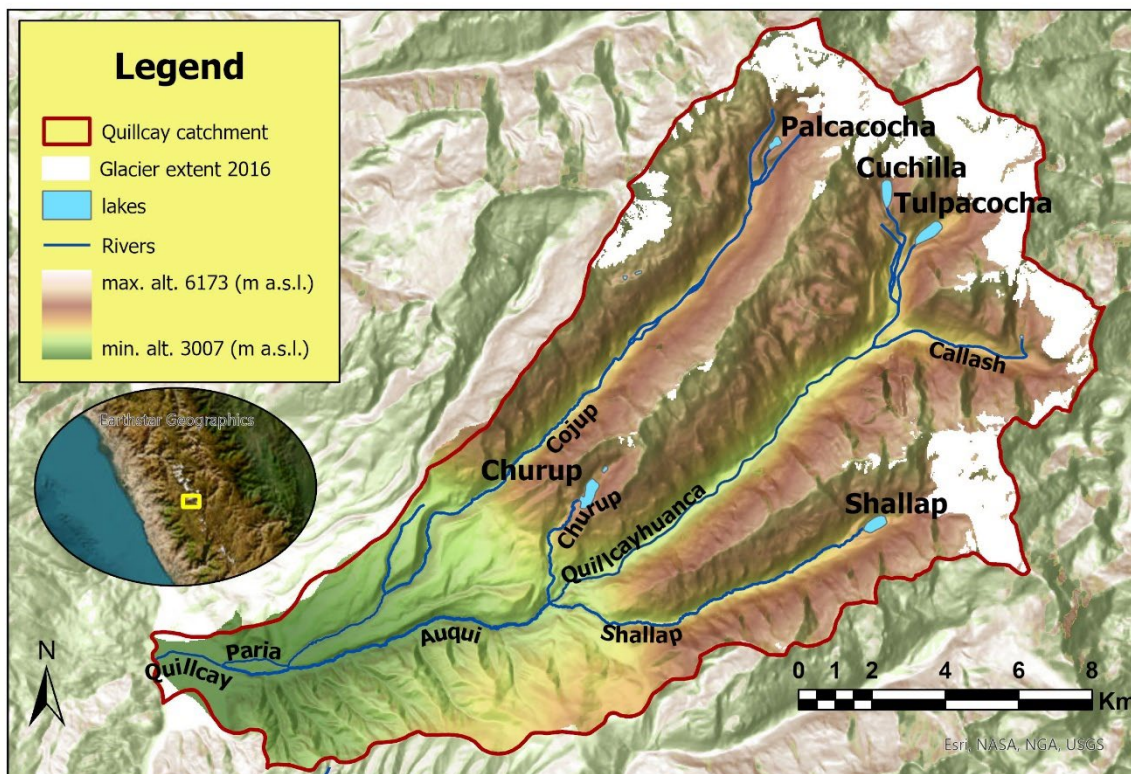


Figure 3. Map of the hydrological system of the Quillcay catchment.

2.3 Agriculture in the Quillcay catchment

Agriculture is a major working sector in Peru representing 65% of the rural population and 23% of the total population (Drenkhan, 2016; MINAM, 2010). Within the Quillcay catchment, a land cover classification derived from satellite imagery determines that 12% of the catchment's area is used for agriculture (MINAM, 2015). The satellite-based classification does not consider the complexity of agricultural practices and their subsequent diverse spatial footprint. It is unlikely that all this area is actively used for agricultural production throughout the year. In fact, area used for agriculture varies between months, with the biggest area cultivated taking place in February with 1304 ha, or about 5% of the catchment area (Quesquén, 2008). Most of the crops are being cultivated in the rainy season, with alfalfa (lat. *Medicago sativa*), wheat, and potato occupying the biggest cultivation areas. In the dry season, only alfalfa, beans (lat. *Pisum Sativum*), and onions are cultivated (Quesquén, 2008).

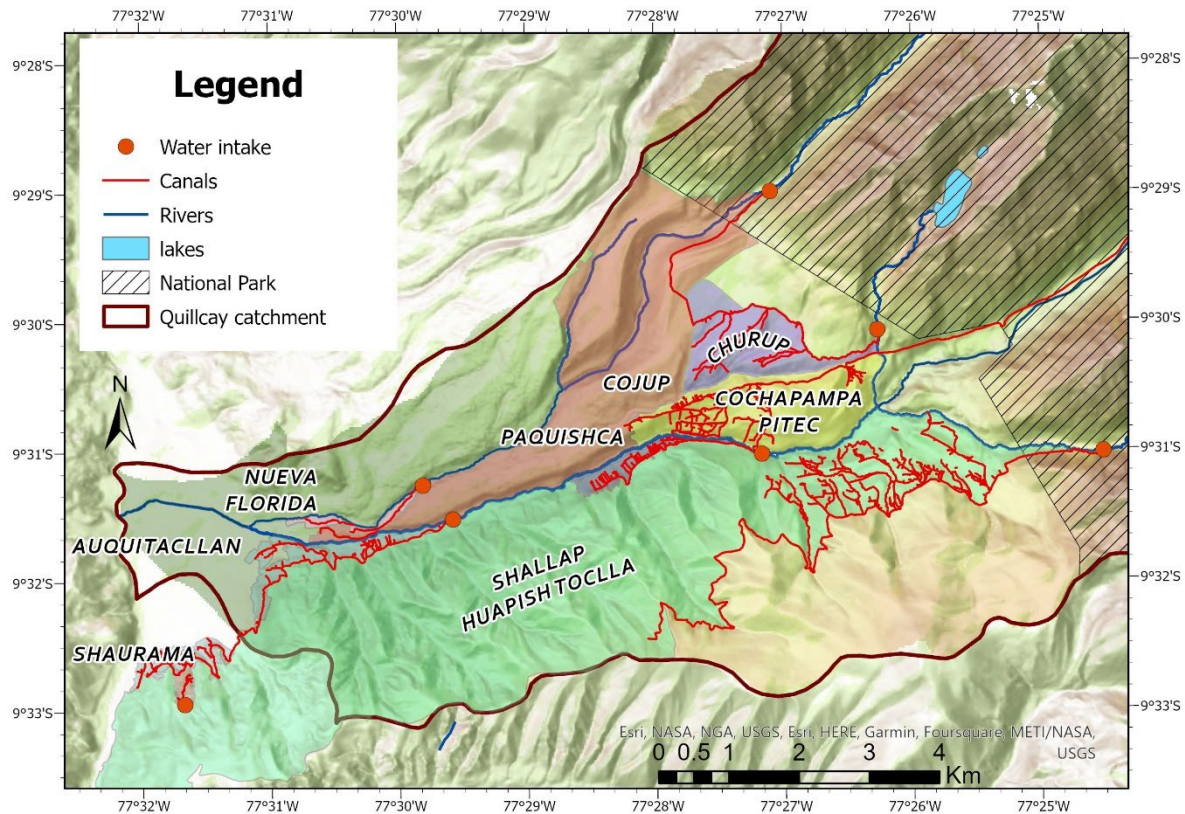


Figure 4. Map of Irrigation blocks and irrigation system.

Agricultural fields are located between about 3000 to 4000 m.a.s.l., which is between the edge of the national park and the city of Huaraz. Small-scale agriculture is dominant in the valley (Motschmann et al. 2020; Mark et al., 2010). During the rainy season, agriculture is mostly rain dependent, whereas a system of canals provides additional water throughout the year. Most of the canals are located at the edge of the national park in the Curup, Cochapampa Pitec, Paquishca and Shallap Huapish Toclla irrigation blocks (Figure 4). Irrigation blocks vary greatly in size from Shallap representing 2'614 ha to Nueva Florida representing 19.4 ha (Appendix I).

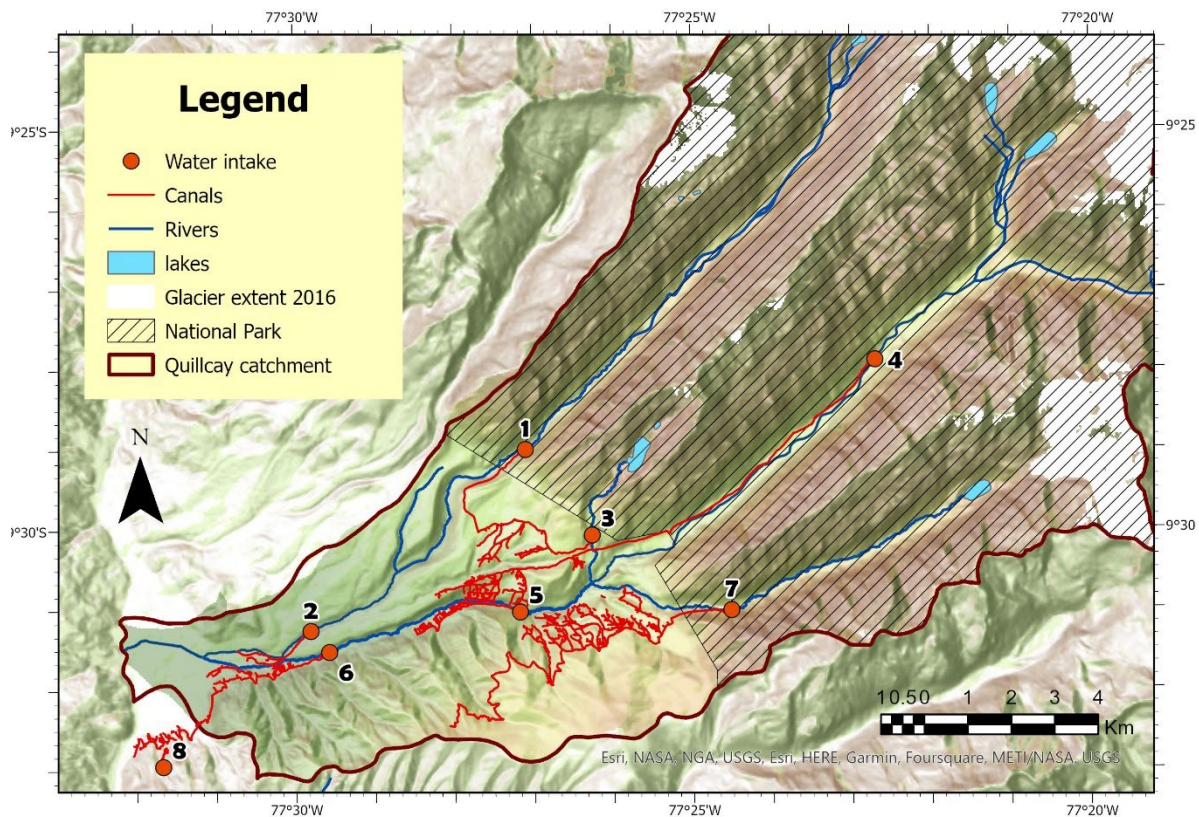


Figure 5. Map of water intake points.

Water intakes are located at every major stream in the catchment and lie at an altitude of between 3'700 to 4'000 m.a.s.l. There is one water intake per irrigation block, each irrigation block is represented by an irrigation committee. The Churup and Cochapampa blocks are represented by one single committee. The intakes number 1,3,4,5 and 7 provide for the main canal system bordering the national park, whereas the intakes number 2 and 6 feed the smaller irrigation system further down in the valley. The water intake number 8 only provides for the Shaurama irrigation block and lies outside of the catchment boundary. For this reason, both the intake point number 8 and the Shaurama block are not further considered in this study (Figure 3, 4 & 5).

2.4 History of GLOFs

The Cordillera Blanca is highly susceptible to high-mountain natural hazards, with more than 30 glacier-related disasters causing a total of more than 15,000 casualties since 1941 (figure 7 & 8) (Carey, 2005; Frey et al., 2018). Events in the high mountain can trigger a cascade of interacting processes which have costly impacts for downstream populations (Huggel et al., 2020, Frey et al., 2018). GLOFs for instance can originate from debris flows or rock/ice avalanches falling into glacier lakes, thus provoking overflowing of the lake. When lakes are dammed by end-moraines, as is the case for lake Palcacocha, an impact wave can flow atop the end moraine. The moraine can also be breached, leading to the sudden lake discharge downstream of the valley. This process happened at lake Palcacocha in 1941. The GLOF resulted in more than 1,800 casualties and the flooding of a third of the city of Huaraz, making it the deadliest GLOF in history (Carey, 2005; Frey et al., 2018).

Even though a GLOF of the same scale as the 1941 disaster is unlikely to occur again in the Quillcay catchment, GLOFs still pose a threat (Carey, 2005, Frey et al., 2018). In 2003, a landslide on the south-west of the glacier tongue fell into lake Palcacocha. Even though the subsequent flood was relatively small, with little material deposited along the river streams, it provoked a 6-day shortage of drinkable water in the city of Huaraz (INAIGEM, 2020). The risk of GLOF is a very present concern for the local population (Carey, 2005). Permafrost thaw as well as high-precipitation events contribute to slope instability in the high mountain.



Figure 6. Photography from NE view of the March 19, 2003 landslide area indicated by the narrow black line (photo by J. Klimes, July 2003, retrieved from Vilimek et al. 2005).

The 2003 landslide shown in the photograph (Figure 6) occurred towards the end of the rain season. It can be hypothesized that a water saturated soil resulted in the detachment of soil mass into the lake, generating a small GLOF.

On the right side of the photograph (figure 7), one can see the moraine breach through which lake Palcacocha emptied out in 1941. A recent dam has been built for a better control over the water reservoir.

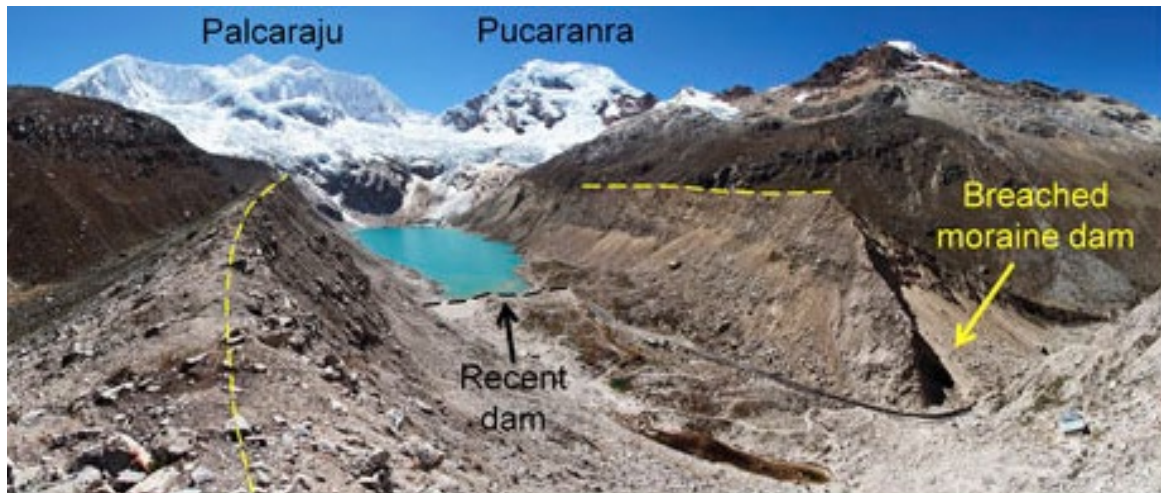


Figure 7. Photograph of the panoramic view over the Palcacocha lake, showing the breached moraine from the 1941 GLOF, by Martin Mergili, July 2017 (retrieved from Mergili et al., 2020).

Figure 8 shows the extent of the 1941 GLOF over the city of Huaraz. The flood extends in urban areas along the Paria and Quillcay river and reaches the Santa River.



Figure 8. Panoramic view over Huaraz and representation of the 1941 GLOF extent, by Martin Mergili, July 2017 (Retrieved from Mergili et al., 2020).

The area covered by lake Palcacocha has significantly increased due to glacier melt since 1941. From 1988 to 2009, the lake has increased from 0.07 km² to 0.52 km² (Figure 9). A decrease of 0.3 km² from 2009 to 2018 is observed, this is due to anthropogenic regulation of the water level.

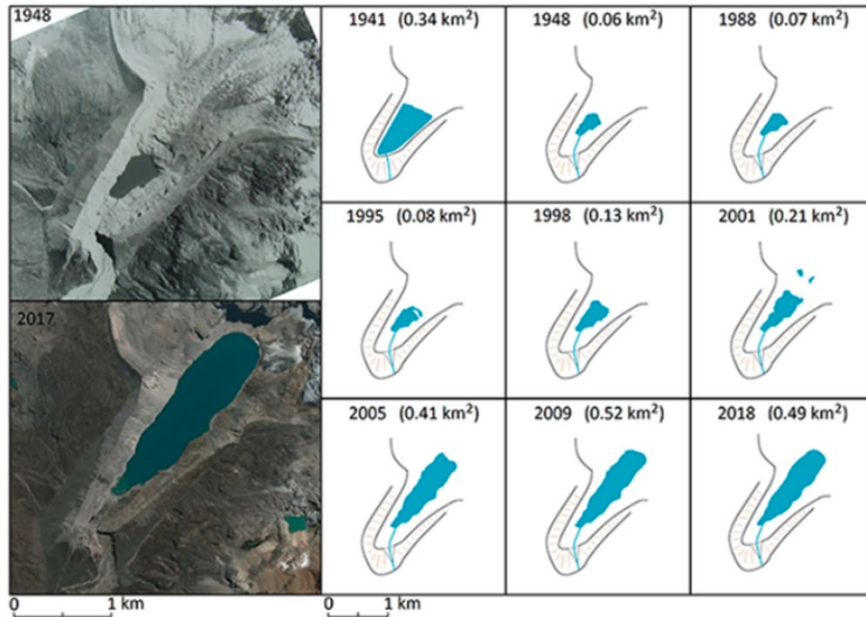


Figure 9. Evolution of the Palcacocha lake since the 1941 GLOF (Retrieved from Huggel et al., 2020)

State of the art

3.1 Glacier's retreat impact on hydrology

The Peruvian Andes contain about 70% of the world's tropical glaciers (Seehaus et al., 2019). The impact of global climate change on the retreat of tropical glaciers has been widely investigated by experts (Mark et al, 2017; Schauerwecker et al., 2017; Seehaus et al., 2019). Changes in melting rates lead to variations of melt-water content in discharges, resulting in new challenges across socio-environmental systems (Mark et al., 2017). Ice loss is also widely felt by local populations, leading to intangible L&D such as loss of identity (Allison, 2015; Huggel et al., 2018). In addition, glacier retreat and permafrost thaw increase slope instability, leading to more likely occurrence of mass movement events such as debris flows or GLOFs (Frey et al., 2018; Drenkhan et al., 2019).

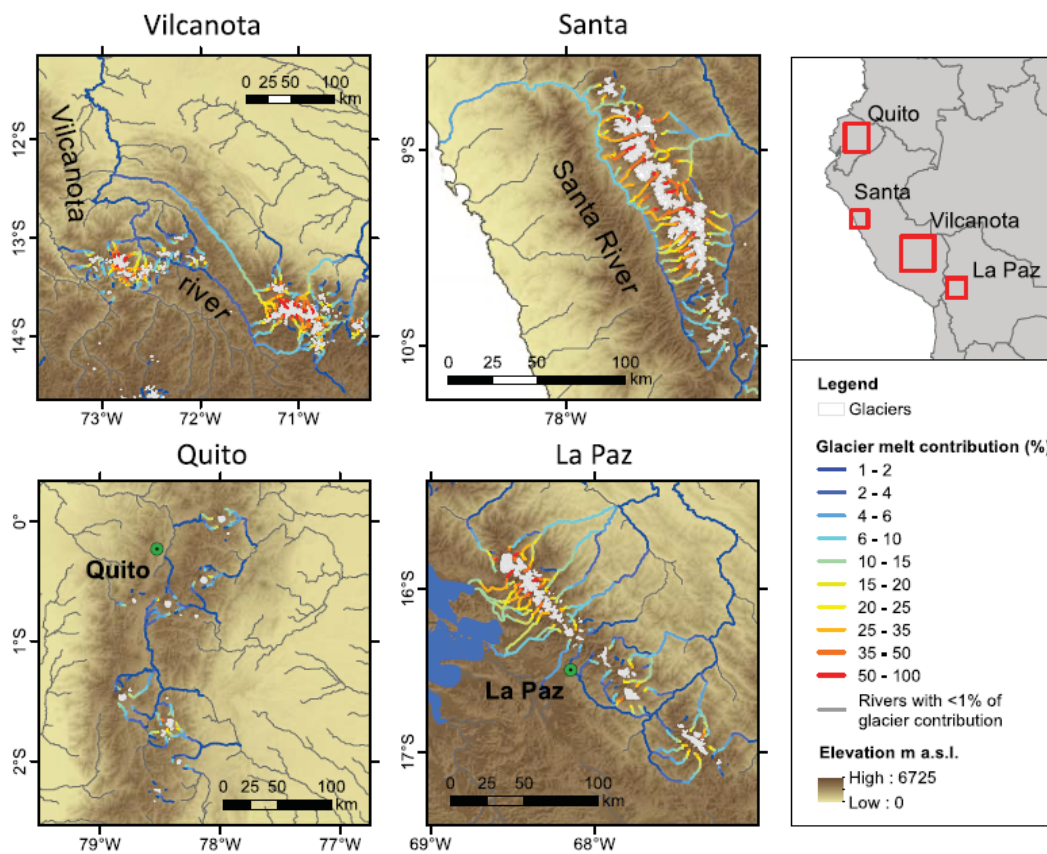


Figure 10. Spatial propagation of the contribution of glacial melt to river flow for four hotspots in the tropical Andes: maps show the annual average during a normal year (Retrieved from Buytaert et al., 2017).

The tropical Andes are marked by a high meteorological seasonality. As a result, tropical glaciers in the Andes show both high accumulation and ablation during the summer period, which corresponds to the rain season between December and February (Drenkhan et al., 2015; Muñoz, 2017). Even though glacier melt peaks in the rain season, glacier melt-water content in percentage of streamflow is highest during the dry season between June and August (Buytaert et al., 2017). Proportion of glacier meltwater in streamflow decreases as river systems run away from glaciers and benefit from the contribution of larger accumulating areas. In figure 10, average annual glacier melt contribution in the tributaries to the Santa River range from above 50% from the glacier tongues to 20% near the Santa River. Glacier meltwater plays a significant role in discharge and is closely connected to glacier retreat, making it a crucial factor in shaping future water supply in the tropical Andes (Buytaert et al., 2017).

3.2 Changes in water availability

Economic development and population increase is expected to contribute to higher water demands until 2050 (Drenkhan et al., 2015; Samir et al., 2017). On the other hand, climate change and the induced glacier retreat alter hydrological cycles. Water availability has therefore become a concern for the local population and is widely investigated by the research community (Gurgiser et al., 2016; Motschmann et al., 2020; Brügger et al., 2021; Calizaya et al., 2021). Precipitation patterns in the last decade are expected to increase north of the 11°S parallel, and to decrease south of this parallel (Drenkhan et al., 2015). In the CB, precipitation has increased by 60 mm per decade from 1983 to 2012 (Drenkhan et al., 2015). Because of the high seasonality of precipitation, it is relevant to understand how precipitation projections could evolve throughout seasons. It is expected that high-precipitation events will increase in number and magnitude in the rainy season and precipitation will become scarcer in the dry season. Such variations in seasonality remain nevertheless difficult to model accurately (Neukom et al., 2015; Guittard et al., 2020). In figure 11, the high variability of precipitation projections for both RCP 2.6 and RCP 8.5 can be observed for the Condorcerro catchment. The Condorcerro catchment includes the Quillcay sub-catchment. Annual mean temperature increases in both RCP scenarios, fostering glacier retreat.

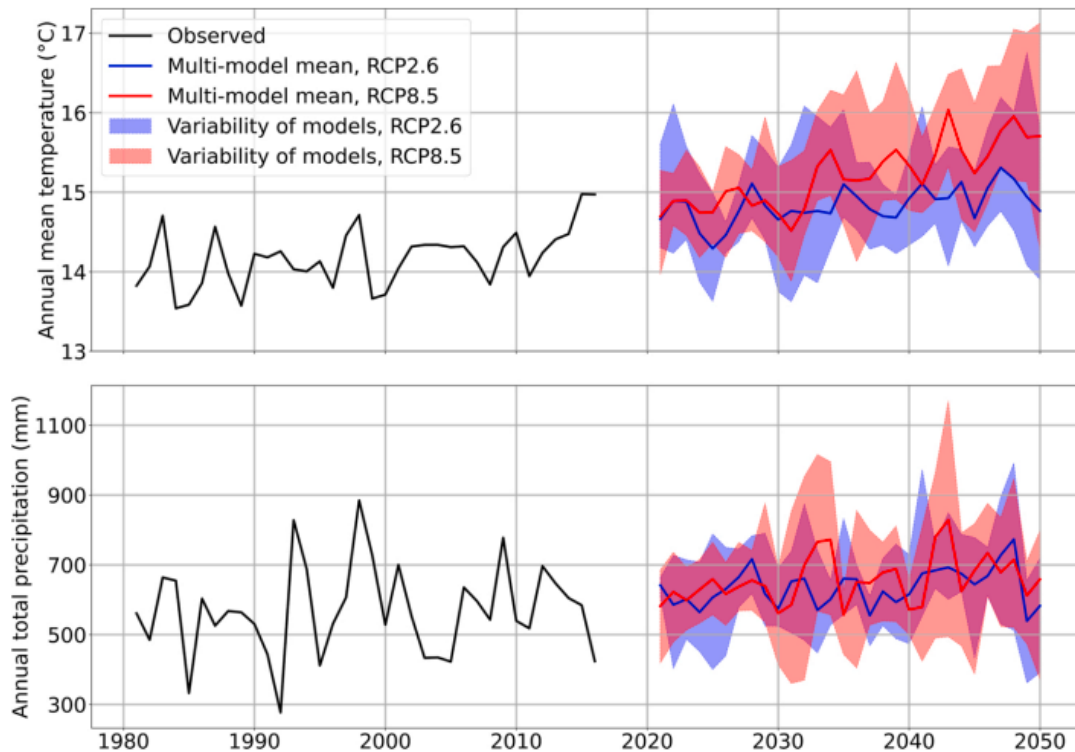


Figure 11. Projected annual precipitation and temperature for the Condorcerro catchment. The Condorcerro catchment is located further downstream of the Santa River and includes the Quillcay catchment. Projections for RCP2.6 and RCP8.5 are based on PISCO data and five different Global circulation Models (Retrieved from Motschmann et al., 2022).

Another component of water availability is glacier-melt water. Due to climate change, glacier retreat is expected to continue until the quasi vanishing of the cryosphere until 2100 (Schauwecker et al., 2017). When the glacierized area is reduced to the point that long-term river discharge is decreasing despite high ice melting rate, the peak water is reached (Motschmann et al., 2022). Guittard et al. suggests that the peak water has already been reached in the Santa catchment (2020).

3.3 Shared Socio-economic Pathways

Climate models are commonly used for assessing risk and vulnerability evolution associated with climate change (Frame et al., 2018). In its sixth report, the International Panel for Climate Change (IPCC) proposes a range of Shared Socio-economic Pathways (SSPs) combined with Representative Concentration Pathways (RCPs) to describe a set of plausible futures. RCPs represent future emissions trajectories and concentrations and are expressed in terms of radiative forcing in Watts per square meters at the top of the atmosphere in 2100. Whereas RCPs are useful tools to represent chemical variables, their defining socio-economic characteristics are not standardized. On the other

hand, SSPs can be understood as a set of narratives describing the development of human societies facing climate change. SSPs propose five different scenarios of societal response, including combinations of challenges to mitigation and adaptation (Figure 12). Each SSP can be connected to multiple RCPs. This makes sense as one socio-economic narrative can be connected to various mitigation ambitions. In this study, SSP1-2.6 and SSP5-8.5 are used (Kriegler et al., 2017; Van Vuuren et al., 2017). These two SSP and RCP combinations are commonly selected to represent a low and a high emission development scenario. The advantage of integrating SSPs into climate modelling rather than solely relying on RCPs lies in the availability of projections of socio-economic variables. In this study, SSP1 and SSP5 baselines projections for agricultural productions for South America were used.

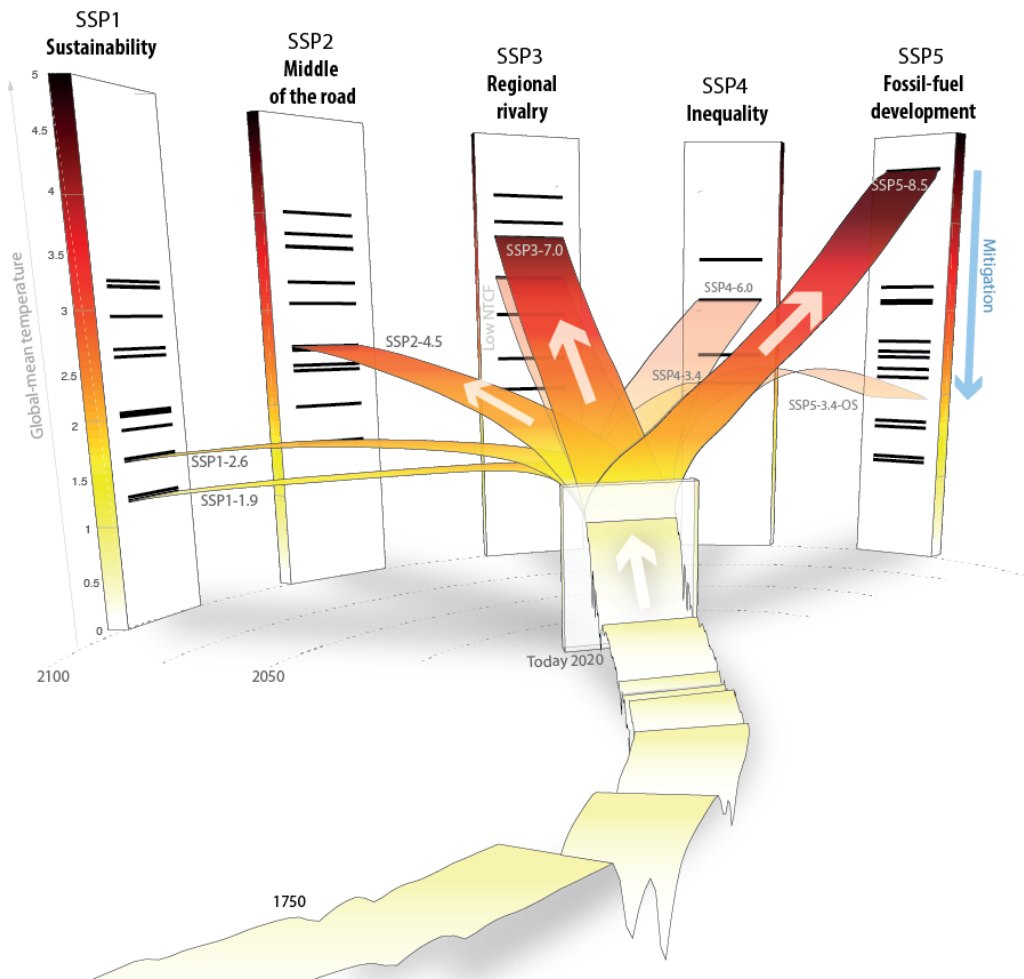


Figure 12. Three-dimensional representation of the SSP scenarios and their five SSP families. The front light-yellow band represent temperature levels relative to pre-industrial era. The branching of SSP scenarios over the 21st century is represented by the 5 vertical pillars (Retrieved from Meinshausen et al., 2020).

3.4 Loss and damage

In November 2013 the Conference of Parties (COP19) established the Warsaw International Mechanism (WIM) for loss and damage associated with climate change impacts (UNFCCC, 2013). Ten years after the WIM's creation, the L&D Fund was operationalized at the COP28. The fund is highly criticized due to the involvement of the World Bank and the composition of the Fund's board only allowing for national representatives (Gibson, 2023). Loss and damage are highly debated concepts within the international politics of climate mitigation (Chiba & Prabhakar, 2017). Consequently, no official definition from the WIM has yet been universally agreed on. In line with previous research on L&D in high-mountain regions, here L&D is defined as a “mechanism of international climate policy that tries to evaluate and reduce negative consequences of climate change for societies” (Motschmann et al., 2020, p.837). L&D focuses on the negative impacts of climate change that cannot be mitigated or adapted (Boyd et al., 2021). More precisely, loss refers to the irrevocable destruction of tangible and intangible objects provoked by climate change, such as loss of lives or ecosystems, or crop failure (Huggel et al., 2018). Damage refers to objects that have not been entirely destroyed by climate change yet. This can for instance be increased vulnerability or disruption of social order (Huggel et al., 2018). L&D therefore inherently recognizes both the impacts of climate change and its structural causes. By assessing impacts, L&D raises the question of compensation and support to affected regions. L&D is therefore also tightly connected to climate justice.

In this work, L&D is being assessed through the framework provided by Huggel et al. (Table 1) (2018). More precisely, L&D to economic productivity through agricultural revenue will be assessed. Damage to and loss of natural resources will be investigated through water shortages. Damage to people and assets, as well as possible loss of lives will be looked at through impacts of GLOFs in terms of number of buildings, agricultural land and people affected.

Table 1. Table showing categorization of L&D originating from cryosphere impacts (Huggel et al., 2018). It is possible that one impact falls into many categories.

Categories of Loss and Damage (L&D)	Examples of L&D
Cultural loss and damage	Cultural and lifestyle changes
Loss of and damage to livelihoods	Shift away from traditional livelihoods
Loss and damage to productivity and revenue	Loss of income, reduced agricultural productivity
Damage to and loss of natural resources	Reduced water access, availability, and
Loss of lives	Loss of human lives
Loss of security and social order	Conflict over water access
Damage to people and assets	Physical damage from cryosphere related

3.5 Integrated Assessments of GLOFs and Water availability

The lack of a clear internationally recognized definition of L&D has also led to the absence of a clear L&D assessment method (Bahinipati & Gupta, 2022). L&D assessment have focused on tangible economic impacts, while paying lesser attention to non-economic impacts (Markantonis et al., 2012; Chiba & Prahakar, 2017; Bahinipati & Gupta, 2022). Rapid-onset events have been paid more attention through post-disaster need assessments (Singh et al., 2021; Bahinipati & Gupta, 2022). L&D of slow-onset events such as drought, have been investigated, yet often with a focus on rural areas and with little consideration for urban impacts of water shortages (Singh et al., 2021). The complexity, interconnectedness and vastness of L&Ds make comprehensive assessments challenging (Westoby et al., 2022).

Motschmann et al. have carried out a combined analysis of water scarcity and GLOFs in the Quillcay catchment through the lens of exposure, probability of occurrence and overall resulting risks (Figure 13) (2020). Beyond permitting a better understanding of differences between these risks, Motschmann’s et al. combined analysis also shows possible scenarios of risk evolution depending on the management actions undertaken (2020). The two risks have distinct characteristics and are assessed using different methods and involving different metrics. This is because while water scarcity is a slow-onset process, GLOFs are sudden-onset processes (Motschmann et al., 2020b). With the proposed framework, both risks’ exposure and probability of occurrence can be compared under different scenarios.

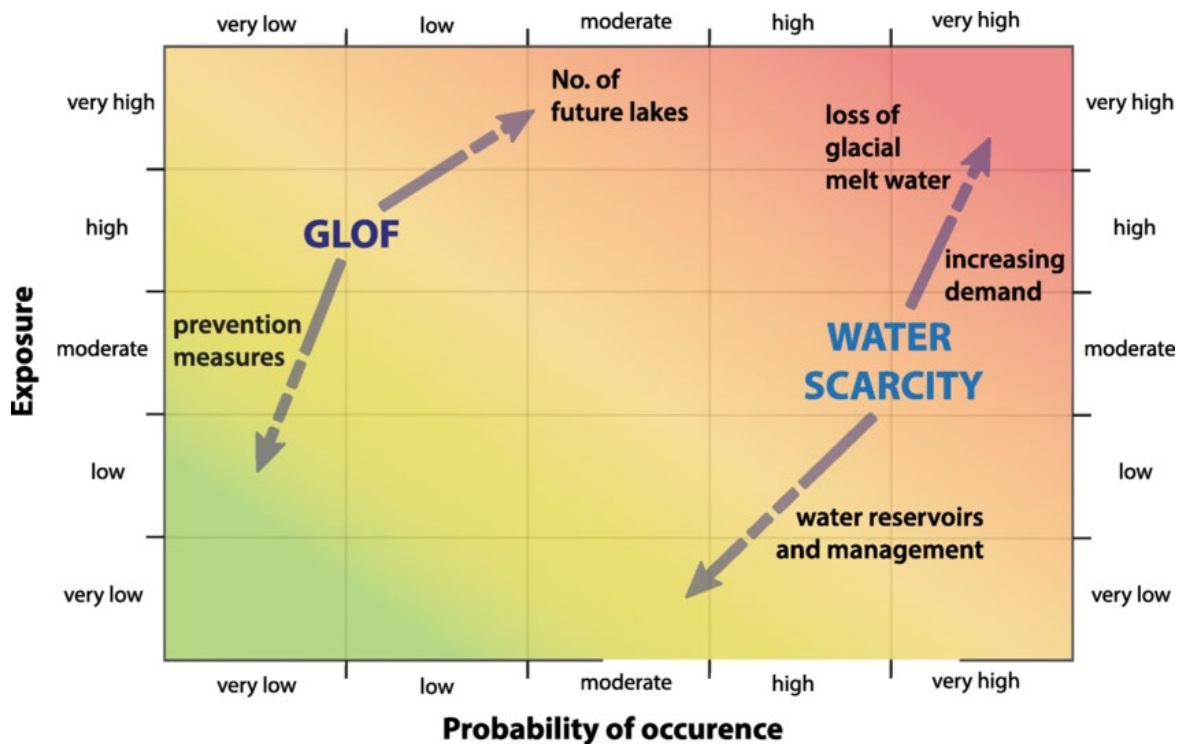


Figure 13. Matrix that compares probability of occurrence and exposure for GLOF and water scarcity. Arrows indicate future tendencies due to named processes (Retrieved from Motschmann et al., 2020b)

Water security indicators are another option for co-assessing water availability and GLOFs. Grey & Sadoff open the way for a joint assessment of GLOFs and water availability by proposing an integrative definition of water security (2007). There, water security is defined as “the availability of an acceptable quantity and quality of water for health, livelihoods, ecosystems and production, coupled with an acceptable level of water-related risks to people, environments and economies”

(Grey & Sadoff, 2007, p. 569). Water is understood as both a necessary resource and a potentially destructive element. Grey & Sadoff explain that countries can, through investments in water institutions and infrastructures, reach water security and make water become an increasingly positive contributor to growth (Grey & Sadoff, 2007).

Another way to perform inclusive assessment of both water availability and GLOFs is to look at cascading L&D. Interconnectedness between L&D through cascading losses have been investigated by Westoby et al. (2022). Although not specific to water availability and GLOFs in high-mountain environment and focusing on non-economic L&D (NELD), Westoby et al. demonstrate that L&D can generate or worsen other types of L&D. This underlines the necessity to assess L&D in a comprehensive way and questions the traditional approach to separated and independent L&D assessments. A research gap remains in evaluating cascading effects of L&D in high-mountain environments.

Methods

This research attempts a comprehensive co-assessment of L&D connected to changes in water availability and GLOFs in the Quillcay catchment until 2050 (Figure 14). Changes in water availability are investigated through simulations from hydrological modelling. Domestic and agricultural demands are estimated from local reports. Future estimations of variables connected to socio-economic developments originate either from local reports or from the SSP literature. Impacts of water availability on agriculture is assessed in financial terms, while impact on domestic consumption is expressed through potential water shortages. Impacts of GLOFs are assessed through spatial analysis of hazard zones. In the city of Huaraz, hazard zones permit to quantify the number of buildings and people affected by floods. In the rural areas, the Normalized Difference Vegetation Index (NDVI) in combination with hazard zones permit to assess the distribution and extent of agricultural areas affected by floods. A descriptive investigation of the relationship between socio-economic drivers and the assessed L&D is led.

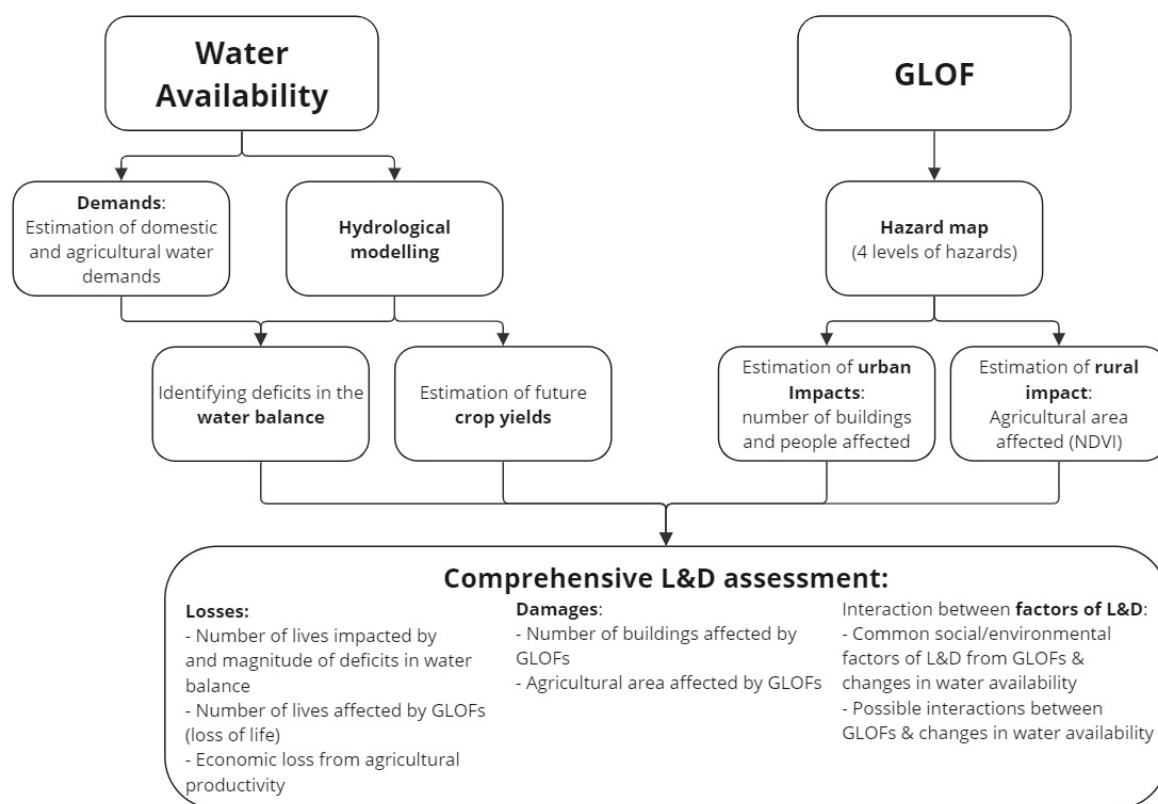


Figure 14. General scheme of the research's method.

4.1 Hydrological Simulations

The hydrological simulations rely on the HBV modelling software. Inputs are PISCO meteorological data and glacier extents from satellite imagery. HBV produces a calibration which can be applied to Global Circulation Models through SSP datasets to simulate future discharges (Figure 15). With future discharges, a comparison with water demands and crop yields permit to identify potential water shortages and quantify loss of agricultural revenue.

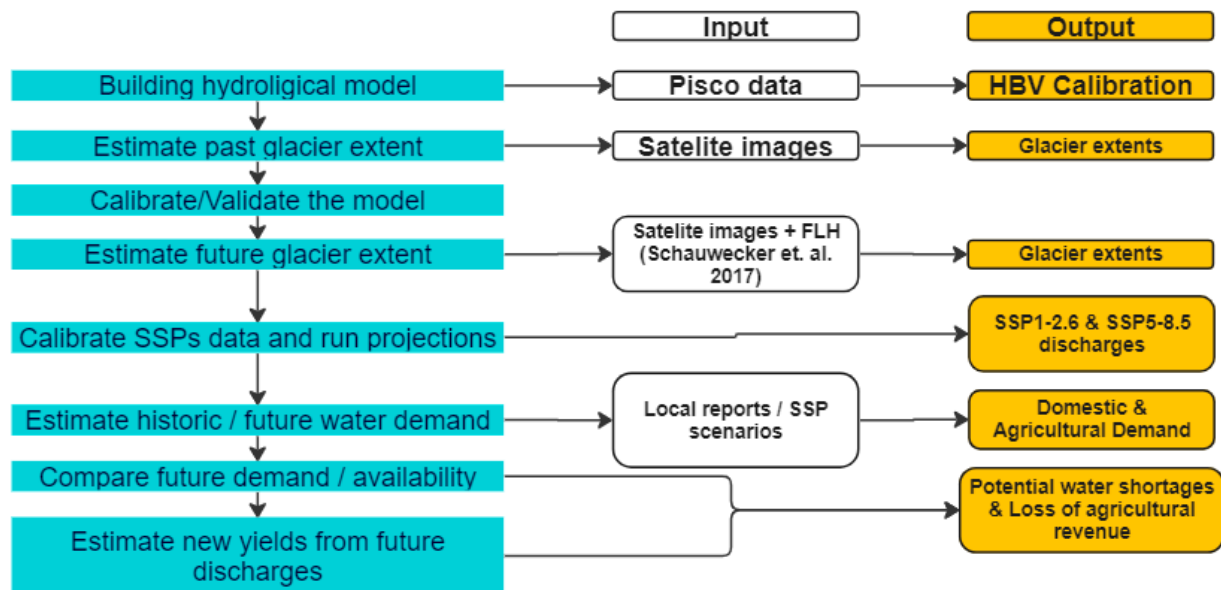


Figure 15. Design of the hydrological modelling method.

4.1.1 The HBV Model

The HBV model is a Swedish hydrological model used since the early 1970's. Since then, it has been widely used by the Swedish Meteorological and Hydrological Institute (SMHI) and has been applied in many studies in more than 30 countries (Seibert, 2005; Konz et al., 2010). HBV is particularly adapted to glacierized catchments as it is composed of a snow, soil moisture, response routine and routing routine. In HBV, the catchment is represented by a set of up to 20 different altitude bands. Each band can be attributed to a vegetation zone or can represent a glacierized area. Bands are weighted in accordance with the percentage of the catchment they represent. HBV requires few input variables; precipitation, average temperature, potential evapotranspiration, and observed discharge.

To simulate topographic differences, precipitation and temperature are distributed according to pre-established height increment variables (PCALT & TCALT) (Figure 16). Precipitation then supplies the snow routine which is set according to the TT, CFMAX, SFCF, CWH and CFR parameters. The resulting rainfall, snow and ice melt supply the soil routine designed by the FC, LP and BETA parameters. As for the snow routine, each elevation band will produce its own output. The saturated upper zone and saturated lower zone are directly dependent on the outputs of the soil routine. Together they are part of the response function relying on the PERC, UZL, K0, K1 and K2 parameters. In addition, the routing routine distributes the runoff between time steps. It relies on the MAXBAS parameters which is used as the base for an equilateral triangular weighting function (Seibert, 2005).

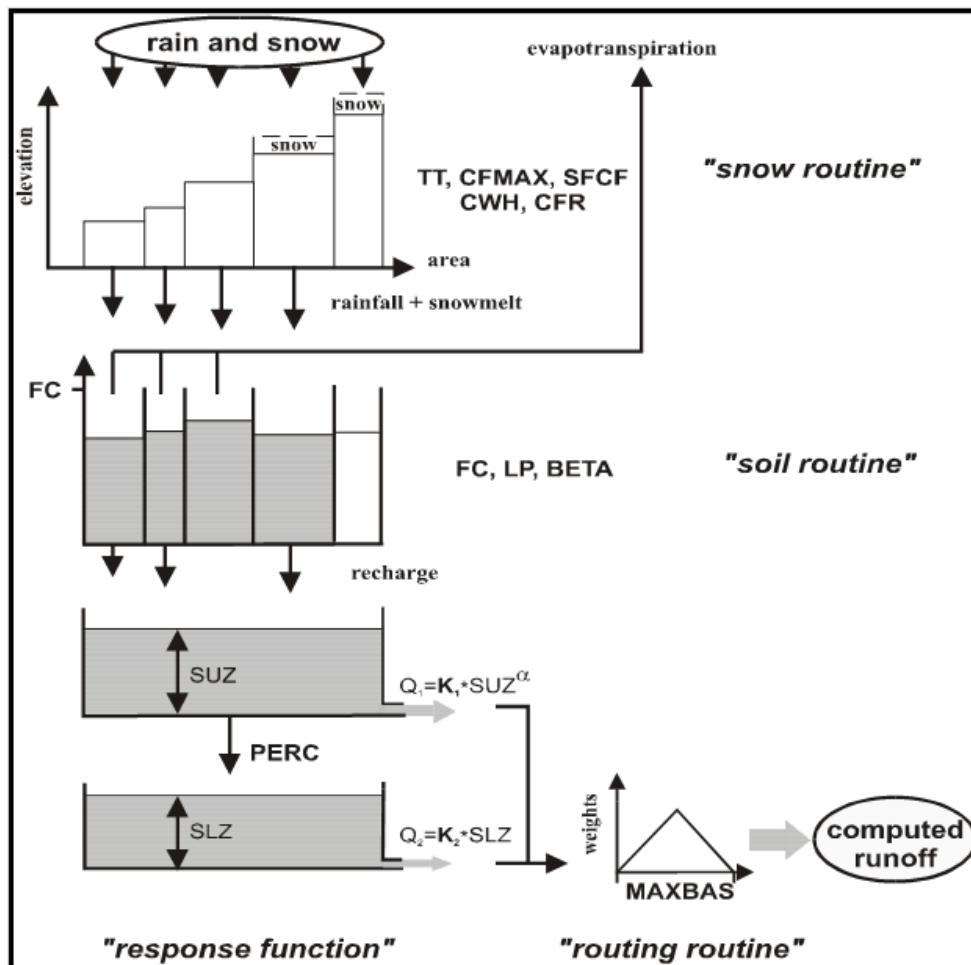


Figure 16. The HBV model (Retrieved from Seibert, 2005).

4.1.2 Reference period simulations

HBV will produce a calibration specific to a catchment which can be used to run future simulation. This calibration is based on a record of observed discharge and a set of meteorological data. HBV simulates discharge based on the meteorological data provided. A comparison between simulated data and observed discharge permits to select the model calibration. To account for glacier retreat, glacier extents must be represented within altitudinal bands.

Input data

The model relies on a historical time series (1981-2015) that is further referenced to as the reference period. This period corresponds to the available data for the Quillcay catchment in the Peruvian Interpolated data of the SENAMHI's Climatological and Hydrological Observations (PISCO) (Aybar et al., 2020). PISCO provides a 0.1° (~10 km) spatial resolution on a monthly timescale (Aybar et al., 2020; Motschmann, 2021). The PISCO dataset has been widely used for climatic and hydrological studies in Peru (Meier, 2021; Motschmann, 2021). Precipitation, streamflow, and maximum and minimum temperature were retrieved from the PISCO dataset for the cells overlapping the Quillcay catchment. As the cells do not perfectly match the catchment's boundaries, a weighted mean was attributed to each cell value depending on their overlap with the catchment (Meier, 2016). Discharge values were then compared with observation from in-situ measurements at the Quillcay station (Quesquén, 2008). Bearing in mind that local measurements could show lower values due to water intakes along the stream, the v1p1 PISCO version was selected as the best fit. The potential evapotranspiration values (ETP) were calculated with the ET0 software from the FAO (2012). The ET0 software uses station characteristics and a minimum and maximum temperature file as input. Station characteristics include location attributes such as coordinates, altitude, proximity with coast, and climatic attributes as general climate and presence of wind (FAO, 2012).

Glacier extents

The major role of glaciers in the hydrological system of the Quillcay catchment and the fast climatic changes in the last decades make it crucial to accurately determine glacier extents for hydrological modeling (Motschmann et al., 2020). Glacier extents were estimated by choosing a representative year for every decade. The years were chosen based on data availability and equal time lapse between each observation. The land cover classification from the ANA maps the glacier extents of both debris

free and debris covered glaciers in the Cordillera Blanca (2016). This classification is based on a Normalized Difference Snow Index (NDSI) from Sentinel-2 images for debris free glacier detection and on a visual assessment of Google Earth satellite imagery for debris covered glaciers. Glacier extents for the years 2008 and 1998 were derived from GLIMS (Raup et al., 2007). GLIMS relies on both automated and manual techniques for glacier extent mapping and have been widely used in determining glacier extents in previous research (Racoviteanu et al., 2008; Cogley et al., 2015; Seier, 2021). Glacier extent for the year 1988 was derived from a visual assessment comparing NDSI and composite band images from landsat-5. The snow cover resulting from the NDSI calculation was faulty due the shadow effect in steep slope areas. A visual comparison with bands showing high reflectivity to ice and snow bodies, such as the blue band, permitted to manually determine the 1988 glacier extent.

Elevation Bands

In HBV, changes in altitude are represented by a maximum of 20 elevation bands. The catchment settings require both the average elevation and the elevation band's weights as inputs. To ensure an accurate representation of elevation changes, 20 elevation bands were created with careful consideration given to effectively represent the areas surrounding glacier tongues. This is important because the proportion of glacier cover on these specific bands changes over time as glaciers retreat. The 20 bands are divided into three categories. The first seven bands cover the area between 3007 and 4400 m.a.s.l., with about 200m elevation gain between each band. The percentage of catchment cover value for these bands do not change over time as glacier are retreating to higher elevations. The second set, band 8 to band 15, covers the rest of the catchment up to 6173 m. a.s.l. yet only represents the non-glacier covered areas. Band 8 to 13 have an elevation gain of 100m each to accurately represent glacier retreat. The last 5 bands, band 16 to ban 20 represent the glaciated areas.

Calibration method

The first two years of the reference period, 1981 and 1982, were dedicated to the model warm-up. A genetic algorithm calibration (GAP calibration) was then performed with value ranges (Appendix II). In HBV, the calibration is made by manual try and error technique (Seibert, 2005). A visual analysis of match between simulated and observed discharge permitted to reject or validate calibrations. The amount of simulated water in the soil box as well as the glacier meltwater content in the streamflow were used to choose a calibration. As recommended by the HBV helper's manual, the model's behaviour under a calibration was observed for a period of up to 10 years (Seibert, 2005). During

this period, a variety of hydrological events such as seasonal droughts and high-precipitation events occurred. If a calibration passed these first assessments, it is then tested on the next decades characterized by their own glacier extents.

4.2.3 Simulation of future discharges

In order to run future hydrological simulations, a Global Circulation Model (GCM) needs to be chosen and calibrated to the reference period data. Then, HBV can run simulations with the parameters set by the reference period's calibration based on the newly calibrated GCM data. To account for glacier retreat, future glacier extents need to be reflected in altitude bands for each decade until 2050.

Choice of Global Circulation Model

Discharge projections are based on climate data from the Coupled Model Intercomparison Project Phase 6 (CMIP6) (Riahi et al., 2017). The model choice was based on data availability for SSP1-2.6 and SSP5-8.5 with the variables of maximum and minimum temperature at surface as well as precipitation. Both SSPs must be of the same variant, which represents a combination of settings including realization, initialization number and forcing scenario. Following this selection and based on its use in previous hydrological modelling efforts in the tropical Andes the MIROC6 model was chosen (Motschmann et al., 2020; Meier, 2021). MIROC6 is the 6th version of the Model for Interdisciplinary Research on Climate. It has a spatial resolution of about 1.4°. Compared to the previous 5th version, in MIROC6 the tropical systems and midlatitude atmospheric circulation are improved (Tatebe et al., 2019). Furthermore, MIROC6 has an updated parametrization for sub-grid-scale snow distribution, which is expected to be particularly relevant for hydrological modelling at high altitudes (Tatebe et al., 2019).

Model Calibration

The Multi-variate Bias Correction (MBC) package was used to perform a calibration based on the MIROC6 historical data and the PISCO reference period (Cannon, 2023). The MBC applies three iterative methods of bias correction and selects the most optimal. These three methods are the Pearson correlation, Rank correlation, and the N-dimensional probability density function transform.

The latter can be understood as a multivariate analogue of univariate quantile mapping (Cannon, 2018). In this work, the N-dimensional probability density function transform was selected as the optimal bias correction method. For consistency, ETP was calculated from the bias-corrected MIROC6 temperature projections with the ETO software.

Future Glacier extents

Future glacier extents are the result of a simple extrapolation technique with a constant lapse rate of $0.0065^{\circ}\text{C}/\text{m}$ applied to the freezing line height (FLH) (Schauwecker et al., 2017). Data scarcity, for instance regarding ice thickness, make it difficult to accurately model glacier extents. The HBV software relying more on percentage of ice cover rather than specific location of glaciated area, the constant lapse rate calculated by Schauwecker et al. is sufficient for this study (2017). The FLH is estimated to approximate the equilibrium line altitude (ELA), above which lies more than 75% of the glacier (Rabatel et al., 2013; Schauwecker et al., 2017). By calculating the FLH with the constant lapse rate technique for 2008 and comparing with the observed glacier extent for that year, it was found that 80% of the glacier was above the FLH (Cogley et al., 2015). The same ratio was therefore applied to estimate future glacier extents. When calculating the weight of elevation bands containing glaciers for future glacier extents, it was assumed that glacier retreat will happen gradually from lower altitudes.

4.3 Water demands

Once future discharges have been simulated, future domestic and agricultural demands must be estimated to identify possible water shortages and assess economic loss on agricultural revenue.

4.3.1 Estimation of agricultural demand and impact on revenue

Current agricultural water demand

Agricultural water demand was retrieved from Quesquén's local report (2008). This report has been used for water demand estimations in previous studies (Muñoz, 2017; Motschmann et al., 2020).

Water demands are provided monthly for each irrigation block. The sum of water demands for June, July and August served as a basis for agricultural water demand during the dry season. The report further indicates the monthly area dedicated to 19 different crops in the whole catchment. Information on the spatial distribution of these areas and crops' yield are nonetheless unavailable in the report. However, the water demands indicated in Quesquén's report cannot be considered representative of the total water need for agriculture. First, because agriculture in the Quillcay catchment is partly rain dependent (Drenkhan, 2015). Secondly, irrigation canals in the Quillcay catchment have an efficiency of about 25%, resulting in the estimated water uptake by crops being one fourth of the water demand, with the rest returning to streams (ANA, 2014b).

Estimation of future agricultural water demand

Yield and economic value of each crop were retrieved from the average monthly yield at the department level for Ancash in 2021 (SIEA, 2021). In some cases, such as with wheat, it was possible to validate the economic value indicated by the SIEA (esp. *Sistema Integrado de Estadísticas Agrarias*) with weekly report from the Central Banque of Reserves of Peru (BCRP, 2021). Three crops, namely in Spanish; *capuli* (lat. *Prunus salicifolia*), *kiwicha* (lat. *Amaranthus caudatus*), *tumbo* (lat. *Welwitschia mirabilis*), were not listed in the SIEA report (2021). These crops were attributed to a negligible area and are therefore left out of the agricultural economic loss estimations. Future agricultural production was retrieved from the SSP1 and SSP5 baseline projections for agricultural production for South America (Detlef et al., 2017; Krieglner et al., 2017). Agricultural production was linearly interpolated for each year, permitting to use the yearly growth coefficient to estimate future agricultural water demand in both SSPs. The future agricultural water demand was then used to identify potential water shortages.

Estimation of impact on agricultural revenue

Future yields were extrapolated from the discharge simulated for SSP1-2.6 and SSP5-8. The 2021 average monthly yield from the SIEA 2021 report was attributed to the reference period 2011-2016 discharge average after deduction of the crop water uptake. For some years in the SSP1-2.6 simulation, discharges higher than the 2011-2016 reference average were observed due to very high precipitation in the rainy season. For these years a maximum yield increase of 20% was set. This value was estimated by the author based on the following reasons:

1. An increase in water availability for agriculture has a limited effect, or can even have a negative effect, on crop yield due to soil water over-saturation in case of high-precipitation event.
2. There is no evidence that the current irrigation infrastructure can maximize increased water supply during high-precipitation events, an increase in yield of more than 20% seems unrealistic.
3. Crop yield depends on a multitude of factors unrelated to water availability. A yield increase higher than 20% would require including additional factors.

4.3.2 Estimation of domestic demand and potential water shortages

Population estimation

Domestic water demand was linearly estimated from population growth. For the reference period, population data for the district of Huaraz and Independencia was retrieved from INEI reports from 1993, 2005, 2007 and 2017. The city of Huaraz lies in both districts and contains between 85% and 90% of the districts' population (INEI, 2017). For future estimations, the SSPs population projections for South America were compared to the INEI projections (INEI, 2009; Riahi et al., 2017; Samir & Lutz, 2017). The difference between the SSPs and INEI population projections differed significantly with population increasing from 2016 to 2050 by factors of 1.21 and 1.18 for respectively SSP1-2.6 and SSP5-8.5 at the continental scale against a factor of 1.44 on the national scale according to the INEI (2009). The INEI projection was selected as it originates from the local country. The trade-off of this selection is that population projection becomes unique and does not include differences between SSP1 and SSP5.

Domestic water demand

Water demand per capita per day was retrieved from the 2014 IMACC report and estimated to an average of 210 liters per capita including a 76% efficiency of water distribution systems (MINAM, 2014). When deducing the water lost in the system, this results in about 160 liters per capita, which is higher than previous estimates fixing the domestic demand to about 97 liters per capita per day

(Drenkhan et al., 2019; Motschmann et al., 2020). Furthermore, differences in water consumption amongst socio-economic groups could not be considered due to data scarcity.

Potential water shortages

Due to the absence of reliable source for estimation of evolution of water demand per capita, domestic demand was estimated to stay constant on average until 2050. Projected domestic demand was then retrieved for each year by multiplying the projected population with the domestic demand per capita. The resulting domestic demands were then compared to available water in the dry season to identify any hypothetical water shortages.

4.4 GLOFs simulations

4.4.1 Overview of GLOF modelling

Estimation of GLOF related losses and damages are based on hazard zones defined by Frey et al. (2018). The four hazard levels mapped rely on floods originating from three rock-ice avalanche scenarios of small, medium, and large size colliding with the Palcacocha, Cuchillacocha, and Tullparaju lakes. Whereas three hazard levels are resulting from the flood simulation from these avalanche scenarios, a fourth low-probability yet high potential impact level based on a moraine breach from Palcacocha lake was added. Intensity maps were created from the flow height distribution, which when connected to probability of occurrence resulted in a multi-source hazard map (Frey et al., 2018). The results from Frey's et al. study have been used by local authorities for hazard mitigation and were widely shared with the local population (2018). With retreating glaciers and permafrost thaw due to climate change, high-mountain landscapes become increasingly unstable (Mark et al., 2017; Frey et al., 2018; Huggel et al., 2018). Rock/ice avalanches seem to be the most likely cause of GLOFs in Quillcay, which makes Frey's et al. approach to flood modelling highly relevant when tackling climate change related L&D in the Quillcay catchment.

4.4.2 Estimation of damage within the city of Huaraz

The GLOFs damage assessment in Huaraz includes Huaraz's administrative neighbourhoods yet excludes the peri-urban area extending towards agricultural fields further up in the catchment or along the Rio Santa's shores. Damage is looked at through the number of buildings within flood hazard zones and number of people affected by floods (Motschmann et al., 2020). Frey's et al. hazard zones are used to determine the extent of flood damage (2018). The spatial distribution of buildings is derived from the Open Buildings Polygon V3 dataset (Sirko et al., 2021). This dataset is the result of an optimized object detection algorithm based on 50 cm high resolution sensors such as Sentinel-2. Part of the purpose for creating this dataset was to contribute to humanitarian response efforts and to minimize the risk of flooding (Sirko et al., 2021). Buildings are classified into three confidence intervals, level 1 (0.75 to 1), level 2 (0.7 to 0.75), level 3 (0.65 to 0.7) (Figure 17). Comparison of confidence level with local expert observations permitted to validate level 1 and 2 for mapping buildings in Huaraz.

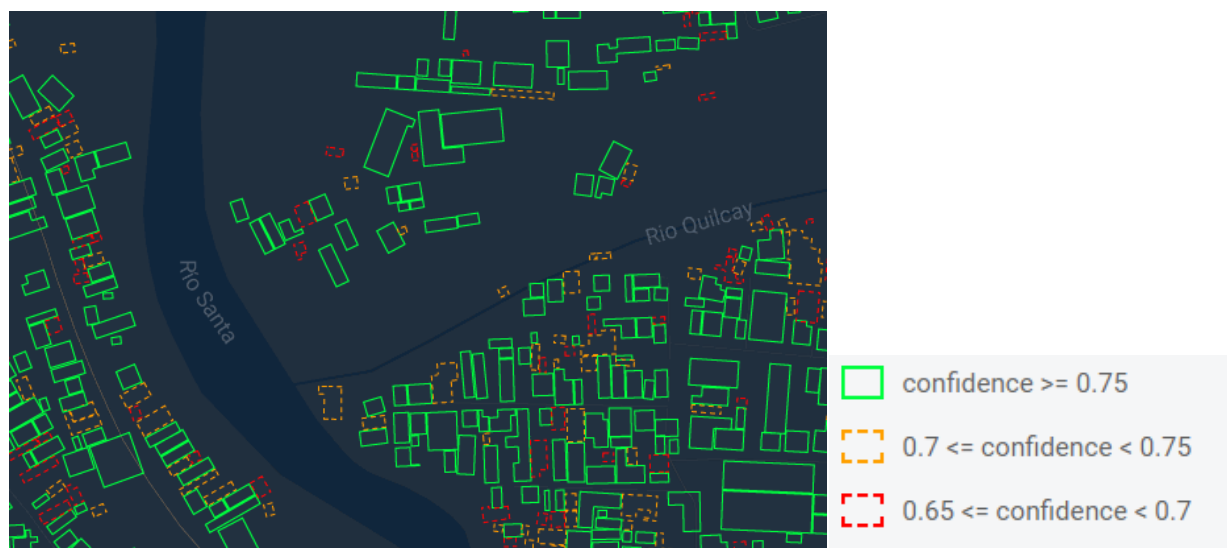


Figure 17. Example of Open Building V3 polygons and confidence intervals at the confluence of Rio Quilcay and Rio Santa in Huaraz.

The number of people affected by floods is directly derived from the number of buildings affected. As the Open Building V3 dataset does not contain information on the building type, an extrapolation was made from the average number of inhabitants per households. The city of Huaraz spreads over the districts of Huaraz and Independencia which are characterized by an average of respectively 3.7 and 3.5 inhabitant per household (ESRI & MBR, 2021). An overall average of 3.6 inhabitant per household

was estimated for the whole city. All buildings were estimated to represent 3.6 inhabitants independently from their size. Height information about buildings could not be found. To test the reliability of this approach, population estimations based on the 3.6 inhabitant per building extrapolation are compared with population data on the quarter (esp. *Manzana*) level (INEI, 2017). Using the building extrapolation approach permits a higher spatial resolution of GLOF impact assessment. Population census at the quarter level typically encompasses large groups of buildings which may intersect the hazard zones' boundaries, making it difficult to accurately estimate the number of people within hazard zones. The spatial division between socio-economic groups and the subsequent differences of population density was tackled by selecting buildings within a 200m buffer of the Quillcay river. It is estimated that the 200m buffer contains an area of higher population density due to higher buildings. This area has seen a rapid population growth in the last two decades (Huggel et al., 2020b). When calculating the number of people affected, the average of 3.6 inhabitant per building in the 200m buffer area was multiplied by a population increase factor. This factor corresponds to the yearly population increase of Peru on a national scale from 2021 to 2050 (INEI, 2009).

4.4.3 Estimation of damage in agricultural areas

Estimation of GLOF damage on agricultural land is based on the overlap between hazard zones and areas of healthy vegetation. To locate areas with healthy vegetation, the Normalized Difference Vegetation Index (NDVI) was used (Hänchen et al., 2022). The NDVI relies on multi-spectral satellite imagery. The infra-red and red bands are used to assess vegetation's health through plant reflectance. NDVI results in a single-band product showing vegetation greenness.

$$NDVI = (NIR - R) / (NIR + R)$$

The NDVI calculation was made from a landsat-8 product with 30m resolution acquired on January 28th, 2018. The middle of the rainy season is expected to show the highest agricultural activity. Land cover was categorized according to NDVI values thresholds, with healthy crops and vegetation shown with NDVI higher than 0.3 (Seehaus et al., 2019).

4.5 Framework for co-assessment of changes in water availability and GLOFs

Despite the lack of clear methodologies for L&D co-assessments, it remains important to devise approaches capable of backing up climate risk management (Hagen et al., 2023). Integrated assessments including both slow and rapid onset processes permit a clearer overview of impacts which could serve as a base for flexible risk management. While a gap has been identified in more comprehensive L&D methodology, the importance of developing such approaches has been pointed out by the scientific community (Bahinipati & Gupta, 2022; Hagen et al., 2023). The co-assessment approach proposed in this study is descriptive and consists in exploring potential contributions of co-assessments to L&D evaluation. First, the investigated L&D of changes in water availability and GLOFs are brought together in order to provide a clear overview. With different metrics, including agricultural economic loss due to changes in water availability, as well as number of people, building, and agricultural area affected by GLOFs, this summary permits a better understanding of the evolution of L&Ds until 2050. In a second step, the relationship between socio-environmental drivers—through population increase and glacier retreat—and L&D of changing water availability and GLOFs is sketched (Huggel et al., 2018). Finally, a framework is suggested to explore potential indirect L&D cascading between changes in water availability and GLOFs.

Results

5.1 Glacio-hydrological simulations

5.1.1 Glacier extents

In the reference period, the combination of GLIMS and ANA assessments reveal a reduction of 2.54 km² of glacier surface from 1998 to 2016. The visual analysis from 1988 Landsat-5 imagery fits well in the observed trend of glacier recession in the catchment with 1.45 km² of glacier surface reduction from 1988 to 1998. Ice loss is distributed in low-altitude glaciated areas, especially around glacier tongues connected to glacier lakes (Figure 18).

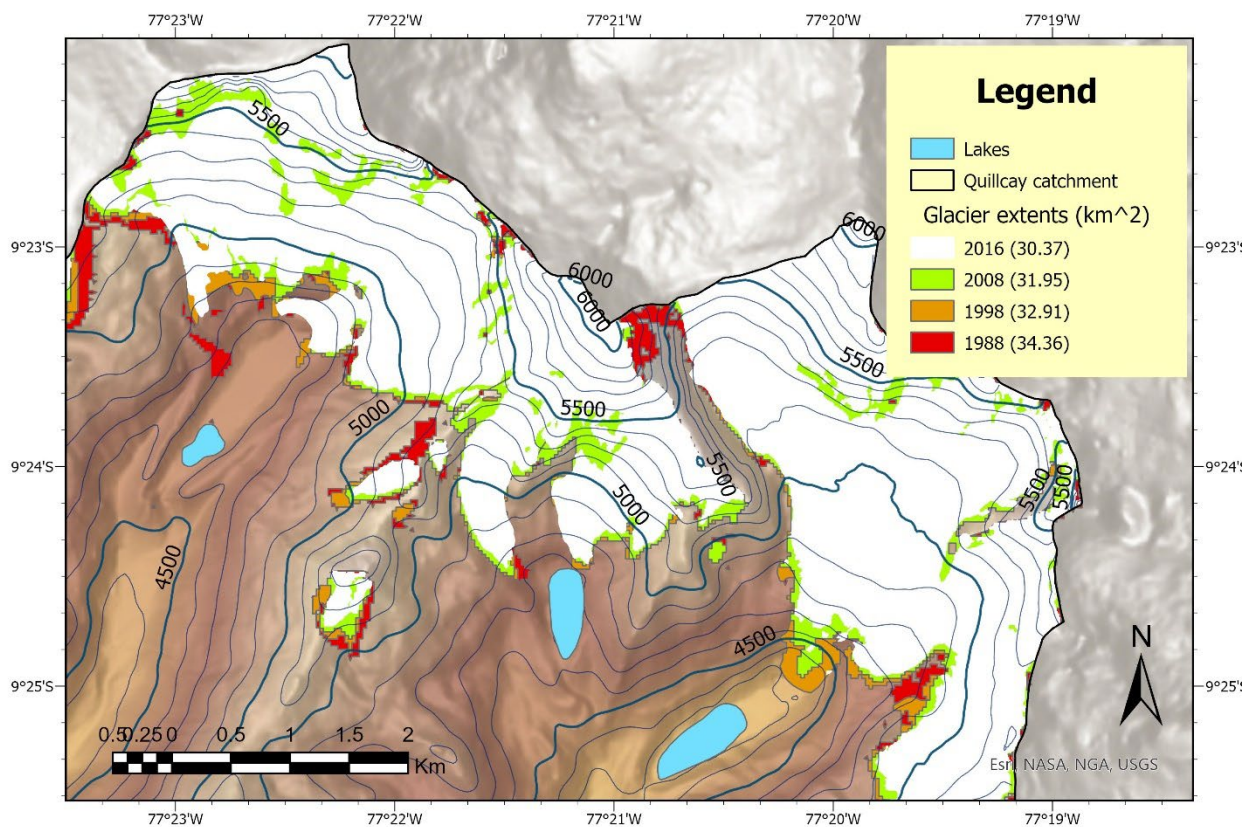


Figure 18. Map of historical glaciers extents from 1988 to 2016. The 1988 glacier extent represents 14.31% of the catchment and was retrieved from visual analysis of Landsat-5 products. The 1998 and 2008 extents correspond to respectively 13.71% and 13.31% of the catchment and were retrieved from GLIMS. The 2016 extent covers 12.65% of the catchment and is retrieved from ANA.

The projections based on the SSP1-2.6 and SSP5-8.5 scenarios result in a continuous, yet nuanced, glacier recession until 2050 (Figure 19). The SSP5-8.5 scenario shows the most severe glacier recession with a loss of 9.76 km² of glacier surface from 2016 to 2015. SSP1-2.6 also projects a reduction of the glacier surface, with a loss of 5.75 km² for the same period. SSP1-2.6 proposes a less linear recession than SSP5-8.5, this is due to a higher variability in annual average temperature projections in SSP1-2.6. Both scenarios indicate a higher rate of ice-melt than in the reference period. There is a 2.43 km² difference between the glacier area estimated from the ELA constant factor projection in 2015 and the observed glacier area by GLIMS in 2016.

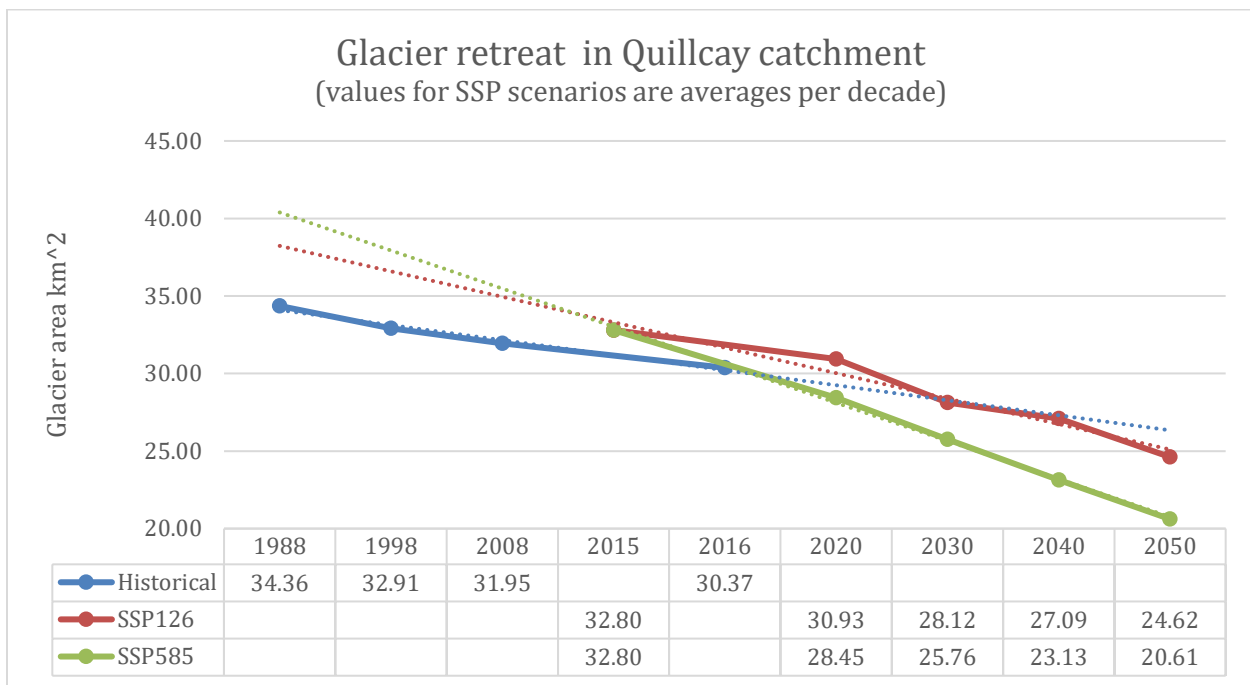


Figure 19. Historical and future glacier extents according to SSPs projections.

5.1.2 Hydrological simulations

In both SSP1-2.6 and SSP5-8.5, simulated discharges present an abnormal pattern in the months of September and October. More specifically, the first discharge peak of the rain season in the reference period, around December, is shifted in both SSPs' projections to September or October. This shift originates from an identical anomaly in the precipitation patterns in both scenarios (Figure 20).

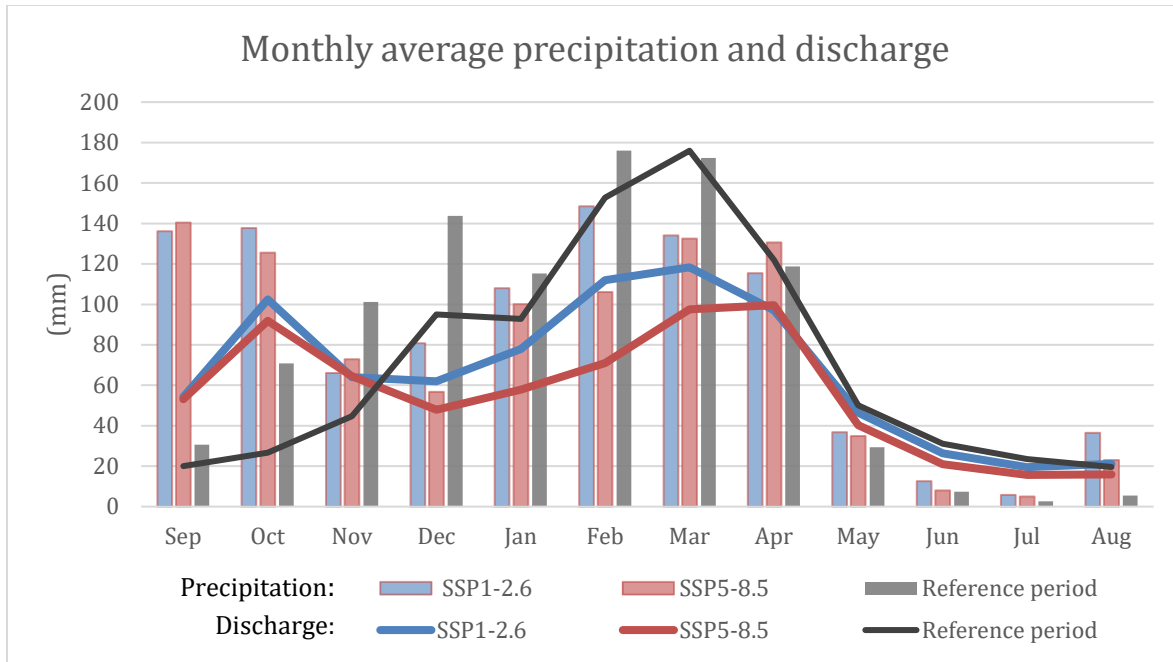


Figure 20. Monthly precipitation compared to discharge during the reference period and for the SSPs' projections.

The one-way ANOVA test applied to the discharges of the reference period (1981-2016) and the SSPs projections on a monthly timescale (2015-2050) reveals a significant difference between the discharges of SSP1-2.6 (Table 2), SSP5-8.5 and the reference period. Post-hoc analysis with the Bonferroni method determined that SSP1-2.6 and the reference period's discharges are not significantly different. However, SSP126 and SSP585, as well as SSP5-8.5 and the reference period show a statistically significant difference in their respective discharges.

Table 2. ANOVA and Post-hoc analysis with the Bonferroni method on the discharges of the reference period and the SSP1-2.6 & SSP5-8.5 projections

Post-hoc test		
Groups	P-value (T test)	Significant ?
SSP585 vs SSP126	0.0009	Yes
SSP126 vs ref. period	0.6392	No
SSP585 vs ref. period	0.0016	Yes

In both scenarios, the dry and the rainy season discharge averages are lesser than in the reference period. SSP1-2.6 shows a higher discharge average in the dry and rainy season than SSP5-8.5 (figure 21 & 22).

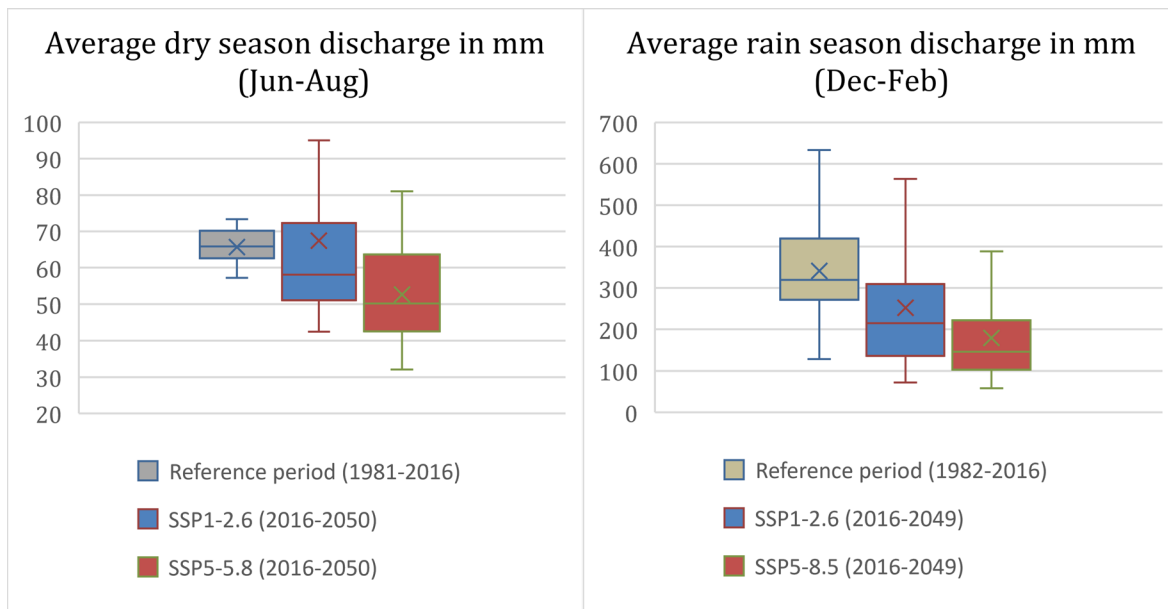


Figure 21 (Left). Average dry season discharge in mm for the reference period and SSPs' projections.
 Figure 22 (Right). Average rain season discharge for the reference period and SSPs' projections. Note that the rain season overlaps between years, therefore the values for 1981 and 2050 were not considered

Compared to the annual 825.7 mm discharge average for the reference period, both scenarios project predominantly lesser yearly discharges. In SSP1-2.6, although some years show annual discharge exceeding the 825.7 average, the overall trend reveals a decrease in yearly cumulated discharge. SSP5-8.5 however, shows an increase in yearly cumulated discharge until 2050. This increase partly originates from a more severe ice-loss in SSP5-8.5 (Figure 23).

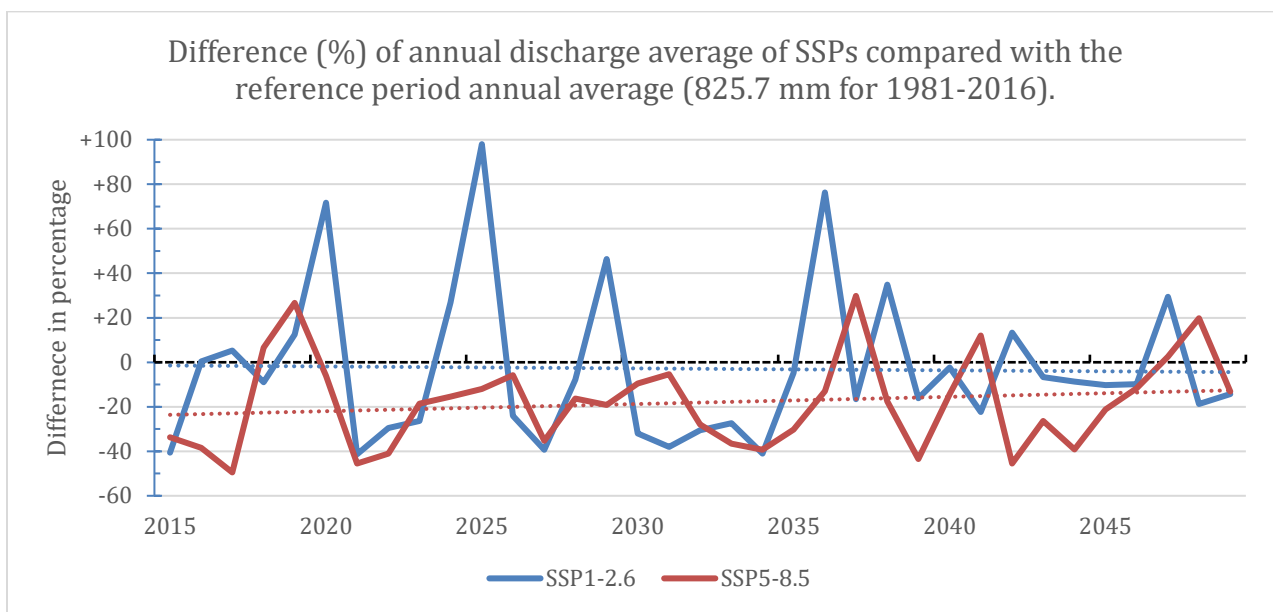


Figure 23. Discharge balance of SSPs' projections compared with the reference period annual average of 825.7 mm for 1981-2016.

The high variability of precipitation in SSP1-2.6 leads to outliers in cumulated discharges in both the dry and rainy season. These are visible for instance in the years 2020, 2025, or 2036. Whereas the reference period doesn't show a clear trend, both SSP projections suggest decreasing dry season discharge until 2050 (Figure 24). The increasing discharge trend for SSP5-8.5 in the rainy season (Figure 25) partly explains the increasing SSP5-8.5 annual discharge trend seen in figure 23.

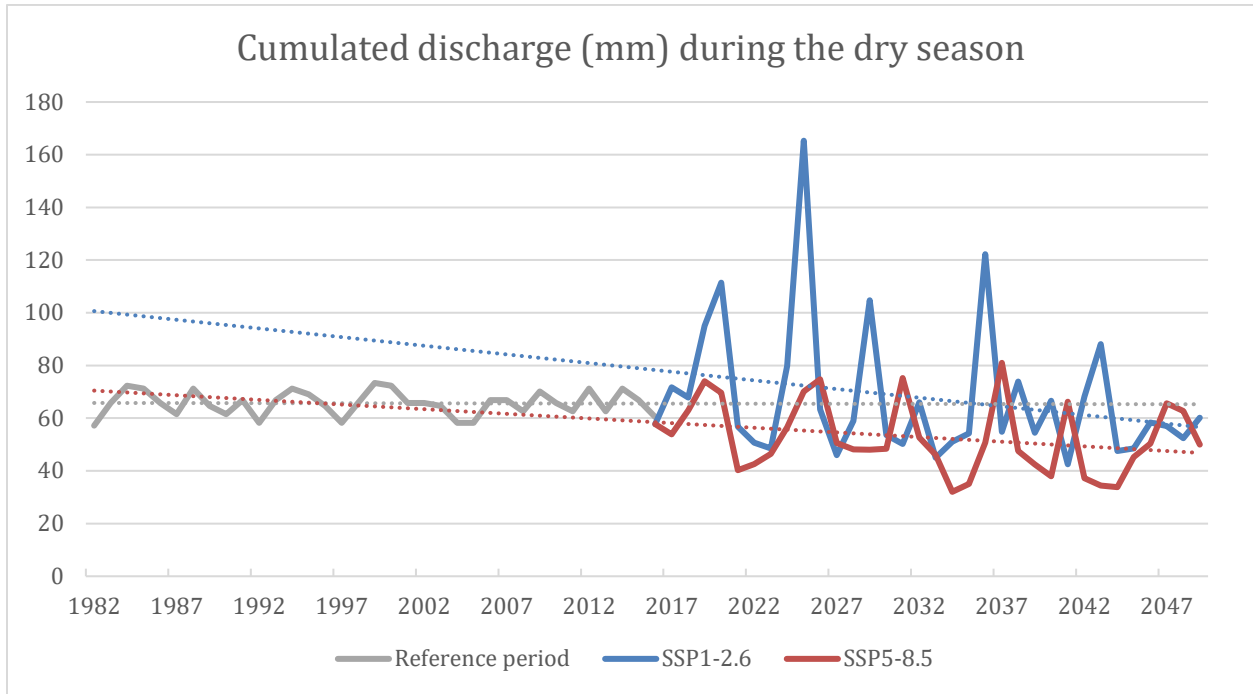


Figure 24. Cumulated discharge during the dry season for the reference period and SSPs' projections.

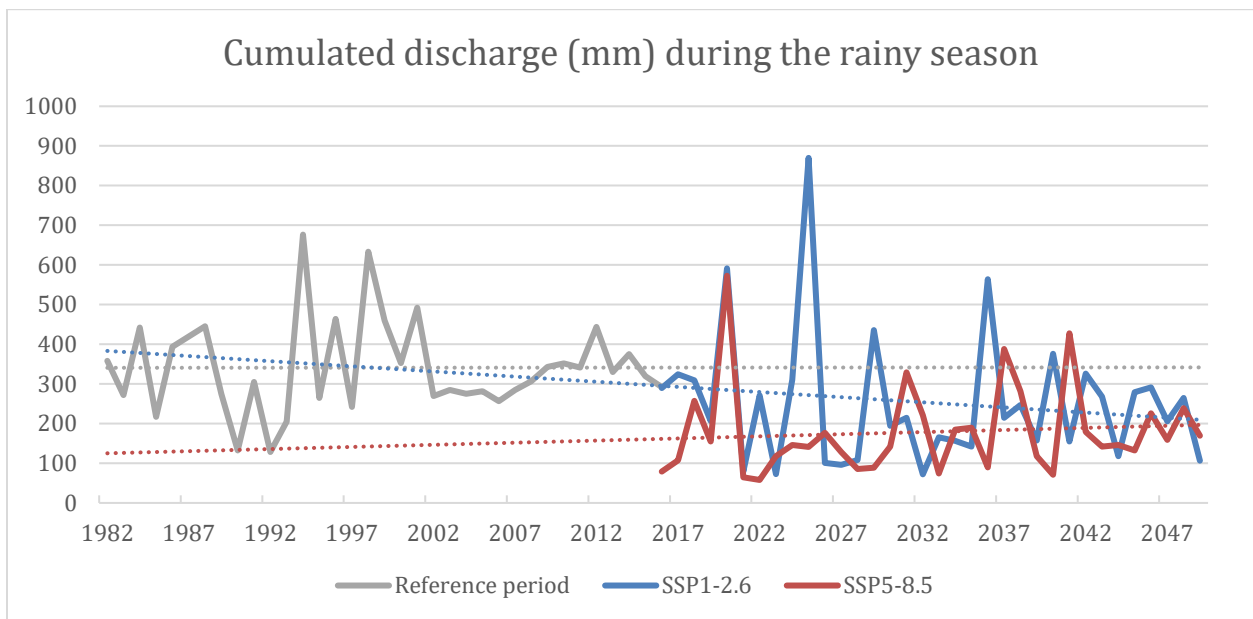


Figure 25. Cumulated discharge during the rainy season for the reference period and SSPs' projections.

In both SSPs' projections, the proportion of water from ice-melt during the dry season decreases until 2050 (Figure 26). The decrease in dry season discharges observed in figure 24 can also be explained by lesser volumes of ice-melt during the dry season until 2050. Here, it is relevant to highlight that despite lesser melt-water contribution in the dry season, higher ice-melt rates are observed until 2050 in figure 19.

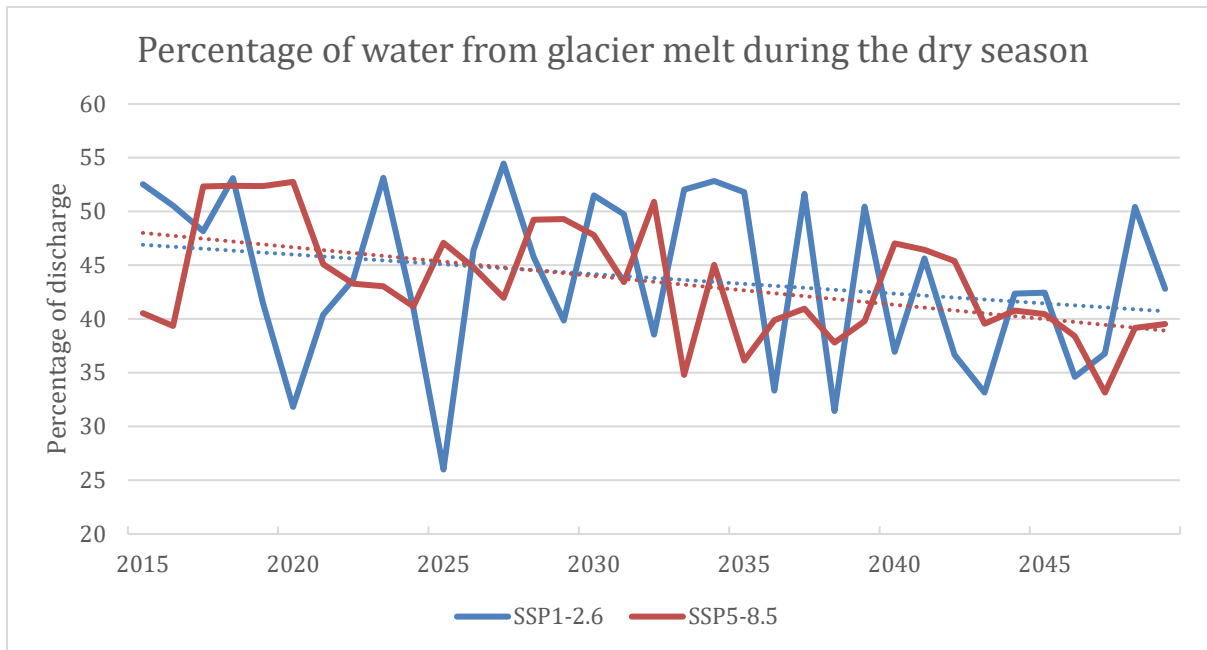


Figure 26. Glacier melt-water content in percentage of the discharge during the dry-season for SSPs' projections.

5.2 Impacts of changing water availability

5.2.1 Impact on water balance

In figure 27, 28, 29 & 30, agricultural and domestic demands accumulate and are then projected over the discharge in order to identify water shortages. The domestic water demand shows the same increase until 2050 for both scenarios because it was estimated from the 2009 report from INEI, independently from SSPs population variables. Corresponding to the agricultural production forecasts in the SSPs scenarios for South America, the estimated water demand for agriculture rises in both SSP1-2.6 and SSP5-8.5. During the dry season, domestic demand remains higher than agricultural demand for both scenarios (Figure 27 & 28). This is due do a constant domestic demand throughout the year and a reduced agricultural demand during the dry season. The results show that discharges are sufficient throughout the whole year to supply the increasing domestic and agricultural demands until 2050.

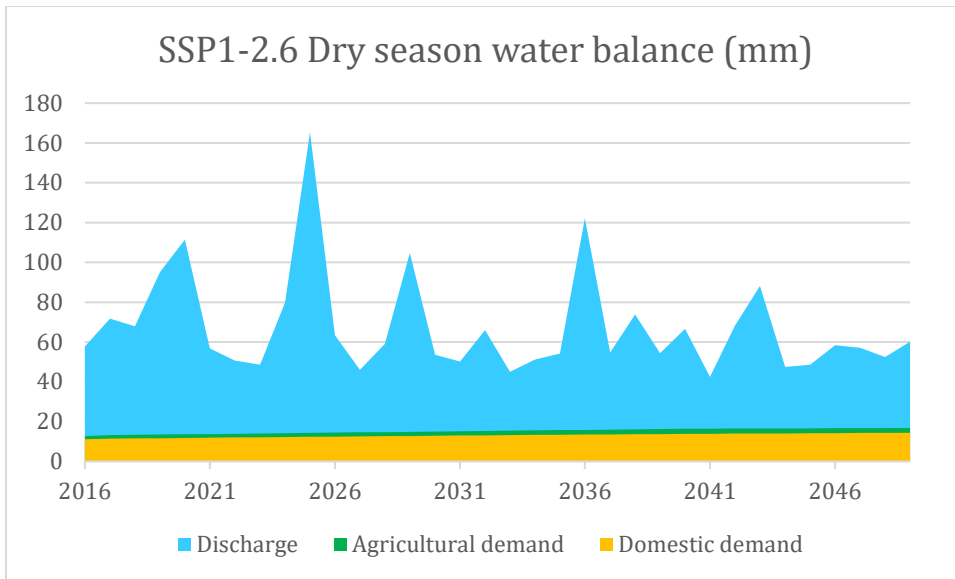


Figure 27. SSP1-2.6 Water balance during the dry season (mm).

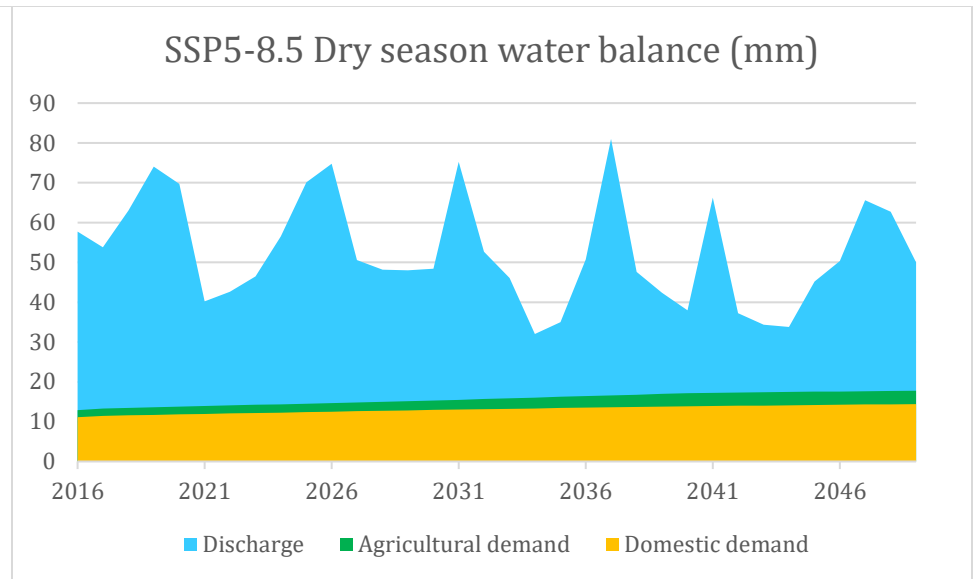


Figure 28. SSP5-8.5 Water balance during the dry season (mm).

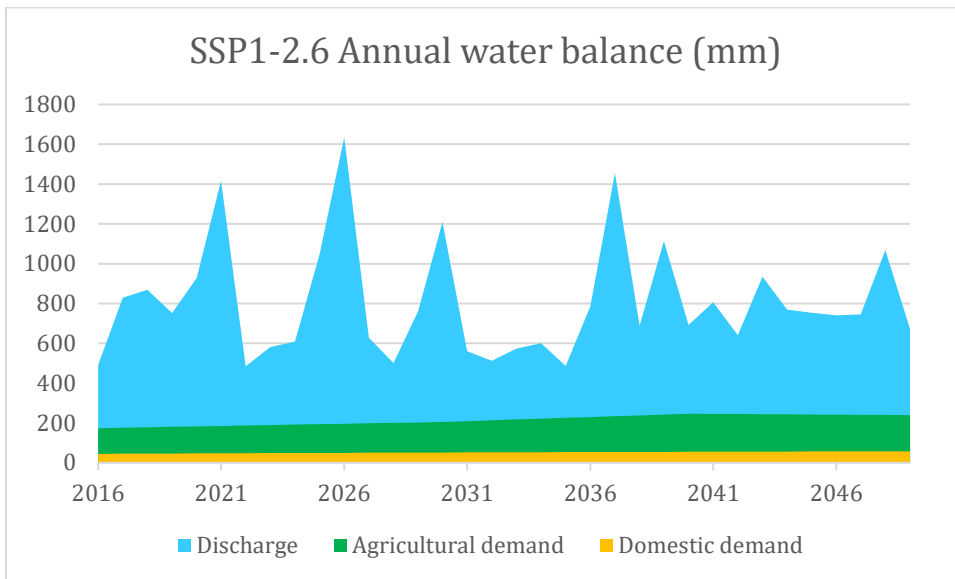


Figure 29. SSP1-2.6 Annual water balance (mm).

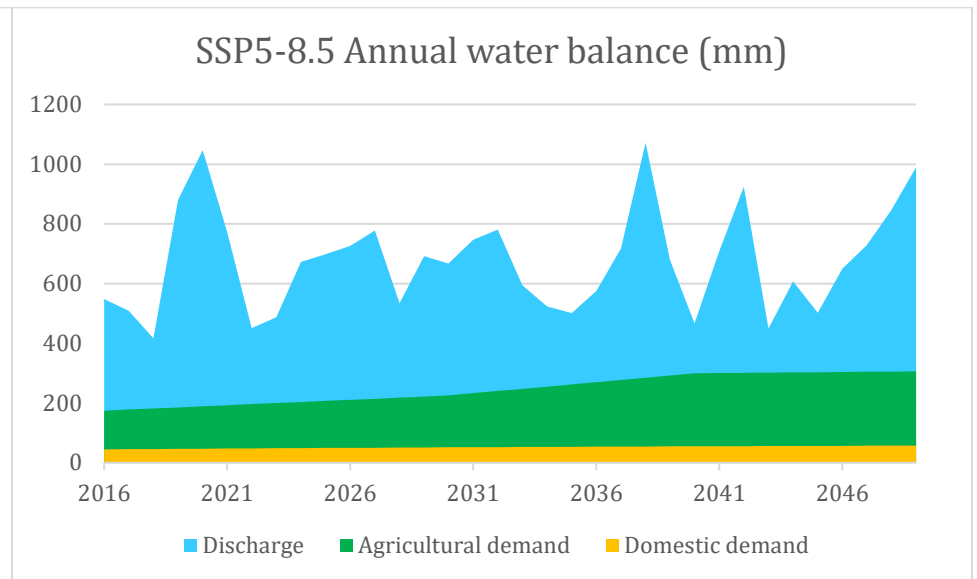


Figure 30. SSP5-8.5 Annual water balance (mm)

5.2.2 Impact on agricultural revenue

SSP1-2.6 depicts an overall diminishing agricultural revenue until 2050 (Figure 31). However, some years show outstanding economic value due to abnormal increase in precipitation. These outstanding values are limited to 120% of the annual revenue reference, due to the set limit on positive impact of water supply on yield. On average, the SSP5-8.5 agricultural revenue is lower than for the SSP1-2.6 scenario. This is due to lower discharges in the SSP5-8.5 scenario. As with the yearly cumulated discharges—to which agricultural revenue is correlated—the agricultural revenue for the SSP5-8.5 scenario shows a slight increase until 2050.

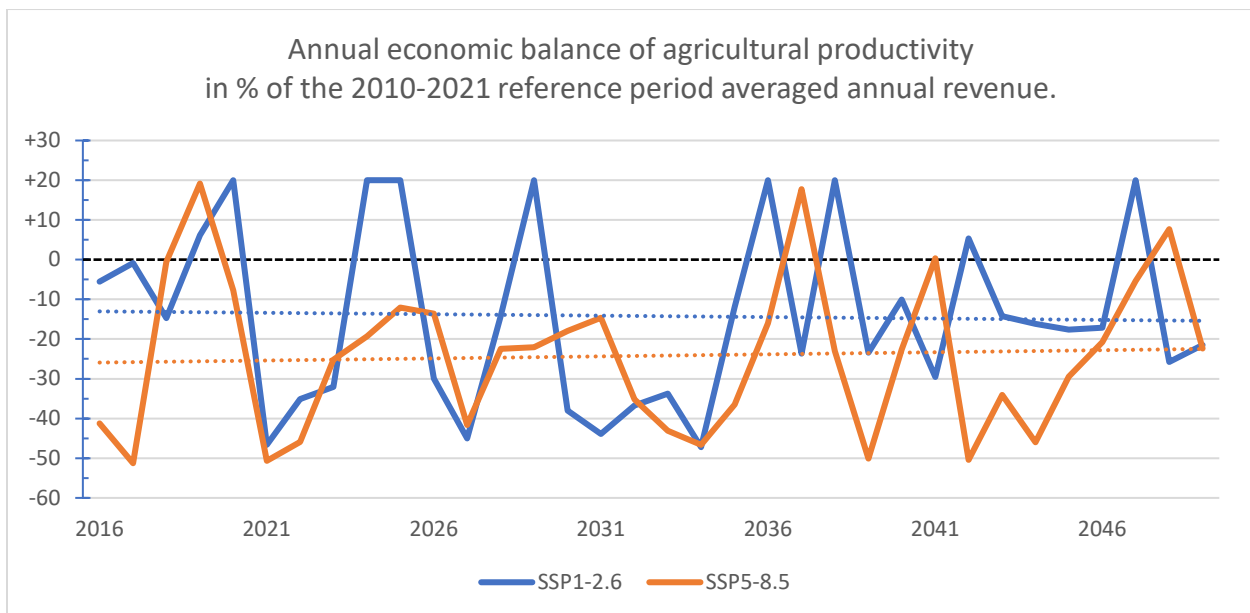


Figure 31. Yearly economic balance of agricultural revenue in percentage of the representative 2010-2021 averaged annual \$38'767'628 revenue. The loss attributed to SSP1-2.6 and SSP5-8.5 from 2016 until 2050 is respectively \$187'372'340 and \$319'054'345.

Patterns of economic balance are similar on the yearly and dry-season scale, with some minor variations due to the subtraction of agricultural demand to discharges when estimating new crop yields (Figure 31 and 32, Appendix V). New yields are the main factor of projected agricultural revenue. Crop yields being derived from future discharges, the resulting balance of agricultural revenue shows similar trends with the yearly cumulated discharges for both scenarios (Figure 23, 31 & 32).

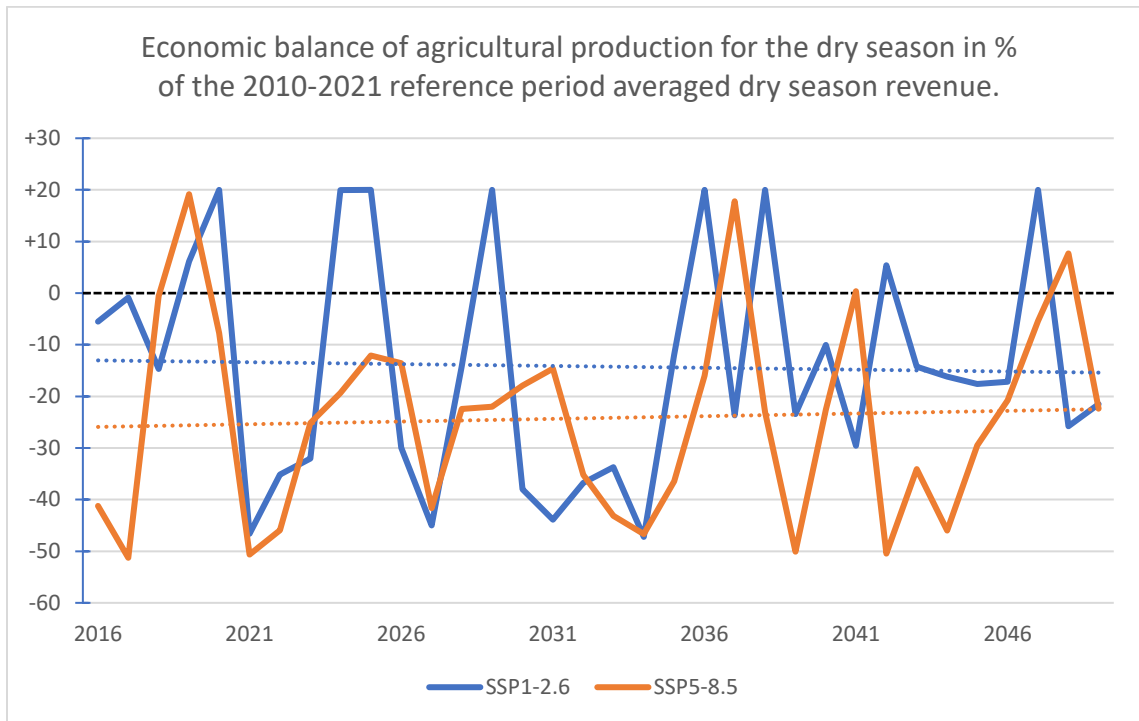


Figure 32. Dry-season economic balance of agricultural revenue in percentage of the representative 2010-2021 averaged yearly value of \$ 3'447'988. The loss attributed to SSP1-2.6 and SSP5-8.5 until 2050 is respectively \$16'665'054 and \$28'376'658.

5.3 Impacts of GLOFs

5.3.1 Impacts within Huaraz

In the city of Huaraz, the 200m buffer zone representing higher population density spans over the very high and high hazard zones (Figure 33). The proportion of buildings within the 200m buffer for each hazard zone decreases with hazard level. The city of Huaraz extends beyond the low hazard zone. Urban sprawling can be anticipated to happen outside of hazard zones. This implies that the number of buildings within hazard zones can be expected to stay constant until 2050.

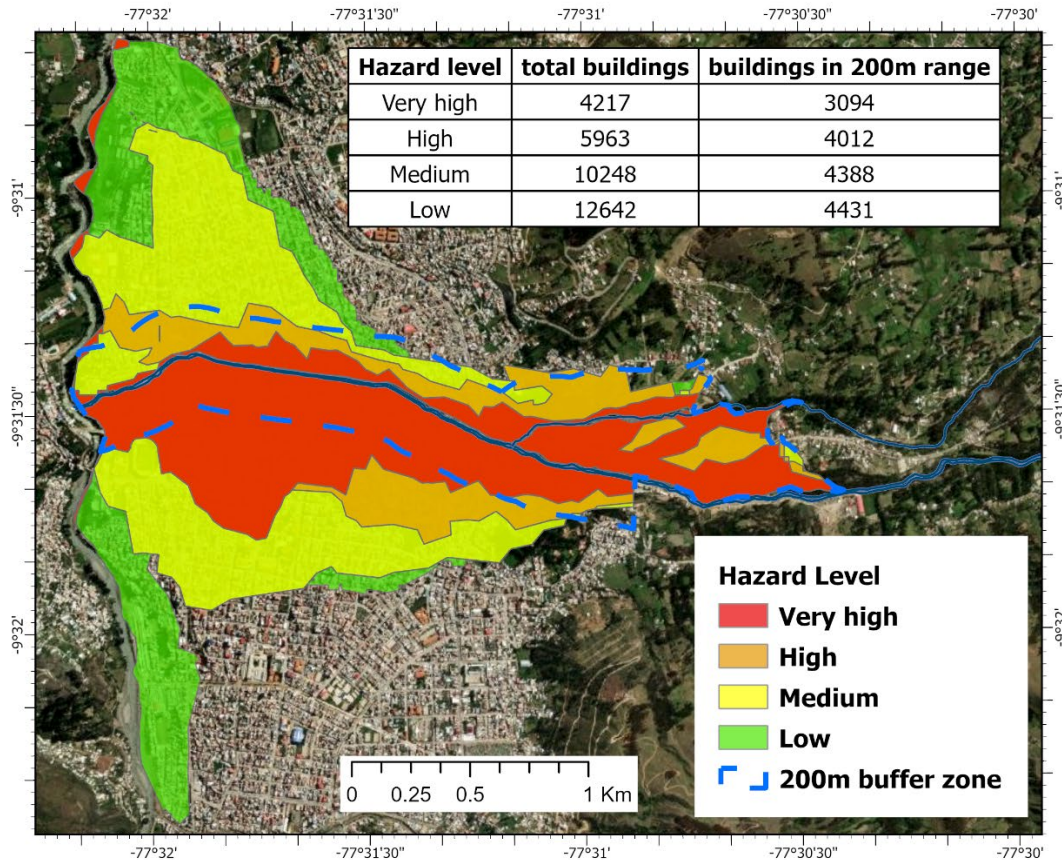


Figure 33. Map of GLOF hazard zones.

As population becomes denser within the 200m buffer, the resulting population within hazard zones increases with time until 2050 (figure 34).

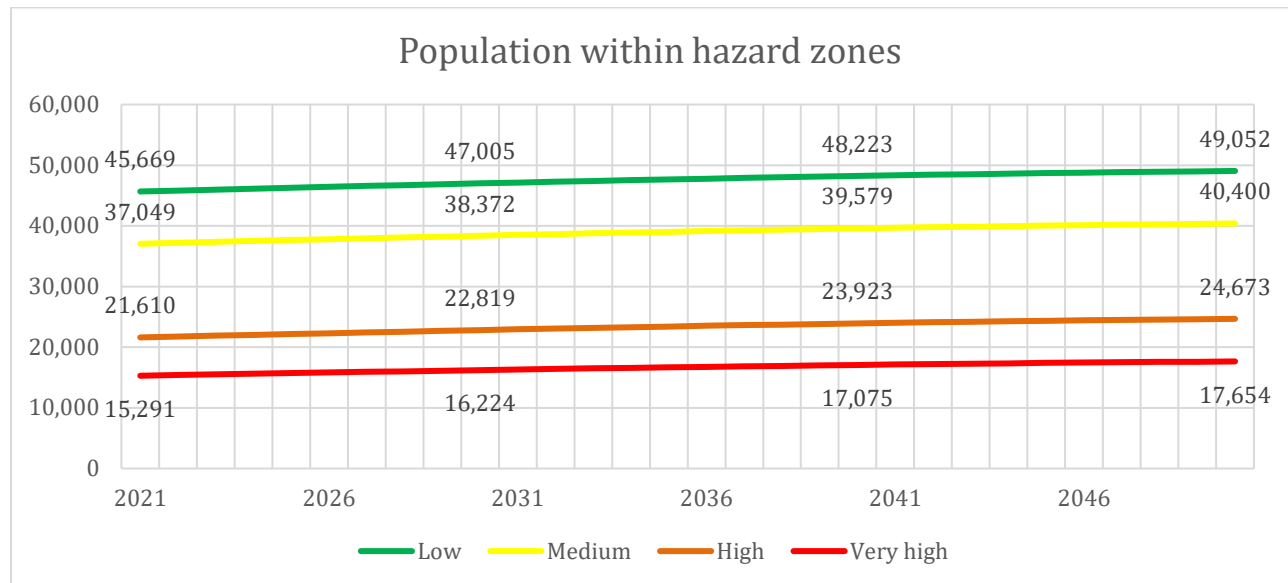


Figure 34. Population within GLOFs hazard zones.

There are differences in population densities obtained by the census at quarter level and the building extrapolation method within hazard zones. Within the 200m buffer zone around the Quilcay river, the population density remains relatively similar in both methods, with 15'457 inh./km² for the building extrapolation method against 15'058 inh./km² for the census. Between the low hazard zone outer limits and the buffer zone, density varies from 18'334 inh./km² with the building extrapolation method to 15'994 inh./km² with the census (Appendix VI).

5.3.2 Impacts on agricultural land

The NDVI reveals that healthy vegetation is located along water bodies (Figure 35). More precisely, high NDVI areas are along rivers or distributed besides irrigation canals. This observation is coherent; cultivated fields are located by agricultural irrigation infrastructures.

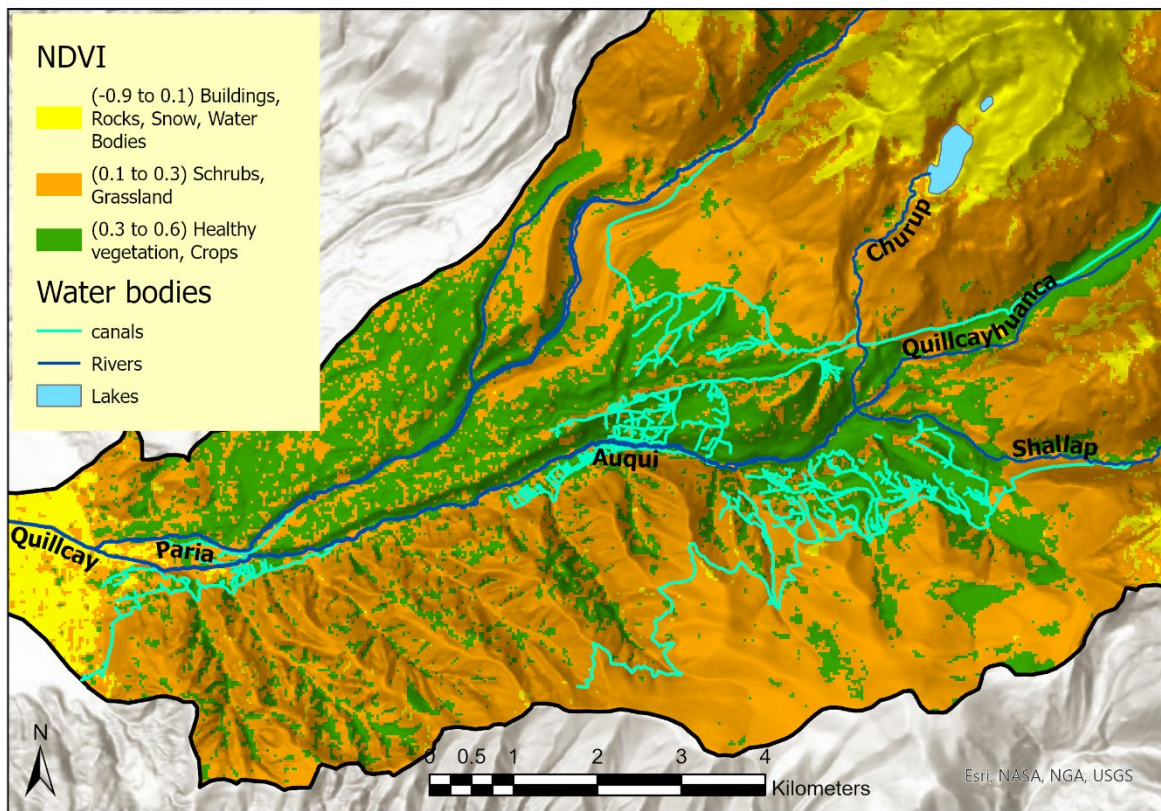


Figure 35. Map of NDVI classification (January 2021).

GLOFs simulations reveal that floods would flow along riverbeds, thus threatening high-NDVI areas (Figure 36; Frey et al., 2018). Smaller irrigation blocks located along river streams such as Nueva Florida, Paquishca and Auqui Tacllan are particularly exposed to floods. On the other hand, bigger irrigation blocks which expend away from the rivers are less affected by GLOFs. Less than 5% of Shallap's high-NDVI area is affected by GLOFs. Churup irrigation block is not affected by any GLOF.

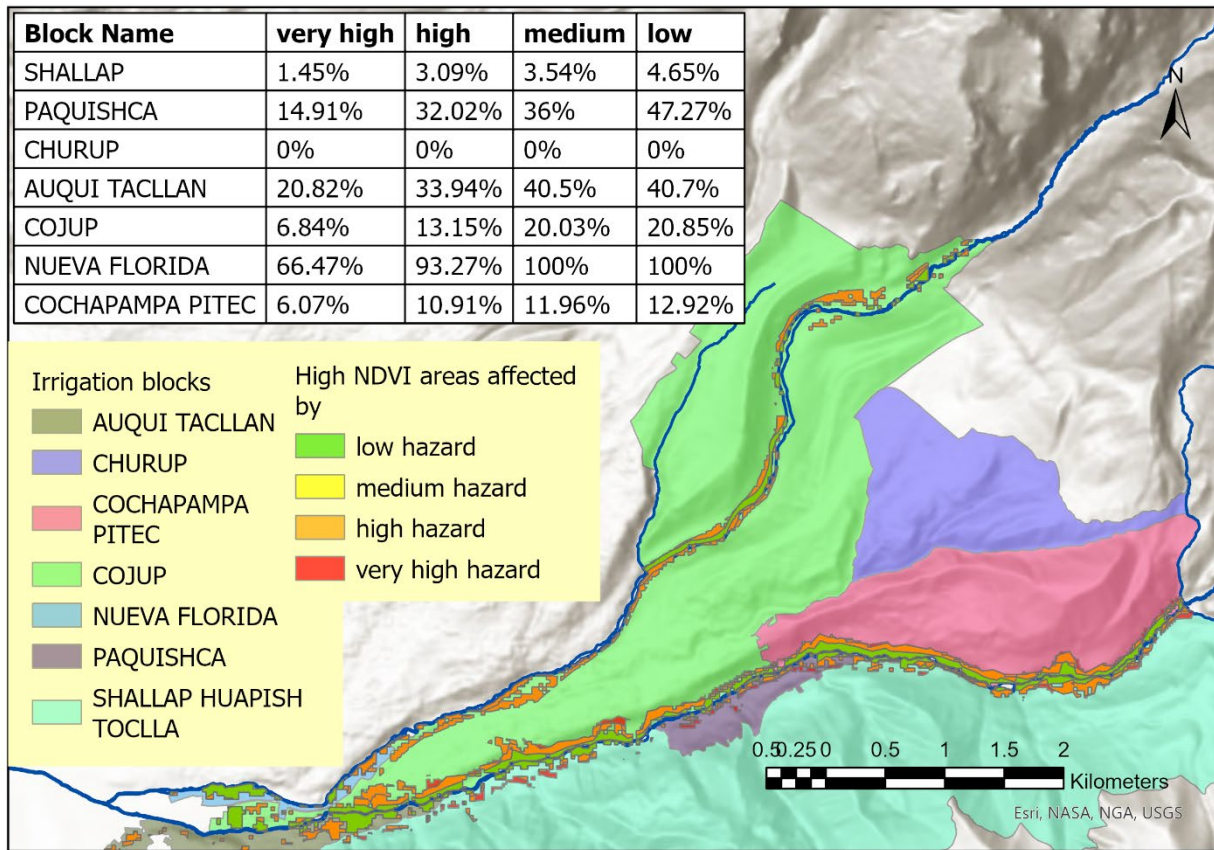


Figure 36. Map of agricultural area (high NDVI) within GLOF hazard zones. The table shows percentage of high-NDVI area within hazard zones compared to the total amount of high-NDVI area in the same irrigation block.

5.4 Co-assessment

5.4.1 Overview of losses and damages

Table 3 proposes an overview of L&Ds assessed in this study. Whereas agricultural revenue lost due to water scarcity and the number of people affected by GLOFS changes over time, GLOFs damages to assets remain constant. This is because agricultural revenue loss and loss of lives are partly driven by, respectively, changes in water availability and population increase. Damages to assets depend on GLOF magnitudes, which are simulated with scenarios unchanging through time.

L&D assessed	Water scarcity		GLOFs											
	Agricultural economic loss (in thousands of \$)		Loss of lives - number of people affected				Damage to assets - number of buildings affected)				Damage to assets - agricultural area affected in (ha)			
Scenario / hazard zone	SSP1-2.6	SSP5-8.5	Low	Medium	High	Very High	Low	Medium	High	Very High	Low	Medium	High	Very High
2020-2029	-\$47'680	-\$101'046	46349	37723	22226	15766	12642	10248	5963	4217	348.26	318.90	245.82	131.96
2030-2039	-\$84'763	-\$102'885	47704	39065	23453	16713								
2040-2049	-\$49'142	-\$86'477	48676	40026	24332	17391								

Table 3. Co-assessment table of L&D directly related to water scarcity and GLOFs. The assessed L&Ds are agricultural economic loss (in thousands of USD), loss of lives due to GLOFs, damage to assets due to GLOFs in terms of number of buildings and agricultural area (ha) potentially affected within hazard zones.

5.4.2 Connecting losses and damages with their drivers

Figure 37 shows the connections between socio-environmental drivers—through population increase and glacier retreat—and the L&Ds directly connected to water availability and GLOFs in the Quillcay catchment. L&Ds from changes in water availability connect to both population increase and glacier retreat. Along with population, domestic water demand increases, resulting in a greater strain on water supply and higher probability of water shortages. Glacier retreat reduces water reserves through ice-melt. Beyond the peak water, the contribution of meltwater to discharge is reduced, resulting in lesser water supply. L&Ds of GLOFs are directly connected to population increase. Higher the population in hazard zones grows, more people are exposed to GLOFs. Glacier retreat increases GLOF hazard due to slope instability around glacier lakes. Glacier retreat does impact probability of occurrence of GLOFs, yet it does not directly impact GLOFs' magnitude. The resulting L&Ds of GLOFs rely on the population exposed and magnitude of the event.

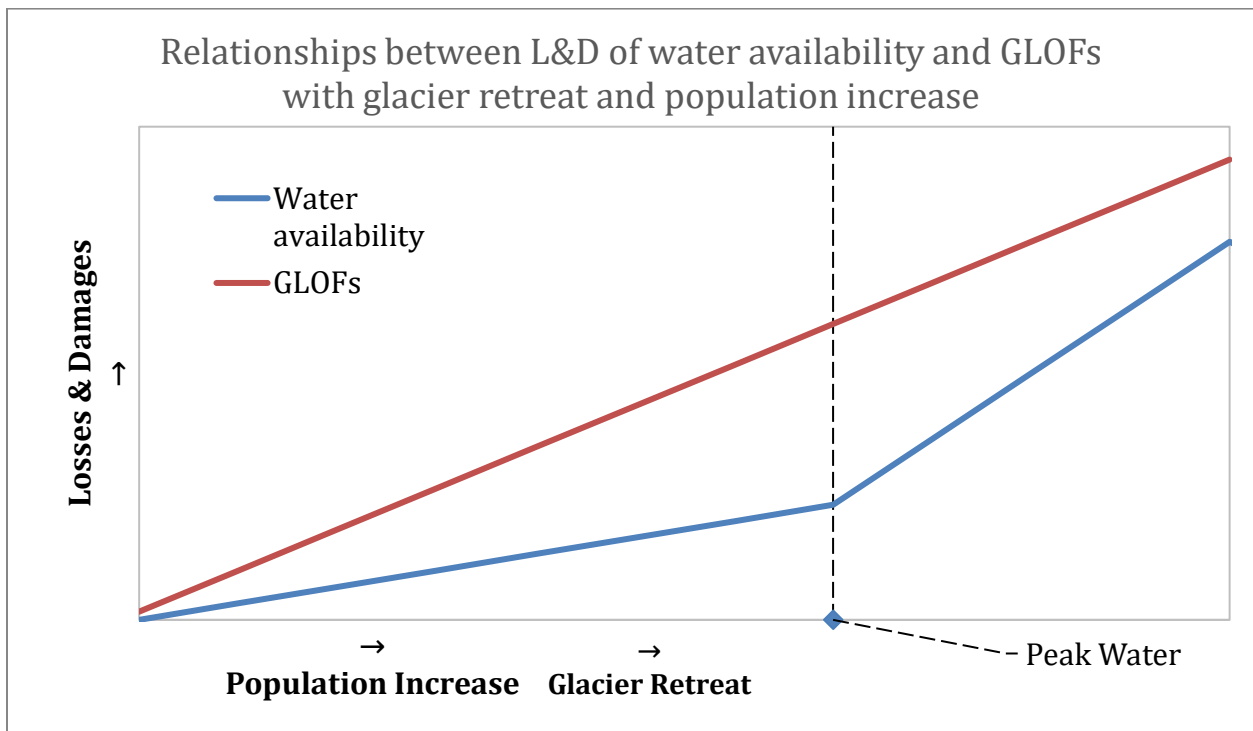


Figure 37. Relationships between glacier retreat, population increase, and L&Ds from water availability and GLOFs in the Quillcay catchment. This sketch is a conceptual figure aiming at representing a general trend and is not based on data.

Discussion

6.1 Robustness of simulations

6.1.1 Glacier retreat

In line with existing literature, projected glacier extents from SSP1-2.6 and SSP5-8.5 indicate a nuanced glacier recession (Schauwecker et al., 2017). The difference of ice area lost between both projections highlights the significance of current societal choices in climate mitigation (Schauwecker et al., 2017, Drenkhan, 2019). Nevertheless, the SSP1-2.6 scenario, which is of both scenarios the one with the lesser ice-melt, still indicates a higher ice-melt rate than in the reference period (Seehaus et al., 2019).

The 2.43 km² mismatch between the glacier area estimated from the ELA constant factor projection in 2015 and the observed glacier area by GLIMS in 2016 originates from two main sources. First, the ELA constant factor method, with an estimate of 80% of the glacier area being located above the FLH, does not systematically fit the satellite derived glacier cover (Schauwecker et al., 2017). Whereas the 80% ratio was derived from a comparison with satellite derived glacier extent in 2008, it does not perfectly transpose to glacier extents from 1998 and 2016. Secondly, the mismatch between the average yearly temperatures in the reference period and the bias-corrected SSPs projections lead to different ELAs. The ELA derived from the reference period 2001-2010 average is 11m higher than the ELA derived from the SSPs scenario for 2016.

Overall, the glacier extents modelled in this research fit with existing literature and modelling efforts (Racovitenau et al., 2008; Cogley et al., 2016; Schauwecker et al., 2017). Even though there remain challenges in modelling the extent and spatial distribution of future glacier recession with higher resolution, the results reached in this study are robust enough to be used as inputs for hydrological simulations.

6.1.2 Hydrological simulations

In line with previous modelling efforts, this study results in lesser discharge on average during the dry and the rainy season for both SSP1-2.6 and SSP5-8.5 scenarios compared to the reference period, indicating scarcer water supplies (Motschmann et al., 2020). The difference in discharge between SSP5-8.5 and the reference period being statistically significantly different for both the rainy, the dry season, and on a yearly timescale, SSP5-8.5 would require considerable adaptation efforts (Drenkhan et al., 2015; Motschmann et al., 2022). Given the difference of projected discharges between SSP5-8.5 and SSP1-2.6, it is highly relevant to aim for the SSP1-2.6 scenario. The SSP1-2.6 discharges not being statistically significantly different to the reference period, this scenario would be more favorable to the local context.

The abnormal discharge peak simulated in September and October and the corresponding abnormal precipitation pattern from the MIROC6 model in the same months prevents assessment of water availability on a monthly timescale. There are many factors influencing precipitation patterns in climate models (Michibata et al., 2016; Hodnebrog et al., 2021; Ferreira et al., 2023). Underestimation of mid-level clouds in the Southern hemisphere within the MIROC6 model might be at the origin of this anomaly (Tatebe et al., 2019).

A recent comparison of cloud microphysical statistics between climate models and satellite-based observations has pointed out that “tuned” model parameters that were adjusted for adequate radiative forcing and realistic SAT (surface air temperature) changes do not necessarily ensure that cloud properties and rain–snow formation will be consistent with observations and implies the presence of error compensations in climate models (e.g. Suzuki et al., 2013; Michibata et al., 2016). (Tatebe et al., 2019).

In line with this observation, it is possible that precipitation patterns, and thus discharges, are inaccurately simulated during the post-dry season in the tropical Andes with the MIROC6 model. This inaccuracy makes a monthly analysis of projected discharges unreliable. However, the dry-season and yearly cumulated discharge and precipitation fit with the reference period patterns. A calibrated L&D assessment for these time periods remains reliable.

Glacier melt-water is an important component of dry season discharge in the Quillcay catchment (Drenkhan et al., 2015; Buytaert et al., 2017; Motschmann et al., 2022). Given the decrease in precipitation and discharge in the dry season observed in both SSPs' projections, the dry-season decline in glacier meltwater from both scenarios is in line with studies suggesting that the peak water has already been reached in the catchment (Baraer et al., 2012; Drenkhan et al., 2015; Guittard et al., 2020). The determination of the peak water is complex due to variations in water supply and demand and is beyond the scope of this study. Nevertheless, with diminishing discharge and increasing flow variability, post peak water systems present challenging conditions for local populations (Drenkhan et al., 2015). The hydrological simulations conducted in this research therefore underlines the relevance of adequate adaptations in water management.

6.2 Losses and damages of changing water availability

6.2.1 Water balance

The water demand per inhabitant was assumed to be constant until 2050. This can be questioned as economic development might lead to higher living standards which have an impact on water consumption (Drenkhan et al., 2015). Similarly, disparities in water consumption between socio-economic groups could not be represented due to data scarcity. The spatial distribution of groups with varying water consumption also impacts stress on water availability. A concentration of high water demand on one intake point could lead to saturation of available water.

The projected agricultural water demands are retrieved from continental SSP projections of agricultural production and do not consider the local context of the Quillcay catchment. Elements of high relevance such as the geographical distribution of new fields and their possible connection with irrigation systems are not projected. It can also be argued that higher agricultural production does not necessarily translates into higher water demand. Irrigation systems can be optimized, agricultural strategies can be adapted to changing climates through scheduling and choice of crop. Given the available data and the scope of this study, the estimations of domestic and agricultural demand are sufficient to present a general overview on possible role of demands as stress-factors on water availability.

Domestic demand outsizes agricultural demand during the dry season due to alfalfa, peas (esp. *Arveja Grano Verde*) and onions being the only crops cultivated in this period. (Quesquén, 2008). Despite that no water shortages were identified in this study, it is important to recall that shortages remain non-excluded. Non-environmental factors such as damage to water distribution and treatment infrastructures can lead to water shortages (Motschmann et al., 2020). Given the limited number of demands included in this study, it is important to raise awareness on the pressure of increasing demands on water availability during the dry season in the SSP5-8.5 scenario.

6.2.2 Loss of agricultural revenue

The economic balance of agricultural revenue is negative for both SSP1-2.6 and SSP5-8.5 from 2016 until 2050 with respectively 187,374,340\$ and 319,054,345\$ loss over the entire period. These results align with the findings of Motschmann et al. showing negative water balances for both RCP 2.6 and RCP 8.5 in the Quillcay catchment (2020). The reduction of water supply calculated by Motschmann et al. is greater in RCP 8.5 than in RCP 2.6 (2020). Water scarcity becomes more severe in the dry season, with again more severe reduction in the RCP 8.5 scenario (Motschmann et al., 2020). Motschmann et al., calculated water balance by subtracting and environmental base, domestic, agricultural, mining demands to simulated discharges (2020). There, water demands were assumed constant until 2050, making the decreasing water balance directly correlated to a decreasing water supply (Motschmann et al., 2020). The estimation of loss of agricultural revenue estimated in this study is a product based on simulated discharges. As such, the decreasing water supplies in Motschmann's et al. study reinforce our estimation of loss of agricultural revenue (2020).

In the same study, Motschmann et al. calculated the agricultural economic loss by determining the water equivalent to the volume of ice lost until 2050 for RCP 2.6 and RCP 8.5. This quantity of water was then converted into tons of wheat or potatoes by assessing the amount of each crop that could have been irrigated with this water. It was found that the economic loss over the entire period amounted to \$18 million and \$77 million with RCP 2.6, or \$220 million and \$617 million USD with RCP 8.5, for wheat and potatoes respectively. This estimation is derived from one factor, glacier retreat, applied to one crop: wheat or potatoes. In contrast, the estimation proposed here in this study is the product of yields derived from simulated discharges and applied to 16 crops. While fitting in

the order of magnitude of Motschmann's et al. estimations, the economic loss calculated in this study proposes a narrower range.

It remains important to underline that methodological choices for assessing loss of agricultural revenue have a direct impact on the resulting loss assessment. Here yields were determined from discharges corrected for future agricultural demand. However, in future scenarios of water scarcity in the dry season, meeting the domestic water demand might be given priority over supplying irrigation systems. In this context, a water balance including domestic demand might become more relevant for assessing future yields. The influence of water availability on crop yields is also highly crop dependent. An in-depth investigation of influence of water availability on crop yield at the crop level in the Quillcay catchment could permit a more accurate estimation.

The economic loss resulting from the impact of changes in water availability on crop yields until 2050 differs of 131'680'005\$ from SSP1-2.6 to SSP5-8.5. This means that leaning towards SSP1-2.6 could avoid a considerable loss of agricultural revenue. Important assumptions, for instance regarding the impact of water supply on crop yield, make the assessed economic loss more useful as an indicator of magnitude rather than a high-resolution prediction tool. Compared to the annual reference for agricultural revenue, the agricultural economic balance for SSP1-2.6 until 2050 manifests in a loss of about 4.8 annual revenues, against a loss of 8.2 annual revenues for SSP5-8.5. In the context of the Quillcay catchment where agriculture is a dominant working sector, the impact of such losses on livelihoods is vital.

6.3 Loss and damage assessment of GLOFs

6.3.1 Losses and damages within Huaraz

As Huaraz's urban population increases, so does the number of people exposed to GLOFs (INEI, 2009; Frey et al., 2018). Until 2050, possible loss of lives increases in the city center where a population densification within the 200m buffer zone is projected. Population increase in surrounding areas is estimated to manifest through urban sprawling and therefore does not affect the number of people exposed to GLOFs.

In 2016, CARE Peru and Frey et al. found that 52'557 people were exposed to GLOF in Huaraz in 2016. The assessment carried out here reveals that 45'669 people are exposed to GLOFs in 2021. Given that the assessment carried out here is limited to the administrative boundaries of Huaraz's

neighbourhoods, both results can be considered as aligning. There is a significant difference between the losses and damages attributed to the smallest and largest GLOF scenarios. The very high hazard zone includes 4'217 buildings against 12'642 in the low hazard zone. This translates into a difference of 30'378 possible losses of lives in 2021 between both scenario extremes. This difference increases to 31'398 possible losses of lives until 2050 due to population densification within the 200m buffer zone (Figure 33 &34).

The differences in population density obtained by the census at quarter level and the building extrapolation method underline the importance of reliable data geocoded data for L&D assessments (Appendix VI). These differences might be due to the spatial resolution of the census level; quarters sometime extend above the limits of hazard or buffer zones (Sirko et al., 2021). Depending on whether the quarter's geometrical center is located within the zone of interest, the quarters might be excluded from the calculation. The higher density outside the buffer zone obtained by both the building extrapolation method and the census contradicts the assumption that poorer neighbourhoods show higher population density along the Quillcay river. The underestimation of population density within the buffer zone with the building extrapolation method could be explained by the fact that height of buildings was not considered.

6.3.2 Damage on agricultural land

Within irrigation blocks, irrigation systems permit to extend fields away from rivers, rendering crops less exposed to GLOFs. It is important to notice that irrigation systems themselves rely on extraction points located in hazard zones along rivers. These extraction points could be damaged, making irrigation ineffective and indirectly affecting agriculture in these blocks. GLOFs impact on agriculture can manifest in degradation or destruction of crops which has a direct effect on farmer's revenue. However, long-term impacts of GLOFs could also be the destruction of agricultural infrastructure such as irrigation systems, and degradation of the soil through rock deposition. It is also important to keep in mind that the NDVI method for locating agricultural area relies on crops' specific spectral signature (Redowan & Kanan, 2012). Certain crop types, such as potatoes, may have high yields but low reflectance to red and infra-red bands due to little above-ground features and different leaf characteristics.

Paradoxically, irrigation in the Quillcay catchment has the advantage of expanding cultivated fields away from hazard zones, while it also creates a high dependence on unique extraction points exposed to GLOFs. The direct impact of GLOFs on agricultural area is not only dependent on GLOFs scenarios, but also on the timing of the event in the agricultural calendar. As less crops are cultivated in the dry season, GLOFs would then have a lesser impact on harvests. The long-term impacts of GLOFs highly depend on sediment and rock deposition triggered by floods.

6.4 Co-assessment of Loss and Damage

The co-assessment of L&Ds related to changes in water availability and GLOFs permits to have a clearer overview of how these L&D evolve through time (Table 35). Combining various L&Ds with different metrics contributes to a holistic understanding of climate change impacts in the Quillcay catchment. Moreover, bringing together L&Ds can help bringing into light the interconnectedness between socio-environmental drivers and the L&Ds themselves.

In line with the conceptual figure representing evolution of L&Ds (Figure 37), Motschmann et al. have shown that L&Ds related to water availability augment with glacier retreat and population increase in the Quillcay catchment (2020). Further, Drenkhan's et al. analysis of increasing water scarcity beyond the peak water reinforces the idea of increasing L&D from water availability after the peak water (2015). Overall, in the specific context of the Quillcay catchment, L&D of GLOFs remain higher as the calculated impacts are highly destructive. This is also because figure 37 does not account for probability of occurrence, and because there remain uncertainties regarding water demand in the catchment. Up-to-date data, or consideration of probability of occurrence, could make L&D of water scarcity more important.

GLOFs and water scarcity are usually assessed separately by experts due to their different nature. Whereas GLOFs are rapid-onset events with low probability of occurrence and high and concentrated impact, water scarcity is a slow-onset event with high-probability of occurrence and more distributed impacts (Motschmann et al., 2020b). However, by performing separate assessment, the opportunity to investigate the interconnections between both phenomena is missed. When assessing L&D, this might lead to significant underestimations. From the L&D assessment and the conceptual exploration carried out in this study emerges a framework for evaluating cascading L&Ds (Table 4):

Step 1: Base variables need to be defined for the co-assessment. If the co-assessment focuses on impacts of GLOF events and water scarcity, categories of L&D could be determined. In the example shown in table 4, cultural L&D and loss of security and social order could be particularly interesting to include as interconnections between these L&Ds for both phenomena remain unexplored.

Step 2: A co-assessment framework for cascading L&Ds GLOFs and water scarcity should prioritize encompassing a wide panel of scenarios while also paying attention to the probability of occurrence of each scenario. For instance, water scarcity could be attributed a higher probability of occurrence than a high-magnitude GLOF event. Social and climatic scenarios could be retrieved from SSPs scenarios. For instance, a scenario proposing increasing water scarcity and a small magnitude GLOF event, along with increasing population, could be attributed a higher probably of occurrence than a scenario proposing little changes to water availability and population evolution, with a high-magnitude GLOF event. Specifying probability of occurrence is important because it makes the co-assessment usable for local authorities.

Step 3: The third step consists in individually exploring impacts from one source of L&D to the other. In table 4, impacts of loss of social order from water scarcity on GLOFs are assessed first, followed by the impact of damage to assets (e.g. water intake points) from GLOF on water scarcity. The resulting possible cascading impacts are highly context dependent; the inclusion of local knowledge is therefore essential.

Step 4: The final step consists in the assessment and integration of cascading impacts. A collaboration between a wide panel of multi-disciplinary experts is recommended due to the different nature of investigated events.

<p style="text-align: center;">Scenario 1:</p> <ul style="list-style-type: none"> • Increasing water scarcity • Small-magnitude GLOF event • SSP5-8.5 scenario 		
Probability of occurrence:	Medium	
Assessed L&Ds:	<ul style="list-style-type: none"> • Loss of social order • Damage to assets 	
Identifying cascading impacts:	Impact of loss of social order from water scarcity on GLOFs	<ul style="list-style-type: none"> • Impact on perception of GLOF • Impact on vulnerability to GLOF • Potential loss of lives due to GLOF
	Impact of damage to assets (e.g. water intake points) from GLOF on water scarcity	<ul style="list-style-type: none"> • Number of lives impacted • Agricultural economic loss
Cascading impact assessment	The assessment is jointly carried out by experts and community insiders	
Resulting impacts	Overview of cascading L&D due to interconnections between GLOF and water scarcity	

Table 4. Suggested framework for co-assessing cascading L&D of GLOFS and water scarcity.

Completing the framework, this work proposes three suggestions as groundwork consideration for future co-assessments efforts:

1. **Finding connections between GLOFs, water scarcity, and their L&D, is an on-going work which should prioritize inclusivity.** By recognizing the diversity of values and perceptions, one reduces the space for underestimation of L&D. Non-economic and intangible L&D in particular could be underestimated. For instance, cultural L&D or loss of security and social order due to water scarcity could in turn affect perception, vulnerability, and exposure to GLOFs, leading to potentially higher L&D overall.
2. **A L&D co-assessment also implies a co-assessment of risks (Reisinger et al., 2020; Westoby et al., 2022).** Interconnections between vulnerability and exposure to, as well as hazard of GLOFs and water scarcity, deserves a close attention. For instance, this research points out that water intake points are located within GLOF hazard zones. A GLOF could therefore provoke water scarcity by damaging water distribution infrastructures. Such cascading effect is also valid for non-economic L&Ds (NELDs), a particular loss or damage from one phenomenon, such as loss of social order due to water scarcity, might impact components of risk from another phenomenon, such as vulnerability and exposure of people to a GLOF. In this line of thought, it is suggested that the results of co-assessments of cascading L&Ds serve as a contribution to risk assessments or water security indices including both water availability and water-related natural hazards (Grey & Sadoff, 2007).
3. **When looking at interconnections between impacts of water scarcity and GLOFs, it seems crucial to have access to reliable geolocated data.** In this study, missing data regarding water access and consumption habits, income, up-to-date agricultural data, and infrastructure resilience to GLOFs, underline the relevance of data availability for L&D assessments. Much important is to collect qualitative data to better assess intangible L&D such as loss of identity or loss of social order. Challenges for collecting such data are multiple and deserve to be further examined.

6.5 Limitations and uncertainties

One of the main challenges when conducting research in the tropical Andes is the scarcity of available and reliable small-scale data (Drenkhan & Castro-Salvador, 2023; Muñoz, 2023). Lack of data concerning agricultural practices and crop-specific water demand make important assumptions necessary in this study. Data on domestic water use amongst socio-economic groups seems to be absent. This hinders the analysis of distribution of impacts within the local population.

The L&D assessment conducted in this research is also limited by abstractions necessary for modelling. For instance, in the HBV model, terrain is simplified into elevation bands which characteristic rely only on average altitude and percentage of catchment covered. Climatic data, from both the PISCO dataset and the MIROC6 model, is grid-based. Grid cells do not fit optimally the catchment, which requires either a weighted mean calculation for the PISCO dataset, or the use of data from a wider cell extending much beyond the catchment's limits in the case of the MIROC6 model. The MIROC6 model has shown limited ability in representing post-dry season precipitation patterns, especially for the months of September and October. This prevented a monthly-based assessment of agricultural revenue. Further, the GLOF hazard map relies on RAMMS simulations based on a DEM which does not include buildings. Even though RAMMS simulations permit a high-resolution assessment of GLOF paths, the evolution of floods in an urban environment full of obstacles remains challenging to model accurately.

Beyond data scarcity and assumptions inherent to modelling, this work also presents methodological limitations. By focusing only on quantifiable L&Ds connected to selected environmental variables and events, this research excludes a wide variety of qualitatively assessed ecological and cultural L&Ds (Bahinipati & Gupta, 2022). These other L&Ds, such as species extinction, habitat degradation, or loss of social cohesion and identity, also impact L&Ds both directly and through cascading effects.

Conclusion

The assessment carried out in this research reveals that the impacts of glacier retreat and changing water availability in the Quillcay catchment are already causing significant L&Ds. Further, L&Ds attributed to both SSP1-2.6 and SSP5-8.5 scenarios have an increasingly negative yet differentiated impact until 2050. SSP5-8.5 shows overall greater negative impacts from water availability due to lesser discharges, subsequently leading to greater strain on water supplies and greater loss in agricultural revenue. The fast glacier retreat simulated in the SSP5-8.5 scenario also contributes to increasing slope instability in the high-mountain, which in turn leads to higher probability of occurrence of GLOF events.

Contributing to existing assessments in the Quillcay catchment, this work innovates by estimating loss of agricultural revenue (Frey et al., 2018; Motschmann et al., 2020). More specifically, this study finds that aiming for the SSP1-2.6 scenario would permit avoiding a loss equivalent to 3.4 agricultural annual revenues compared to SSP5-8.5. Moreover, water balances estimated in this work reinforce findings revealing an increasing strain on water supply during dry season (Motschmann et al., 2020). Even though estimations of future water balance did not reveal water shortages in this study, the strain on water supply will be greater with SSP5-8.5 than with SSP1-2.6. Further research should pay particular attention to the weight of domestic water demand in future water balances in the dry season.

This study also consolidated Frey's et al. efforts in estimating L&Ds of GLOFs in the Quillcay catchment (2018). The innovative use of the Open Buildings Polygon V3 dataset permitted to confirm the magnitudes of L&D from Frey's et al. findings (Frey et al., 2018; Sirko et al., 2021). This study has found that the number of lives affected vary significantly between GLOFs scenarios, from 17'654 to 49'052 in 2050 between the most extreme scenarios. The direct impacts of GLOFs on agricultural land is distributed along the river streams and is very nuanced between irrigation blocks. Indirect impacts caused for instance by damage to irrigation infrastructure and water intake points must be further investigated.

It remains important to recall that this work does not entail a fully comprehensive assessment of all L&D due to climate change in the Quillcay catchment. The assessed L&D categories were pre-established and calculated from a limited number of factors, this is to say water availability and GLOF hazard. Many other factors may influence the assessed L&Ds. For instance, loss of agricultural

revenue may be impacted by soil degradation or political and economic instability. Further, limitations due to data scarcity prevented an assessment of the distribution of L&Ds within socio-economic groups. Necessary assumptions within the glacio-hydrological models, as well as within the agricultural revenue balance and the GLOF L&D estimations, made high-resolution results challenging.

Despite its limited scope, this research contributes to the on-going effort to better understand and define L&D in high-mountain environments. A combination of different metrics of L&Ds was proposed, providing a better overview of climate change impacts in the Quillcay catchment. This research also finds that impacts of climate change become more complex when pictured together. Interactions between socio-environmental drivers and L&D, as well as cascading effects of L&D, deserve close attention to avoid underestimations of L&D. To lay the ground for further investigations, an innovative framework for cascading L&D assessments was brought forward. In view of strengthening the robustness and resolution of future assessments, responsible actors are encouraged to support the acquisition of reliable geolocated data and prioritize inclusivity when determining and evaluating L&D.

References

- ANA (2014a). Inventario Nacional de Glaciares (resumen). Huaraz, Perú: Autoridad Nacional del Agua.
- ANA (2014b). Inventario Nacional de Glaciares de la Cordillera Blanca. Huaraz, Perú: Autoridad Nacional del Agua.
- ANA (2023). Infraestructura de datos especiales. Autoridad Nacional del Agua.
- Allison, E.A. (2015) The spiritual significance of glaciers in an age of climate change. *Wiley Interdisciplinary Review of Climate Change*, vol.6, p.493–508. DOI: 10.1002/wcc.354
- Aybar, C., Fernández, C., Huerta, A., Lavado, W., Vegaaand, F., Felipe-Obando, O. (2020). Construction of a high-resolution gridded rainfall dataset for Peru from 1981 to the present day. *Hydrological Sciences Journal*, vol.65, issue 5, p.770-785. Doi: 1080/02626667.2019.164941
- Bahinipati, S.C., Gupta, A.K. (2022). Methodological challenges in assessing loss and damage from climate-related extreme events and slow onset disasters: Evidence from India. *International Journal of Disaster Risk Reduction*, vol.83. Doi: 10.1016/j.ijdr.2022.103418
- Baraer, M., Mark, B.G., Mckenzie, J.M., Condom, T., Bury, J., Huh, K-I., Portocarrero, C., Gómez, J., Rathay, S. (2012). Glacier recession and water resources in Peru's Cordillera Blanca. *Journal of Glaciology*, vol.58, p. 134–150. DOI:10.3189/2012JoG11J186.
- Boyd, E., Chaffin, B.C., Dorkenoo, K., Jackson, G., Harrington, L., N'Guetta, A., Johansson, E.A., Nordlander, L., De Rosa, S.P., Raju, E., Scown, M., Soo, J., Stuart-Smith, R. (2021). Loss and damage from climate change: A new climate justice agenda. *One Earth*, vol.4, issue 10. DOI: 10.1016/j.oneear.2021.09.015
- Brouwer, C., Heibloem, M. (1986). Irrigation Water Management: Irrigation Water Needs, *Training manual no.3*. FAO, Rome.
- Brügger, A., Tobias, R., Monge-Rodríguez, F.S. (2021). Public Perceptions of Climate Change in the Peruvian Andes. *Sustainability*, vol.13, issue 5. DOI: 10.3390/su13052677

- Burhans, Z. (2022). Research Report Two: Lliuya v. RWE AG. *Res Publica, Journal of Undergraduate Research*, vol.27. Retrieved from: <https://digitalcommons.iwu.edu/respublica/vol27/iss1/11>
- Buytaert, W., Moulds, S., Acosta, L., De Bievre, B., Olmos, C., Villacis, M., Tovar, C., Verbist, K.M.J. (2017). Glacial melt content of water use in the tropical Andes. *Environmental Research Letters*, vol.12. Doi: 10.1088/1748-9326/aa926c
- Calizaya, E., Mejía, A., Barboza, E., Calizaya, F., Corroto, F., Salas, R., Vásquez, H., Turpo, E. (2021). Modelling Snowmelt Runoff from Tropical Andean Glaciers under Climate Change Scenarios in the Santa River Sub-Basin (Peru). *Water*, vol.13. DOI: 10.3390/w13243535
- Cannon, A.J. (2018). Multivariate quantile mapping bias correction: An N-dimensional probability density function transform for climate model simulations of multiple variables. *Climate Dynamics*, vol.50, p. 31-49. DOI:10.1007/s00382-017-3580-6
- Cannon, A.J. (2023). Multivariate Bias Correction of Climate Model Outputs. Comprehensive R Archive Network, Canada.
- Carey, M. (2005). Living and dying with glaciers: people's historical vulnerability to avalanches and outburst floods in Peru. *Global and Planetary Change*, vol.47, p.122-134. DOI:10.1016/j.gloplacha.2004.10.007
- Chiba, Y., Prabhakar, S.V.R.K. (2017). Addressing Non-economic Losses and Damages Associated with Climate Change: Learning from the Recent Past Extreme Climatic Events for Future Planning. Kobe, Japan: Asia-Pacific Network for Global Change Research (APN) and Institute for Global Environmental Strategies (IGES). DOI: 10.30852/p.4492
- Cogley, G., Kienholz, C., Miles, E., Sharp, M., Wyatt, F. (2015). GLIMS Glacier Database. Boulder, Colorado, National Snow and Ice Data Center. DOI: 10.7265/N5V98602
- Condom, T., Escobar, M., Purkey, D., Pouget, J.C., Suarez, W., Ramos, C., Apaestegui, J., Tacsí, A., Gomez, J. (2012). Simulating the implications of glaciers' retreat for water management: a case study in the Rio Santa basin, Peru. *Water International*, vol.37, p.442-459. DOI:10.1080/02508060.2012.706773
- Drenkhan, F., Carey, M., Huggel, C., Seidel, J., Oré, M.T. (2015). The changing water cycle: climatic and socioeconomic drivers of water-related changes in the Andes of Peru. *Wiley Interdisciplinary Reviews, Water*, vol.2, p.715-733. DOI: 10.1002/wat2.1105

- Drenkhan, F. (2016). En la sombra del Cambio Global: hacia una gestión integrada y adaptativa de recursos hídricos en los Andes del Perú. *Espacio y Desarrollo*, vol.28, p.25-51. DOI:10.18800/espacioydesarrollo.201601.002
- Drenkhan, F., Guardamino, L., Huggel, C., Frey, H. (2018). Current and future glacier and lake assessment in the deglaciating Vilcanota-Urubamba basin, Peruvian Andes. *Global Planet Change*, vol.169, p.105–118. DOI: 10.1016/J.
- Drenkhan, F., Huggel, C., Guardamino, L., Haerberli, W. (2019). Managing risks and future options from new lakes in the deglaciating Andes of Peru: The example of the Vilcanota-Urubamba basin. *Science of the Total Environ*, vol.665, p.465–483. DOI: 10.1016/j. scitotenv.2019.02.070
- Drenkhan, F., Huggel, C., Hoyos, N., Scott, C. A. (2023). Hydrology, water resources availability and management in the Andes under climate change and human impacts. *Journal of Hydrology: Regional Studies*, vol.49. DOI: 10.1016/j.ejrh.2023.101519
- Drenkhan F., Castro-Salvador S. (2023). Una aproximación hacia la seguridad hídrica en los Andes tropicales: desafíos y perspectivas. *Revista Kawsaypacha: Sociedad Y Medio Ambiente*, vol.2. DOI: 10.18800/kawsaypacha.202302.A006
- ESRI Demographics & Michael Bauer Research GmbH. (2021). Population density dataset available through ArcGIS online. Nuremberg, Germany. Dataset information available at: <https://doc.arcgis.com/en/esri-demographics/latest/reference/michael-bauer.htm>
- FAO. (2012). ET0 calculator. Land and Water Digital Media Series N°36. Rome, Italy.
- Ferreira, G.W.d.S., Reboita, M.S., Ribeiro, J.G.M., de Souza, C.A. (2023). Assessment of Precipitation and Hydrological Droughts in South America through Statistically Downscaled CMIP6 Projections. *Climate*, vol.11, issue 166. DOI: 10.3390/cli11080166
- Frame, B., Lawrence, J., Ausseil, A-G., Reisinger, A., Daigneault, A. (2018). Adapting global shared socio-economic pathways for national and local scenarios. *Climate Risk Management*, vol.21, p.39-51. Doi: 10.1016/j.crm.2018.05.001
- Gibson, S. (2023, December 6). Don't applaud the COP28 climate summit's loss and damage fund deal just yet – here's what's missing. *The Conversation*. Retrieved (December 20, 2023) from: <https://theconversation.com/dont-applaud-the-cop28-climate-summits-loss-and-damage-fund-deal-just-yet-heres-whats-missing-218093>

- Grey, D., Sadoff, C.W. (2007). Sink or swim? water security for growth and development. *Water Policy*, vol.9, p.545– 571. DOI:10.2166/wp.2007.021.
- Guittard, A., Baraer, M., McKenzie, J.M., Mark, B.G., Rapre, A.C., Bury, J., Carey, M., Young, K.R. (2020). Trace metal stream contamination in a post peak water context: lessons from the cordillera Blanca, Peru. *ACS Earth Space and Chemistry*, vol.4, p.506-514. DOI:10.1021/acsearthspacechem.9b00269
- Gurgiser, W., Juen, I., Singer, K., Neuburger, M., Schauwecker, S., Hofer, M., Kaser, G. (2016). Comparing peasants' perceptions of precipitation change with precipitation records in the tropical Callejón de Huaylas, Peru. *Earth System Dynamics*, vol.7, p.499–515. DOI: 10.5194/esd-7-499-2016
- Hagen, I., Allen, S., Bahinipati S.C., Frey, H., Huggel, C., Karabaczek, V., Kienberger, S., Mechler, R., Petutschnig, L., Schinko, T. (2023). A reality check for the applicability of comprehensive climate risk assessment and management: Experiences from Peru, India and Austria. *Climate risk management*, vol.41. DOI: 10.1016/j.crm.2023.100534
- Hänchen, L., Klein, C., Maussion, F., Gurgiser, W., Calanca, P., Wohlfahrt, G. (2022). Widespread greening suggests increased dry-season plant water availability in the Rio Santa valley, Peruvian Andes. *Earth System Dynamics*, vol.13, p.595–611. DOI: 10.5194/esd-13-595-2022
- Hodnebrog, Ø., Steensen, B.M., Marelle, L., Alterskjær, K., Dalsøren, S.B., Myhre, G. (2021). Understanding model diversity in future precipitation projections for South America. *Climate dynamics*, vol.58, p. 1329-1347. DOI: 10.1007/s00382-021-05964-w
- Huggel, C., Muccione, V., Carey, M., James R., Jurt, C., Mechler, R. (2018). Loss and damage in the mountain cryosphere. *Regional Environmental Change*, vol.19, p.1387–1399. DOI: 10.1007/s10113-018-1385-8
- Huggel, C., Carey, M., Emmer, A., Frey, H., Walker-Crawford, N., Wallimann-Helmer, I. (2020). Anthropogenic climate change and glacier lake outburst flood risk: local and global drivers and responsibilities for the case of lake Palcacocha, Peru. *Natural Hazards and Earth System Sciences*, vol.20, p.2175-2193. Doi:10.5194/nhess-20-2175-2020
- Huggel, C., Carey, M., Emmer, A., Frey, H., Walker-Crawford, N., Wallimann-Helmer, I. (2020b). Interactive comment on “Anthropogenic climate change and glacier lake outburst flood risk: local

and global drivers and responsibilities for the case of Lake Palcacocha, Peru". *Natural Hazards and Earth System Sciences*, Discussion. DOI:10.5194/nhess-2020-44-AC1

INAIGEM. (2020). *Evaluación del riesgo por aluvión en la ciudad de Huaraz, distritos de Huaraz e Independencia, provincia de Huaraz, departamento de Áncash*. Lima, Perú.

INEI. (1993). Censos Nacionales 1993: IX de Población y IV de Vivienda. Dataset: Sistema de Consulta de Base de Datos REDATAM.

Available at: <http://censos1.inei.gob.pe/censos1993/redatam/>

INEI. (2005). Censos Nacionales 2005: X de Población y V de Vivienda. Dataset: Sistema de Consulta de Base de Datos REDATAM.

Available at: <http://censos1.inei.gob.pe/Censos2005/redatam/>

INEI. (2007). Censos Nacionales 2007: XI de Población y VI de Vivienda. Dataset: Sistema de Consulta de Base de Datos REDATAM.

Available at: <http://censos1.inei.gob.pe/Censos2007/redatam/>

INEI. (2009). Perú: Estimaciones y Proyecciones de Población Total, por Años Calendario y Edades Simples, 1950-2050. Dirección Técnica de Demografía e Indicadores Sociales. *Boletín Especial N° 17*. Lima, Perú.

INEI. (2017). Censos Nacionales 2017: XII de Población, VII de Vivienda y III de Comunidades Indígenas. Dataset: Sistema de Consulta de Base de Datos REDATAM.

Available at: <https://censos2017.inei.gob.pe/redatam/>

Kriegler, E., Bauer, N., Popp, A., Humpenöder, F., Leimbach, M., Strefler, J., Baumstark, L., Bodirsky, B.L., Hilaire J., Klein, D. Mouratiadou I. , Weindl, I., Bertram, C., Dietrich, J-P. Luderer G., Pehl, M., Pietzcker, R., Piontek, F., Lotze-Campen, H., et al. (2017). Fossil-fueled development (SSP5): An energy and resource intensive scenario for the 21st century. *Global Environmental Change*, vol.42, p. 297-315. DOI: 10.1016/j.gloenvcha.2016.05.015

Mark, B.G., French, A., Baraer, M., Carey, M., Bury, J., Young, K.R., Polk M.K., Wigmorea, O., Lagosh, P., Crumleya, R., McKenzie, J.M., Lautz L. (2017). Glacier loss and hydro-social risks in the Peruvian Andes. *Global Planet Change*, vol.159, p.61–76. DOI: 10.1016/j.gloplacha.2017.10.003

- Markantonis, V., Meyer, V., Schwarze, R. (2012). Valuating the intangible effects of natural hazards – review and analysis of the costing methods. *Natural Hazards and Earth System Sciences*, vol.12, p.1633-1640. Doi: 10.5194/nhess-12-1633-2012
- Meier, S. (2021). *Impact of climate change on water availability in Tropical Andean catchments: a case study in the Vilcanota catchment, Peru*. Master thesis, University of Zurich.
- Meinshausen, M., Nicholls, Z.R.H., Lewis, J., Gidden, M.J., Vogel, E., Freund, M., Beyerle, U., Gessner, C., Nauels, A., Bauer, N., Canadell, J.G., Daniel, J.A., John, A., Krummel, P.B., Luderer, G. Meinshausen, N., Montzka, S., Reynier P.J., Reimann S., et al. (2020). The shared socioeconomic pathway (SSP) greenhouse gas concentrations and their extensions to 2500. *Geoscientific Model Development*, vol.13, issue 8. DOI: 10.5194/gmd-13-3571-2020
- Mergili, M., Pudasaini, S.P., Emmer, A., Fischer, J-T., Cochachin, A., Frey, H. (2020). Reconstruction of the 1941 GLOF process chain at Lake Palcacocha (Cordillera Blanca, Peru). *Hydrology and Earth System Sciences*, vol.24, p.93-114. DOI: 10.5194/hess-24-93-2020
- Michibata, T., Suzuki, K., Sato, Y., Takemura, T. (2016). The source of discrepancies in aerosol–cloud–precipitation interactions between GCM and A-Train retrievals. *Atmospheric Chemistry and Physics*, vol.16, p.15413–15424. DOI: 10.5194/acp-16-15413-2016
- MINAM. (2010). *El Perú y el cambio climático - Segunda Comunicación Nacional del Perú a la CMNUCC 2010*. Lima, Perú.
- MINAM. (2014). Demanda de agua municipal en la ciudad de Huaraz. Modelo de recursos hídricos de la subcuenca de Quillcay. *Nota técnica 4*, Austin, USA.
- MINAM. (2015). Mapa Nacional de Cobertura Vegetal. Lima, Perú.
- Motschmann, A., Huggel, C., Carey, M., Moulton, H., Walker-Crawford, N., Muñoz, R. (2020). Losses and Damages connected to glacier retreat in the Cordillera Blanca, Peru. *Climatic Change*, vol.162, issue 2, p.837-858. DOI: 10.1007/s10584-020-02770-x
- Motschmann, A., Huggel, C., Muñoz, R., Thür, A. (2020b). Towards integrated assessments of water risks in deglaciating mountain areas: water scarcity and GLOF risk in the Peruvian Andes. *Geoenvironmental Disasters*, vol.7, issue 26. DOI: 10.1186/s40677-020-00159-7
- Motschmann, A., Teutsch, C., Huggel, C., Seidel, J., León, C.D., Muñoz, R., Siemel, J., Drenkhan, F., Weimer-Jehle, W. (2022). Current and future water balance for coupled human-natural systems –

Insights from a glacierized catchment in Peru. *Journal of Hydrology: Regional Studies*, vol.41. Doi: 10.1016/j.ejrh.2022.101063

Muñoz R.A. (2017). *Impacto del cambio climático en los recursos hídricos de la subcuenca Quillcayhuanca, Perú*. Master thesis, Universitat Politècnica de València.

Muñoz, R. (2023). *Toward adaptive water management in the glacierized and data-scarce Peruvian Andes*. University of Zurich, Faculty of Science.

Neukom, R., Rohrer, M., Calanca, P., Salzmann, N., Huggel, C., Acuña, D., Christie, D.A., Morales, M.A. (2015). Facing unprecedented drying of the Central Andes? Precipitation variability over the period AD 1000–2100. *Environmental Research Letters*, vol.10. DOI: 10.1088/1748-9326/10/8/084017

Quesquén, A. (2008). *Propuesta de asignaciones de agua en bloque. Volúmenes anuales y mensuales, para la formalización de los derechos de uso de agua Cuenca Alto Santa en la comisión de regantes Quillcay*. Lima, Perú.

Rabatel, A., Francou, B., Soruco, A., Gomez, J., Caceres, B., Ceballos, J.L., Basantes, R., Vuille, M., Sicart, J.-E., Huggel C., Scheel, M., Lejeune, Y., Arnaud, Y., Collet, M., Condom, T., Consoli, M., Favier, V., Jomelli, V., Galarraga, R., et al. (2013). Current state of glaciers in the tropical Andes: a multi-century perspective on glacier evolution and climate change. *The Cryosphere*, vol.7, p. 81–102. DOI: 10.5194/tc-7-81-2013

Racoviteanu, A.E., Arnaud, Y., Williams, M.W., Ordonez, J. (2008). Decadal changes in glacier parameters in the Cordillera Blanca, Peru, derived from remote sensing. *Journal of Glaciology*, vol.54, p.499–510. DOI:10.3189/002214308785836922

Raup, B.H., Racoviteanu, A.E., Khalsa, S.J.S., Helm, C., Armstrong, R., Arnaud, Y. (2007). The GLIMS Geospatial Glacier Database: a New Tool for Studying Glacier Change. *Global and Planetary Change*, vol.56, p.101-110. DOI: 10.1016/j.gloplacha.2006.07.018

Redowan, M., Kanan, A.H. (2012). Potentials and Limitations of NDVI and other Vegetation Indices (VIS) for Monitoring Vegetation Parameters from Remotely Sensed Data. *Bangladesh Research Publications Journal*, vol.7, issue 3, p. 291-299. Available at Researchgate.net

Reisinger, A., Howden, M., Vera, C., et al. (2020). *The Concept of Risk in the IPCC Sixth Assessment Report: A Summary of Cross-Working Group Discussions, Intergovernmental Panel on Climate Change*. Geneva, Switzerland.

- Riahi, K., Van Vuuren, D.P., Kriegler, E., Edmonds, J., O'Neill B.C., Fujimori, S., Bauer, N., Calvin, K., Dellink, R., Fricko, O., Lutz, W., Popp, A., Cuaresma, J.C., Samir, K.C., Leimbach, M., Jiang, L., Kram, T., Rao, S., Emmerling, J., et al. (2017). The Shared Socioeconomic Pathways and their energy, land use, and greenhouse gas emissions implications: An overview. *Global Environmental Change*, vol.42, p. 153-168, DOI: 10.1016/j.gloenvcha.2016.05.009
- Samir, K.C., Lutz, W., (2017). The human core of the shared socioeconomic pathways: Population scenarios by age, sex and level of education for all countries to 2100. *Global Environmental Change*, vol.42, p. 181-192. DOI: 10.1016/j.gloenvcha.2014.06.004
- Schauwecker, S., Rohrer, M., Acuña, D., Cochachin, A., Dávila, L., Frey, H., Giráldez, C., Gómez, J., Huggel, C., Jacques-Coper, M., Loarte, E., Salzmann, N., Vuille, M. (2014). Climate trends and glacier retreat in the Cordillera Blanca, Peru, revisited. *Global Planet Change*, vol.119, p.85–97. Doi: 10.1016/j.gloplacha.2014.05.005
- Schauwecker, S., Rohrer, M., Huggel, C., Endries, J., Montoya, N., Neukom, R., Perry, B., Salzmann, N., Schwarb, M., Suarez, W. (2017). The freezing level in the tropical Andes, Peru: An indicator for present and future glacier extents. *Journal of Geophysical Research*, vol.122, p.5172–5189. Doi: 10.1002/2016JD025943
- Seehaus, T., Malz, P., Sommer, C., Lippl, S., Cochachin, A., Braun, M. (2019). Changes of the tropical glaciers throughout Peru between 2000 and 2016 – mass balance and area fluctuations. *The Cryosphere*, vol.13, p.2537–2556, DOI: 10.5194/tc-13-2537-2019
- Seibert J. (2005). *HBV light version 2 User's Manual*. Sweden, Uppsala.
- Singh, C., Jain, G., Sukhwani, V., Shaw, R. (2021). Losses and damages associated with slow-onset events: urban drought and water insecurity in Asia. *Current Opinion in Environmental Sustainability*, vol.50, p.72-86. DOI: 10.1016/j.cosust.2021.02.006
- Sirko, W., Kashubin, S., Ritter, M., Annkah, A., Bouchareb, Y.S.E, Dauphin, Y., Keyzers, D., Neumann, M., Cisse, M., Quinn, J.A. (2021). Continental-scale building detection from high resolution satellite imagery. DOI: 10.48550/arXiv.2107.12283
- Suzuki, K., Golaz, J.-C., Stephens, G. L. (2013). Evaluating cloud tuning in a climate model with satellite observations. *Geophysical Research Letters*, vol.40, p.4464–4468. DOI: 10.1002/grl.50874

- Tatebe, H., Ogura, T., Nitta, T., Komuro, Y., Ogochi, K., Takemura, T., Sudo, K., Sekiguchi, M., Abe, M., Saito, F., Chikira, M., Watanabe, S., Mori, M., Hirota, ., Kawatani, Y., Mochizuki, T., Yoshimura, K., Takata, K., O'ishi, R., et al. (2019). Description and basic evaluation of simulated mean state, internal variability and climate sensitivity in MIROC6. *European Geosciences Union*, vol.12, issue 7. DOI: 10.5194/gmd-12-2727-2019
- UNFCCC. (2013). Decision 2/CP.19 Warsaw international mechanism for loss and damage associated with climate change impacts.
- UNFCCC. (2023). Operationalization of the new funding arrangements, including a fund, for responding to loss and damage referred to in paragraphs 2–3 of decisions 2/CP.27 and 2/CMA.4. Draft decision -/CP.28 -/CMA.5. Available at: <https://unfccc.int/documents/634215>
- Van Vuuren, D.P., Stehfest, E., Gernaat, D.E.H.J., Doelman, J.C., Van den Berg, M., Harmsena, M., Sytze de Boera, H., Bouwmana, L.F., Daiogloua, V., Edelenboscha, O.Y., Girodd, B., Krama, T., Lassalettaa, L., Lucasa, P.L., Van Meijle, H., Müller, C., Van Ruijveng, B.J., Van der Sluisa, S., Tabeau, S. (2017). Energy, land-use and greenhouse gas emissions trajectories under a green growth paradigm. *Global Environmental Change*, Vol.42, p. 237-250. DOI: 10.1016/j.gloenvcha.2016.05.008
- Vilímek, V., Luyo Zapata, M., Klimeš, J., Patzelt, Z. (2005). Influence of glacial retreat on natural hazards of the Palcacocha Lake area, Peru. *Landslides*, vol.2, p.107-115. DOI: 10.1007/s10346-005-0052-6
- Vuille, M., Francou, B., Wagnon, P., Juen, I., Kaser, G., Mark, B.G., Bradley, R.S. (2008). Climate change and tropical Andean glaciers: Past, present and future. *Earth-Science Reviews*, vol.89, p.79–96. Doi: 10.1016/j.earscirev.2008.04.002
- Westoby, R., Clissold, R., McNamara, K.E., Latai-Niusulu, A., Chandra, A. (2022). Cascading loss and loss risk multipliers amid a changing climate in the Pacific Islands, *Ambio*, vol.51, p. 1239-1246. DOI: 10.1007/s13280-021-01640-9
- Yap, A. (2015). *Análisis multitemporal de glaciares y lagunas glaciares en la Cordillera Blanca e identificación de potenciales amenazas GLOFs*. Tesis de Licenciatura. Lima, Pontificia Universidad Católica del Perú.

Appendix

Appendix I. Irrigation blocks and water intake points attributes (Source: Quesquén, 2008).

Water intake Nbr.	Source of intake	Altitude (m.a.s.l.)	Irrigation committee	Irrigation block	Block area (ha)
1	RIO PARIA	3783	COJUP	COJUP	844.8
2	RIO PARIA	3228	NUEVA FLORIDA	NUEVA FLORIDA	19.4
3	LAGUNA CHURUP	3921	COCHAPAMPA CHURUP	CHURUP	196.6
4	QDA. QUILLCAYHUANCA	3906		COCHAPAMPA PITEC	267.3
5	RIO AUQUI	3511	PAQUISHCA - QUERUPAMPA	PAQUISHCA	45.5
6	RIO AUQUI	3223	AUQUI TACLLAN	AUQUI TACLLAN	124.5
7	QDA. SHALLAP	3990	SHALLAP HUAPISH TOCLLA	SHALLAP HUAPISH TOCLLA	2614.0

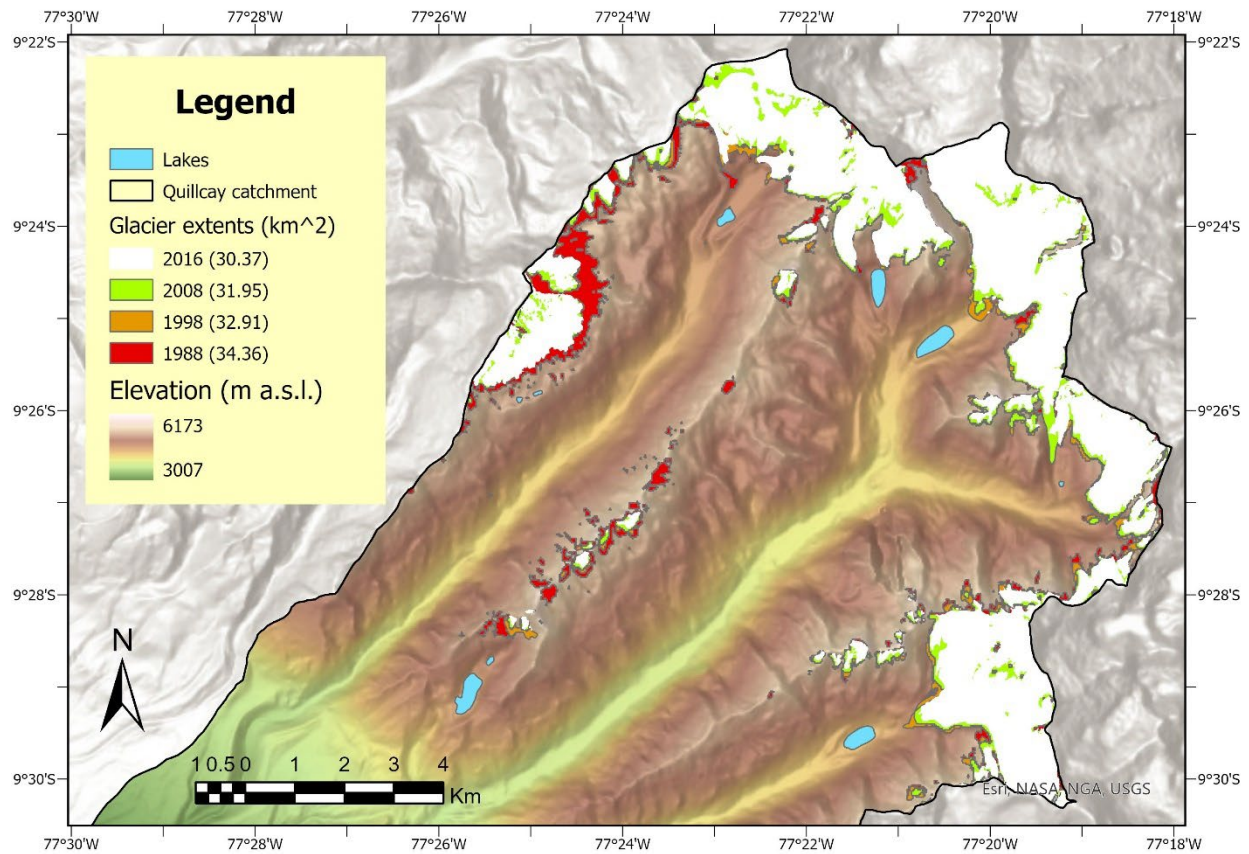
Appendix II. HBV parameters and their ranges for the Quillcay catchment.

	Abbreviation	Description	Realistic Values for Quillcay
Snow Routine	TT	threshold temperature for snow melt	from -2 to 0.5 °c
	CFMAX *	degree- Δt factor (mm oC-1 Δt -1) (mm of snow melt / degree)	from 0.5 to 4
	SP	Seasonal variability in degree- Δt factor (-)	from -1 to 0
	SFCF	Snowfall correction factor	from 0.5 to 0.9
	CFR	Refreezing coefficient	0.05
	CWH	Water holding capacity	0.1
	CFGlacier **	Correction factor glacier	from 0.5 to 1
	CFSlope **	Correction factor slope	1
Soil Moisture Routine	FC	Maximum soil moisture storage (mm)	from 100 to 550
	LP	Soil moisture value above which AET reaches PET	from 0.3 to 1
	BETA	Parameter that determines the relative contribution to runoff from rain or snowmelt	from 1 to 5
Glacier Routine	KSI	Snow to Ice conversion factor (Δt -1)	0.001
	Kgmin ***	Minimum outflow coefficient	from 0.01 to 0.2
	dKg	Maximum minus minimum outflow coefficient	from 0.02 to 0.5
	AG	Calibration parameter (mm-1)	from 0 to 1
Response fonction	PERC	Threshold parameter (mm Δt -1)	from 0 to 4
	UZL	threshold parameter (mm)	fro 0 to 70
	K0	storage (or recession) coefficient (Δt -1)	from 0.1 to 0.6
	K1	storage (or recession) coefficient (Δt -1)	from 0.1 to 0.6
	K2	storage (or recession) coefficient (Δt -1)	from 0.00005 to 0.1
Routing Routine	MAXBAS	Length of triangular weighting function (Δt)	from 1 to 2.5

* CFMAX: for monthly time-setp this value is multiplied by 30.

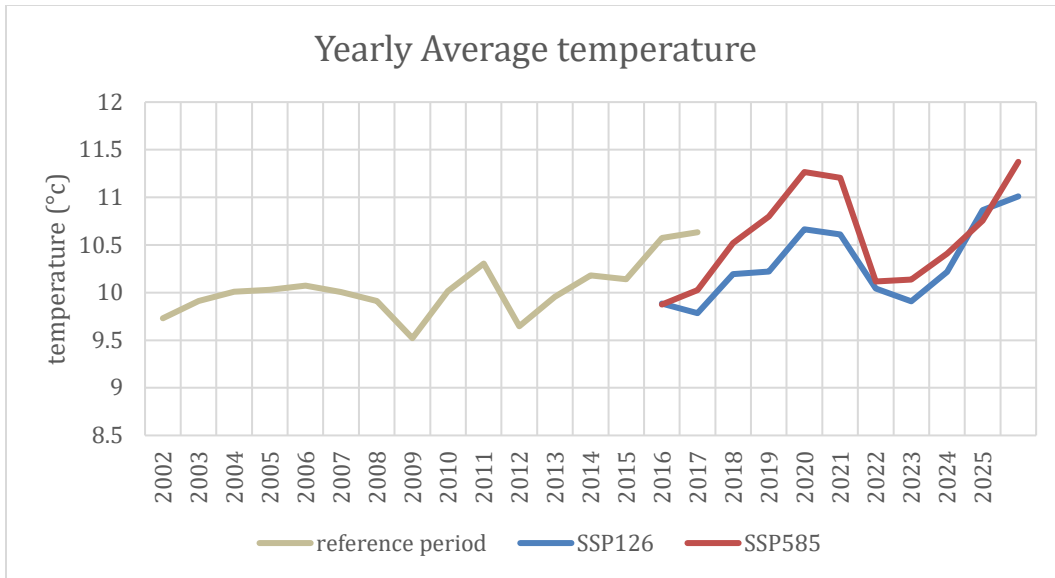
** CFGlacier & CFSlope: Corrects CFMAX depending on north/south facing slopes

***Kgmin: The relationship between glacial water content and outflow varies over time to represent the seasonal development of the subglacial drainage system.

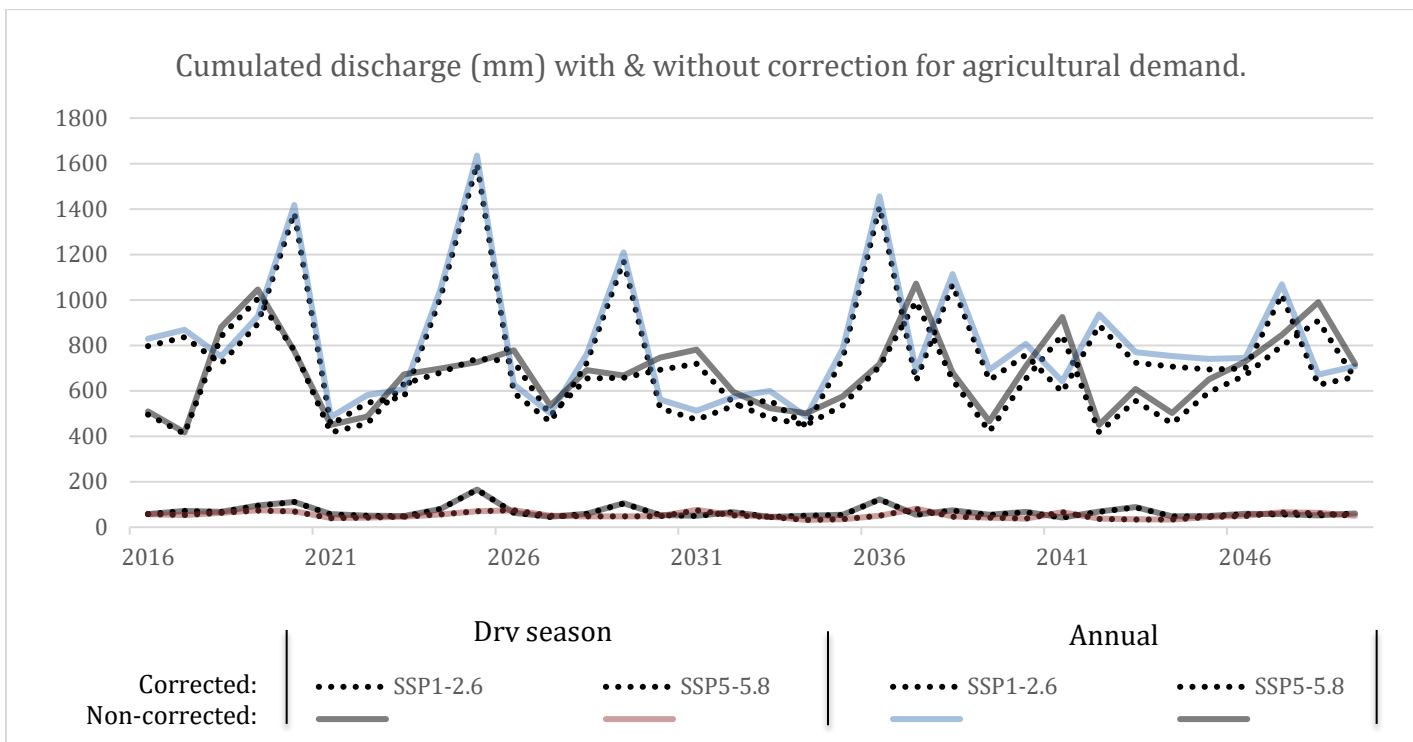


Appendix III. Map of historical glaciers extents from 1988 to 2016. The 1988 glacier extent represents 14.31% of the catchment and was retrieved from visual analysis of Landsat-5 products. The 1998 and 2008 extents correspond to respectively 13.71% and 13.31% of the catchment and were retrieved from GLIMS. The 2016 extent covers 12.65% of the catchment and is retrieved from ANA.

Note on appendix III: The 2.54 km² reduction of glacier surface from 1998 to 2016 observed fits with the magnitudes of ice melt observed in previous studies (Racovitenau et al., 2008; ANA, 2014b; Cogley et al., 2016). The glacier area for 1988 extends outstandingly on the north-western side of the catchment. This extension would need to be verified with further remote sensing investigations. The mapping of the 1988 glacier extent relies on a visual assessment of the blue, red, and near-infrared bands of Landsat-5. The resulting overall glacier extent retrieved from the visual assessment fits with the observed glacier recession trend in the catchment. However, the precise geographical distribution of the glacierized areas should be further investigated. Ice melt is observed at lower altitudes, more specifically at the edges of glacier tongues (Yap, 2015). Ice melt leads to an increased slope instability and contributes to augmenting glacier lake volumes (Huggel et al., 2018).



Appendix IV. Yearly average temperatures in the reference period and in SSPs projections. The 2001-2010 reference period is characterized by an temperature average of 9.95 °c and an ELA of 4'973 m.a.s.l. In contrast, both SSPs average temperature value for 2016 is 9.88°C with an ELA of 4'962 m.a.s.l.



Appendix V. Cumulated discharges (mm) with & without correction for agricultural demand.

Note on Appendix V: As new crop yields were extrapolated from discharge projections, it is relevant to investigate whether subtracting future agricultural water demands from discharges makes a significant difference on future water balances, and thus on yield estimation. The difference between both methods is negligible due to the poor efficiency of the irrigation systems. Indeed, 76% of irrigation water returns to the discharge (MINAM, 2014). In the figure above (appendix V), the differences on discharge resulting from both methods are made visible. The differences in discharges from both methods are due to the increasing agricultural water demand until 2050. For higher accuracy, in this study future crop yields are therefore extrapolated from discharges to which agricultural demand has been subtracted.

Appendix VI. Population density (inhabitants/km²) within and out of the 200m buffer according to the building extrapolation method and the INEI 2017 Census at quarter level.

	Density within the 200m buffer (inhabitants /km ²)	Density outside of the buffer (inhabitants /km ²)
Building extrapolation method	15'457	18'334
Census at quarter level	15'058	15'994

Appendix VII. Economic annual revenue of crops (SSP1-2.6), values are in thousands of USD\$. (Esp. Ingresos económicos anuales de los cultivos (SSP5-8.5), los valores están en miles de USD\$).

Año	Alfalfa	Arveja Grano verde	Cebolla	Cebada Grano	Trigo	Haba Grano Seco	Quinua	Frijol Grano Seco	ARVEJA GRANO SECO	TARHUI GRANO SECO	HABA GRANO VERDE	MAIZ AMILACEO	MAIZ CHOCCLO	OCA	OLLUCO	PAPA	SUMA
2016	8'529	2'412	1'341	3'114	3'295	895	1'282	198	817	119	811	1'298	3'376	389	1'762	6'993	36'631
2017	8'951	2'531	1'407	3'268	3'458	939	1'346	208	858	125	851	1'362	3'543	408	1'849	7'339	38'442
2018	7'699	2'177	1'210	2'811	2'975	808	1'157	179	738	107	732	1'171	3'048	351	1'590	6'312	33'065
2019	9'580	2'709	1'506	3'497	3'701	1'005	1'440	223	918	133	911	1'458	3'792	437	1'979	7'855	41'144
2020	10'832	3'063	1'703	3'954	4'185	1'137	1'628	252	1'038	151	1'030	1'648	4'288	494	2'238	8'881	46'521
2021	4'818	1'362	757	1'759	1'862	506	724	112	462	67	458	733	1'907	220	995	3'950	20'693
2022	5'854	1'655	920	2'137	2'262	614	880	136	561	82	557	891	2'318	267	1'209	4'800	25'143
2023	6'133	1'734	964	2'239	2'370	644	922	143	588	85	583	933	2'428	280	1'267	5'028	26'340
2024	10'829	3'062	1'702	3'953	4'184	1'136	1'628	252	1'038	151	1'029	1'648	4'287	494	2'237	8'879	46'509
2025	10'832	3'063	1'703	3'954	4'185	1'137	1'628	252	1'038	151	1'030	1'648	4'288	494	2'238	8'881	46'521
2026	6'325	1'788	994	2'309	2'444	664	951	147	606	88	601	962	2'504	288	1'307	5'186	27'163
2027	4'963	1'403	780	1'812	1'918	521	746	115	476	69	472	755	1'965	226	1'025	4'069	21'315
2028	7'746	2'190	1'218	2'828	2'993	813	1'164	180	742	108	736	1'179	3'067	353	1'600	6'351	33'269
2029	10'832	3'063	1'703	3'954	4'185	1'137	1'628	252	1'038	151	1'030	1'648	4'288	494	2'238	8'881	46'521
2030	5'597	1'583	880	2'043	2'163	587	841	130	536	78	532	852	2'216	255	1'156	4'589	24'039
2031	5'064	1'432	796	1'849	1'957	531	761	118	485	71	481	770	2'005	231	1'046	4'152	21'748
2032	5'709	1'614	897	2'084	2'206	599	858	133	547	80	543	869	2'260	260	1'179	4'681	24'519

Año	Alfalfa	Arveja Grano verde	Cebolla	Cebada Grano	Trigo	Haba Grano Seco	Quinua	Frijol Grano Seco	ARVEJA GRANO SECO	TARHUI GRANO SECO	HABA GRANO VERDE	MAIZ AMILACEO	MAIZ CHOCLO	OCA	OLLUCO	PAPA	SUMA
2033	5'984	1'692	941	2'185	2'312	628	900	139	573	83	569	910	2'369	273	1'236	4'906	25'700
2034	4'764	1'347	749	1'739	1'841	500	716	111	457	66	453	725	1'886	217	984	3'906	20'461
2035	7'950	2'248	1'250	2'902	3'072	834	1'195	185	762	111	756	1'210	3'147	363	1'642	6'518	34'144
2036	10'832	3'063	1'703	3'954	4'185	1'137	1'628	252	1'038	151	1'030	1'648	4'288	494	2'238	8'881	46'521
2037	6'889	1'948	1'083	2'515	2'662	723	1'036	160	660	96	655	1'048	2'727	314	1'423	5'648	29'587
2038	10'832	3'063	1'703	3'954	4'185	1'137	1'628	252	1'038	151	1'030	1'648	4'288	494	2'238	8'881	46'521
2039	6'909	1'953	1'086	2'522	2'669	725	1'039	161	662	96	657	1'051	2'735	315	1'427	5'665	29'673
2040	8'120	2'296	1'276	2'964	3'138	852	1'221	189	778	113	772	1'235	3'215	370	1'677	6'658	34'875
2041	6'357	1'797	999	2'321	2'456	667	956	148	609	89	604	967	2'517	290	1'313	5'212	27'302
2042	9'511	2'689	1'495	3'472	3'675	998	1'430	221	911	132	904	1'447	3'765	434	1'965	7'798	40'849
2043	7'741	2'189	1'217	2'826	2'991	812	1'164	180	742	108	736	1'178	3'064	353	1'599	6'347	33'246
2044	7'565	2'139	1'189	2'762	2'923	794	1'137	176	725	105	719	1'151	2'995	345	1'563	6'203	32'492
2045	7'435	2'102	1'169	2'714	2'873	780	1'118	173	713	104	707	1'131	2'943	339	1'536	6'096	31'932
2046	7'477	2'114	1'175	2'729	2'889	785	1'124	174	717	104	711	1'138	2'960	341	1'545	6'130	32'111
2047	10'832	3'063	1'703	3'954	4'185	1'137	1'628	252	1'038	151	1'030	1'648	4'288	494	2'238	8'881	46'521
2048	6'698	1'894	1'053	2'445	2'588	703	1'007	156	642	93	637	1'019	2'651	305	1'384	5'492	28'766
2049	7'088	2'004	1'114	2'587	2'739	744	1'065	165	679	99	674	1'078	2'806	323	1'464	5'811	30'440

(Continuation of Appendix VII)

Appendix VIII. Economic annual revenue of crops (SSP5-8.5), values are in thousands of USD\$. (Esp. Ingresos económicos anuales de los cultivos (SSP5-8.5), los valores están en miles de USD\$.)

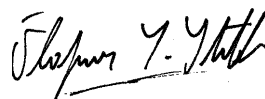
Año	Alfalfa	Arveja Grano verde	Cebolla	Cebada Grano	Trigo	Haba Grano Seco	Quinua	Frijol Grano Seco	ARVEJA GRANO SECO	TARHUI GRANO SECO	HABA GRANO VERDE	MAIZ AMILACEO	MAIZ CHOCLO	OCA	OLLUCO	PAPA	SUMA
2016	5'305	1'500	834	1'937	2'050	557	797	123	508	74	504	807	2'100	242	1'096	4'349	22'783
2017	4'399	1'244	691	1'606	1'700	462	661	102	422	61	418	669	1'741	201	909	3'606	18'892
2018	8'977	2'538	1'411	3'277	3'468	942	1'349	209	860	125	853	1'366	3'554	409	1'854	7'360	38'554
2019	10'756	3'041	1'691	3'927	4'156	1'129	1'617	250	1'031	150	1'023	1'636	4'258	491	2'222	8'819	46'196
2020	8'328	2'355	1'309	3'040	3'218	874	1'252	194	798	116	792	1'267	3'297	380	1'720	6'828	35'767
2021	4'456	1'260	700	1'627	1'722	468	670	104	427	62	424	678	1'764	203	921	3'654	19'139
2022	4'879	1'380	767	1'781	1'885	512	733	113	468	68	464	742	1'932	223	1'008	4'000	20'955
2023	6'754	1'910	1'062	2'466	2'610	709	1'015	157	647	94	642	1'028	2'674	308	1'395	5'538	29'009
2024	7'281	2'059	1'145	2'658	2'813	764	1'095	169	698	101	692	1'108	2'882	332	1'504	5'970	31'272
2025	7'937	2'244	1'248	2'897	3'066	833	1'193	184	761	111	754	1'207	3'142	362	1'640	6'507	34'086
2026	7'800	2'205	1'226	2'848	3'014	819	1'173	181	748	109	741	1'187	3'088	356	1'611	6'395	33'500
2027	5'264	1'488	827	1'922	2'034	552	791	122	504	73	500	801	2'084	240	1'087	4'316	22'609
2028	7'001	1'979	1'100	2'556	2'705	735	1'052	163	671	98	666	1'065	2'771	319	1'446	5'740	30'067
2029	7'038	1'990	1'106	2'569	2'719	739	1'058	164	674	98	669	1'071	2'786	321	1'454	5'770	30'227
2030	7'409	2'095	1'165	2'705	2'862	777	1'114	172	710	103	704	1'127	2'933	338	1'530	6'074	31'818
2031	7'706	2'179	1'211	2'813	2'978	809	1'158	179	739	107	733	1'172	3'051	351	1'592	6'318	33'097

Año	Alfalfa	Arveja Grano verde	Cebolla	Cebada Grano	Trigo	Haba Grano Seco	Quinua	Frijol Grano Seco	ARVEJA GRANO SECO	TARHUI GRANO SECO	HABA GRANO VERDE	MAIZ AMILACEO	MAIZ CHOCLO	OCA	OLLUCO	PAPA	SUMA
2032	5'850	1'654	920	2'136	2'260	614	879	136	561	81	556	890	2'316	267	1'208	4'796	25'124
2033	5'134	1'452	807	1'874	1'984	539	772	119	492	72	488	781	2'032	234	1'061	4'209	22'049
2034	4'813	1'361	757	1'757	1'860	505	724	112	461	67	458	732	1'905	220	994	3'946	20'673
2035	5'736	1'622	902	2'094	2'216	602	862	133	550	80	545	873	2'270	262	1'185	4'703	24'633
2036	7'582	2'144	1'192	2'768	2'930	796	1'140	176	727	106	721	1'154	3'002	346	1'566	6'217	32'564
2037	10'632	3'006	1'671	3'881	4'108	1'116	1'598	247	1'019	148	1'011	1'618	4'209	485	2'196	8'717	45'663
2038	6'946	1'964	1'092	2'536	2'684	729	1'044	161	666	97	660	1'057	2'750	317	1'435	5'695	29'830
2039	4'503	1'273	708	1'644	1'740	473	677	105	432	63	428	685	1'783	205	930	3'692	19'341
2040	6'987	1'976	1'098	2'551	2'700	733	1'050	162	670	97	664	1'063	2'766	319	1'443	5'729	30'010
2041	9'060	2'562	1'424	3'307	3'500	951	1'362	211	868	126	861	1'378	3'586	413	1'872	7'428	38'910
2042	4'474	1'265	703	1'633	1'729	470	673	104	429	62	425	681	1'771	204	924	3'668	19'214
2043	5'950	1'682	935	2'172	2'299	624	894	138	570	83	566	905	2'355	271	1'229	4'878	25'554
2044	4'877	1'379	767	1'781	1'885	512	733	113	467	68	464	742	1'931	222	1'008	3'999	20'948
2045	6'363	1'799	1'000	2'323	2'458	668	956	148	610	89	605	968	2'519	290	1'314	5'217	27'326
2046	7'151	2'022	1'124	2'610	2'763	750	1'075	166	685	100	680	1'088	2'831	326	1'477	5'863	30'710
2047	8'538	2'414	1'342	3'117	3'299	896	1'283	198	818	119	812	1'299	3'380	389	1'764	7'000	36'668
2048	9'723	2'749	1'528	3'549	3'757	1'020	1'462	226	932	135	924	1'479	3'849	443	2'009	7'972	41'757
2049	7'009	1'982	1'102	2'559	2'708	736	1'054	163	672	98	666	1'066	2'775	320	1'448	5'747	30'102

(Continuation of Appendix VIII)

Personal declaration:

I hereby declare that the submitted thesis is the result of my own, independent work. All external sources are explicitly acknowledged in the thesis.

A handwritten signature in black ink, appearing to read 'Ólafur Yngvi Stítelmann', written in a cursive style.

Sion, 2024-01-25

Ólafur Yngvi Stítelmann